2021

Remediation of Roadway Runoff Nutrients: Querying Sources Delivery Mechanism, Efficacy of Stormwater Best Management Practices, and Stormwater Routing Through Karst Geology

Mohammad Shokri
University of Central Florida

REMEDIATION OF ROADWAY RUNOFF NUTRIENTS: QUERYING SOURCE DELIVERY MECHANISMS, EFFICACY OF STORMWATER BEST MANAGEMENT PRACTICES, AND STORMWATER ROUTING THROUGH KARST GEOLOGY

by

MOHAMMAD SHOKRI

B.S. University of Tehran, 2009

M.S. Shahrood University of Technology, 2012

M.S. West Virginia University, 2017

A dissertation submitted in partial fulfillment of the requirements

for the degree of Doctor of Philosophy

in the Department of Civil, Environmental and Construction Engineering

in the College of Engineering and Computer Science

at the University of Central Florida

Orlando, Florida

Fall Term

2021

Major Professor: Kelly Kibler

ABSTRACT

Stormwater road runoff is a widespread non-point source of contaminants such as nutrients, which endangers water bodies, especially in vulnerable karst areas such as Florida. While roadside vegetated filter strips (VFSs) and stormwater basins are generally accepted best management practices (BMPs) for stormwater management, uncertainties about VFS nutrient removal are reported and stormwater basins are concerned of facilitating contaminant transport. In this dissertation, the application and efficacy of engineered infiltration media was tested as a subgrade for the enhanced nutrient removal from roadway runoff. Results of field-scale laboratory testing indicated that a VFS with engineered biosorption activated media (BAM) outperformed a Control with sandy soil concerning nitrate removal (mean 94±6% reduction vs. 23±64% increase) and total nitrogen removal (mean 80±5% vs. 38±23% reduction) within a 6 m filter width. However, BAM and soil performed similarly with respected to total phosphorus removal within the first 1.5 m filter width (84±9% vs. 82±12% reduction). Next, field sampling was conducted to characterize nutrient load and delivery in stormwater road runoff in different events, providing insights to improve design of BMPs. Three types of runoff events were characterized, where nutrients are transported differently under the controls of nutrient supply and transport conditions. Antecedent dry period was strongly related to nutrient supply and runoff volume was correlated to nutrient transport capacity. Finally, the configuration of the subsurface in stormwater basins and runoff movement to and within karst aquifer near Silver Springs in central Florida were investigated using geophysical surveys (ground penetrating radar and frequency domain electromagnetics) and tracer tests. Numerous subsurface anomalies and surface sinkholes were detected in the basins. High groundwater velocities in the surficial aquifer (10^{-6} to 10^{-3} ms^{-1}) and Upper Floridan Aquifer

(maximum on the order of 10^{-1} ms^{-1}) indicated that the basins act as hotspots of groundwater contamination in the area.

Keyword: Vegetated filter strips, road runoff, nutrients, karst aquifers, Silver Springs, Florida

In Loving Memory of

Maryam Kazemi

My Beloved Mother

1949 - 2021

She was my constant source of inspiration.

ACKNOWLEDGMENTS

I want to express my outmost gratitude to my advisor, Dr. Kelly Kibler, for her patience, support, comprehensive knowledge, and precious advices during my PhD program. Dr. Kibler was always helpful and the exploration of this research would not have been so rich and fulfilling without her guidance. I would also like to thank my dissertation committee members, Drs. Dingbao Wang, Thomas Wahl, and Melanie Beazley. Your constructive advice and suggestions have been very helpful. I would also like to thank Mr. Mike Wightman and Geo-view Inc. for providing geophysical equipment and training me on collecting and analyzing the collected data. Special thanks to Erik Stuart for his help during construction of our VFS models.

I want to acknowledge my colleagues, Dr. Yuan Gao, Dr. Dan Wen, Chris Hagglund, Andrew Corrado, Andrea Valencia, Diana Ordonez, Eranildo Lustosa, Gabriela Ford, Jordyn Washington, Olatoyin Olasimbo, Sam Maldonado, and Iris Peterson for their helps during data collections and insightful ideas. In addition, thanks to my friends in Orlando that have been like my family when I have been away from my own family in these years. Special thanks and gratitude to the University of Central Florida and Civil, Environmental and Construction Engineering Department for services and offering me to teach as teaching assistant. Also, thanks to the Florida Department of Transportation for funding this research.

Last and most importantly, I want to give my sincere appreciations to my family for their endless love, support, and encouragement. Mam, I did it by your prayer and always felt your positive energy. Thank you for being such a great and kind mom and I am so sorry I could not come back to see you again when you were not fine. I wish to see you again in the afterlife.

TABLE OF CONTENT

LIST OF FIGURES

LIST OF TABLES

CHAPTER 1 INTRODUCTION

1.1 Problem statement

Urbanization and expansion of impervious surfaces associated with infrastructure affect hydrological properties of watersheds by increasing pollution and runoff volume as well as decreasing infiltration rate (Booth and Jackson, 1997; Chabaeva et al., 2009; Ebrahimian et al., 2016). Stormwater runoff from roadways has been recognized as one of the major non-point sources of contaminants such as nutrients, heavy metals, sediments, and toxic substances (Carsel et al., 1985; Arias-Estévez et al., 2008; McKenzie et al., 2009; Chai et al., 2012; Kayhanian et al., 2012; LeFevre et al., 2014). Degrading water quality in Florida's lakes, rivers, and springs, such as Silver Springs in Central Florida, have directed attention to identifying and remediating sources of excess nutrient pollution (Heffernan et al., 2010; Hicks and Holland, 2012; Liao et al., 2019; Wen et al., 2020). Excess nutrients from roadway runoff endangers surface and groundwater bodies and can lead to algal blooms, ecosystem degradation, loss of biodiversity, and eutrophication in receiving water bodies (Bouchard et al., 1992; Pitt et al., 1999; Mallin et al., 2009; Suthar et al., 2009; Eller and Katz, 2017). Groundwater resources in Florida are karstic aquifers, which are highly susceptible to dissolution, subsurface features, and sinkholes that make aquifers highly vulnerable to contamination by surface water (Harper and Baker, 2007; Moore and Beck, 2018). Given vulnerable karst aquifers in Florida, particular attention is required with respect to stormwater management and treatment to protect groundwater aquifers. This dissertation addresses such concerns to enhance nutrient removal from roadway runoff within green infrastructure designs and inform nutrient delivery from roadway runoff and movement from stormwater basins to groundwater and within karst aquifers.

1.2 Literature review

A set of regulations were evolved in the United States to preserve water resources from pollution and restore water quality, known as the Clean Water Act of 1972 (Boger et al., 2018). Based on these regulations, stormwater management with the aim of water quality improvement has been considered extensively, especially from non-point sources of pollutants such as roadways and urbanized area (Harper and Baker, 2007; Boger et al., 2018). Green infrastructure including vegetated filter strips (VFSs) and vegetated swales were brought to attention as best management practices (BMPs) for roadside shoulders (Gavrić et al., 2019). The green infrastructure strategies have been attractive to the department of transportations (DOTs) for water quality improvements because of the ease and economics of incorporation to road shoulders (Yu et al., 2001). Stormwater management basins are another BMP strategies designed usually in urbanized areas to collect stormwater runoff and inhibit flood occurrence, provide infiltration, and assist with groundwater recharge (Harper and Baker, 2007). Per collecting stormwater runoff, significant amount of runoff volumes are usually delivered to stormwater management basins. In order to preserve water resources from pollution and restore water quality, we need to deepen our understanding about stormwater management through such BMP systems.

1.2.1 Roadway runoff nutrient delivery

Roadway runoff is characterized as a widespread non-point source of contaminates such as nutrients, heavy metals, sediments, and toxic substances (Hu et al., 2020; Jeong et al., 2020). Contaminants can be accumulated over road surfaces then washed off and transported during rainfall-runoff events to finally reach water bodies (e.g. Wang et al., 2010; Winston and Hunt,

2016; Zhao et al., 2018). While different sources of excess nutrients are documented including agriculture, septic tanks, fertilizers, livestock waste, and wastewater discharges (Badruzzaman et al., 2012; Eller and Katz, 2017), urban stormwater runoff is characterized as a potential source of excess nutrients degrading water quality in Florida and the US (Abdul-Aziz and Al-Amin, 2016; Trenouth and Gharabaghi, 2016). Excess nutrients in roadway runoff derive from varied sources including atmospheric deposition, sediment and particulate colloids, and incoming pollutants from nearby surfaces like fertilizers and animal wastes in agricultural and residential areas (Miguntanna, 2009; Eller and Katz, 2017). For example, anthropogenic sources of burning fossil fuels can increase nitrogen deposited through atmospheric deposition (Paerl, 1997; Lapointe et al., 2004).

Nutrients can be accumulated over road surfaces during dry conditions and then delivered in rainfall-runoff events in dissolved and particulate forms (Wang et al., 2010; Winston et al., 2016; Hong et al. 2016; Zhao et al., 2018). The first several days after a rain event are characterized as the greatest rate of pollutant accumulation (Borris et al., 2014; Trenouth and Gharabaghi, 2016). Nitrate, nitrite, and ammonia are inorganic nitrogen species, which are highly soluble in urban runoff and aquatic systems (Feth, 1966; Galloway et al., 2003; Oms et al., 2000) and dominantly transport in dissolved form in roadway runoff (Taylor et al., 2005). Organic nitrogen and phosphorus tend to transport more in particulate forms, even though they may also transport in dissolved form (Taylor et al., 2005). While the proportion and dominant nitrogen species forming total nitrogen may be different site to site, stormwater treatment systems are suggested to be designed to improve dissolved nitrogen removal, as they can transport to receiving water bodies with ease and promoting their removal is critical (Taylor et al., 2005).

Nutrient delivery from roadways can vary within and between runoff events and characterizing these dynamics can provide important insights into better design of BMPs (Stahre and Urbonas, 1990; Wanielista and Yousef, 1993; Bertrand-Krajewski et al., 1998). For example, when the majority of the pollutant load is transported during the initial runoff phases and contaminant concentrations decrease through the tail of the event, this dynamic is recognized as a first flush delivery (Lee et al., 2002; Miguntanna, 2009). Based on the first flush concept, BMPs may be deigned to capture and treat the initial runoff volume (20 to 50%) which is assumed to deliver the majority of pollutant mass (Stahre and Urbonas, 1990; Wanielista and Yousef, 1993; Bertrand-Krajewski et al., 1998). However, first flush behavior is not observed in all runoff events and increase in total nitrogen mass has been reported at the end of runoff events, a so-called end-flush delivery (Bach et al., 2010). Analysis of nutrient delivery dynamics is traditionally conducted by examining the variation in cumulative pollutant mass delivery (normalized by event total) against normalized cumulative runoff volume, known as the M(V) curve (Bertrand-Krajewski et al., 1998; Lee et al., 2002; Jiang et al., 2010). The M(V) curve allows for comparison of contaminant transport dynamics between events (Figure 1). First flush behavior occurs when cumulative pollutant mass exceeds cumulative runoff volume and conversely end flush behavior is defined when pollutant mass lags behind cumulative runoff volume (Bertrand-Krajewski et al., 1998). The strength of first flush is acknowledged by deviation of the curve with respect to the bisector (1:1) line (Bertrand-Krajewski et al., 1998; Lee et al., 2002). In Figure 1 for example, event 1 represents a first flush event as a larger share of the total pollutant mass is delivered early in the runoff event, while event 2 represents an end flush event delivering the majority of the pollutant mass over the tail of the runoff event.

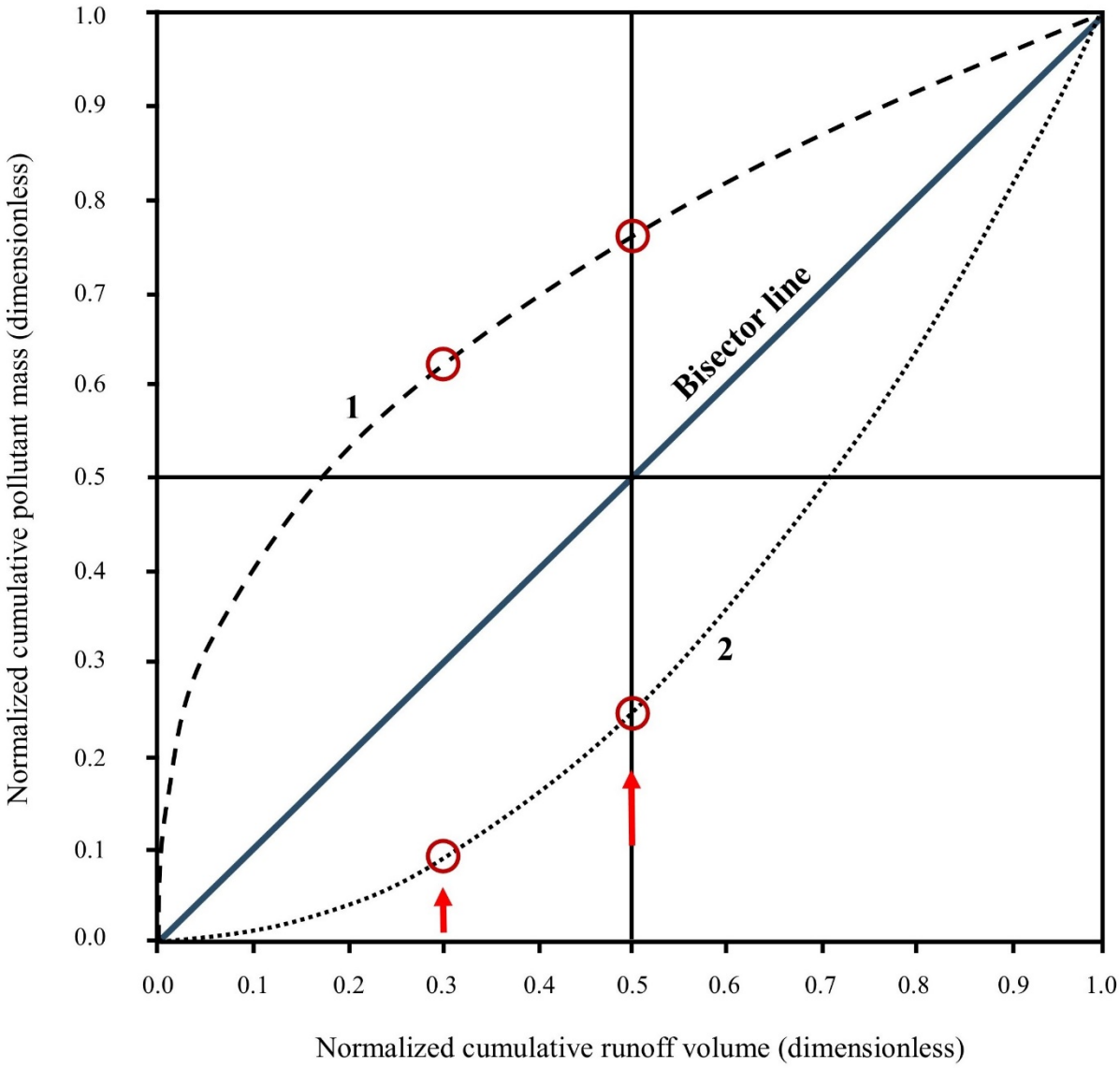

Figure 1. Variation of cumulative pollutant mass against cumulative runoff volume in two different roadway runoff events: (1) a first-flush curve, and (2) an end-flush curve. The bisector line represents 1:1 variation of pollutant mass and runoff volume. Greater pollutant mass delivery earlier in event (1) can be observed by comparing relative mass delivery at the 30% or 50% of runoff volumes. Figure is adapted from (Lee et al., 2002).

While the M(V) curve approach is generally accepted as a method for analyzing pollutant delivery dynamics of runoff events, some issues are reported about the approach. For example, the method neglects to account for variation in absolute characteristics of runoff events (cumulative depth, precipitation intensity and intensity profile), where large and small events are normalized relative to the total volume and compared. Similarly, variation of accumulated pollutant available for transport is not considered among different events (Bach et al., 2010). Bach et al., (2010) have proposed a sliced-based approach instead, and their approach has been endorsed by others (e.g. Christian et al., 2020). However, the method requires collecting continuous water quality data over runoff events (sampling at 60 seconds) which may not be always possible. Introducing a complementary approach based on understanding the physics of nutrient mobilization from roadways may improve understanding of excess nutrient delivery in road runoff and lead to better design of BMPs and mitigation or avoidance strategies.

Pollutant transport dynamics are affected by many factors such as drainage size and impervious area, rainfall intensity, antecedent dry period, and dominant tendency of pollutant species to transport in dissolved vs. particulate forms (Wanielista and Yousef, 1993; Lee et al., 2002; Kayhanian et al., 2012). For example, pollutant transport from smaller and more compact catchment areas (less than 10 to 20 ha) are likely to be characterized by more frequent first flush events as compared to larger watershed areas (Lee et al., 2002; Harper and Baker, 2007; Kayhanian et al., 2012). The relationship between rainfall characteristics and pollutant wash-off from roadways is investigated by Liu et al., [2013] where rainfall intensity, duration, and antecedent dry days were considered. Highly intense events are generally characterized as having higher kinetic energy, and thus greater potential for particle detachment and wash off, greater competence for

sediment entrainment, and likely more contaminant transport (Kleinman et al., 2006; Liu et al., 2013). While a positive correlation between rainfall intensity and duration with pollutant wash off may be expected, research indicates that behavior is non-linear, similar to a step-wise function, indicating that key thresholds may control pollutant delivery (Egodawatta et al., 2007; Liu et al., 2013). For instance, intense events (> 20 mm/h) delivered greater event mean concentrations (EMC) of nutrients as compared to lower intensity events because of greater kinetic energy during wash-off processes (Liu et al., 2013). Similarly, intense events with shorter duration (< 2 h) were characterized as delivering greater EMC than same intensity (> 20 mm/h) but with longer duration (> 2 h) (Liu et al., 2013). In addition, the effect of rainfall duration was minimal in wash off in low intensity events (Liu et al., 2013). Contrarily, relationships between roadway runoff nutrient concentrations with rainfall intensity or depth were not observed in research conducted in Tampa Bay, Florida (Yang and Toor, 2017). The varied outcomes observed in different studies suggest that the role of rainfall characteristics (especially intensity) on nutrient delivery may be highly complex and context-specific.

The concept of transport-limited vs. supply-limited flows is well known within the sediment transport literature (Lane, 1955; Grant et al., 2003). For example, when transport capacity is higher than sediment supply in a river channel, more erosion and sediment transport occur but sediment deposits when transport capacity is lower than sediment supply. Characterizing stormwater runoff events as transport or supply limited may have applications to stormwater management. Borris et al. [2014] conducted a modelling study that illustrated the role of rainfall and runoff as a primary controlling factor of total suspended solids (TSS) in urban runoff. Transport-limited events occurred when rainfall depth and intensity were low and generated runoff did not effectively

transport all available solids, thus concentrations were low. However, by increasing runoff volume by a certain threshold (larger storms), transport limited flow regimes shifted to become supply limited, where runoff effectively mobilized pollutants to the point where available transport capacity exceeded pollutant mass, also resulting in low pollutant concentrations (Borris et al., 2014). Similarly, Bach et al. [2010] stated that if runoff volume was not be sufficiently large enough to wash off contaminants, concentrations may be constant through runoff event. However, when contaminant supply is limited and runoff volume is sufficient, contaminant concentrations will decrease with cumulative runoff volume (Bach et al., 2010).

1.2.2 Vegetated filter strip

Stormwater BMPs generally intercept stormwater runoff after the contaminant wash off process. VFS, also called filter strip or buffer strip, is a type of infiltration-based BMP technique of stromwater management where inflow runoff disperses as a sheet flow uniformly over vegetated side slopes (Hager et al., 2019; Qin, 2020). They usually implement to drain runoff and prevent inundation of roadways, and additionally remediate contaminants through biological and physicochemical processes of sorption, filtration, sedimentation, and precipitation (Strock et al., 2010; Winston et al., 2011; Horstmeyer et al., 2016). While they are widely-accepted BMPs to provide infiltration and primary treatment of runoff from roadways (Abu-Zreig et al., 2003; Dierkes et al., 2015; Horstmeyer et al., 2016), variation in nutrient removal performance has been reported for roadside shoulder VFS applications (e.g. Boger et al. 2018; Hager et al., 2019). Negative nutrient removal (i.e. generation) has been reported in roadside VFS (Stagge et al., 2012; Hager et al. 2019). In some cases, VFS was considered as sources of contamination by

accumulating pollutants (Barrett et al. 1998; Barrett et al. 2004; Koch et al. 2015; Liu et al. 2017; Yu et al. 2019). Given runoff from roadways as a major source of nutrient and variations in nutrient removal performance of roadside VFS, a new strategy of improving nutrient removals within VFS roadside application is required.

Runoff flowing into roadside VFS infiltrates into surface soil over shoulder side-slopes or bypasses the filter as overland flow to receiving water bodies or bottom channel. Within VFSs, the vegetated area helps with runoff velocity reduction and promotes infiltration within subgrade media, where potential contaminants may be sequestered or removed. The subsurface properties of soil and surface characteristics such as roughness and depression storage will influence runoff and infiltration process over side-slopes. Soil texture (relative percentages of sand, silt, and clay), compaction, soil organic content, and soil moisture content are important parameters affect infiltration capacity of subgrade media (Winston et al., 2011). Fine textural soils (e.g. clayey soils) or compacted soils, which characterized by lower permeability, promote more runoff, sooner than coarser soils with little compaction (Martinez-Mena et al., 1998; Vahabi and Ghafouri, 2009). Soil compaction may occur because of human activities during roadway constructions, equipment used for spreading fertilizers, grazing animals, or naturally due to raindrops (Dingman, 2015). Soil organic content provides habitat for biota that positively increase pore space and soil infiltration rate through root growth and decay process, burrowing, and soil insects (Jones, 1971; Vahabi and Ghafouri, 2009; Dingman, 2015). Some influential properties such as soil moisture content, vegetation cover, and precipitation intensity (rate of runoff production) may be dynamic and vary seasonally or over a storm (Garcia de la Serrana Lozano, 2017). High initial soil moisture causes low infiltration rate of soil and then faster response to runoff generation (Tarboton, 2003). Soil

content moisture is impacted by evapotranspiration rate, plant cover, and irrigation activities. In addition, some soils which contain clay minerals swell in wet condition and shrink in dry condition which consequently causes a decrease and increase in permeability and infiltration rate of soil, respectively (Römkens and Prasad, 2006; Dingman, 2015).

The surface hydraulic process over VFS is mainly controlled by slope, surface roughness, and vegetation cover, particularly when ponding begins (Dingman, 2015). The rate of generating overland flow is directly related to slope and inversely related to surface roughness. Thus, steeper slope and smoother surfaces facilitate rapid overland flow and lower infiltration rate. Steep side-slopes of road shoulders may also make the soil susceptible to erosion. Soil surface roughness can be also increased during maintenance operations (Dingman, 2015). Two general type of surface micro-structure depressions can be identified in roadside shoulder with respect to side-slope direction (Garcia de la Serrana Lozano, 2017). Surface depressions with downslope orientations can increase runoff generation while surface depressions with cross-slope orientations can decrease runoff generation (Römkens and Wang, 1986; Helmers and Eisenhauer, 2006; Thompson et al., 2010; Kirkby, 2014). Intense vegetation cover can lead to increase in soil surface roughness, which then delay runoff generation by water retention in depressions (Garcia de la Serrana Lozano, 2017). In addition, soil vegetation cover can assist soil protection and the consensus is that denser vegetation cover will promote infiltration rate and more protected the soil from the erosion (Loch, 2000). Accordingly and in summary, infiltration capacity of a VFS depends usually upon soil type and compaction, rainfall-runoff event, inflow runoff volume, slope, filter size, and vegetation type and density (Stagge et al. 2012; Boger et al. 2018; Qin, 2020).

Engineering of roadway shoulder filters must be considered within the context of road shoulder design standards, for instance, as regulated by FDOT (e.g. Florida Department of Transportation, 2005). While removal efficiency of BMPs are usually calculated based mean annual runoff (Harper and Baker, 2007), a significant amount of the annual pollutant mass is typically carried from roadways to shoulders by small frequent storm events (Pappas et al., 2008; Arias-Estévez et al., 2008; McKenzie et al., 2009; Chai et al., 2012; Kayhanian et al., 2012; LeFevre et al., 2014; Borris et al., 2014). Therefore, the design of VFS within roadway should be directed to the frequent event sizes that most likely deliver the greatest pollutant loads.

Enhanced roadway runoff treatment may be possible within right-of-ways through implementing VFSs containing engineered infiltration media (e.g. CTS Bold & Gold BAM) along roadways. CTS Bold & Gold Biosorption activated media (BAM) is a type of engineered media which has been developed for stormwater nutrient removals (Kibler et al., 2020). BAM contains expanded clay, tire crumb, sand and topsoil (Hanson Professional Services INC, 2017). BAM contains more than 2% and less than 6% mineral materials by volume smaller than #200 sieve size (0.0029 in or 0.074 mm). The density of CTS BAM is about 1.6 g/cm^3 (2700 lb/cy) and does not contain organic material. CTS BAM is composed of approximately 15% sorption materials including tire crumb of 0.04 to 0.2 in (~1 to 5 mm) size with density of about 0.43 g/cm^3 (730 lbs/cy) and light colored mined clay (more than 99% clay content) with medium plasticity and density of about 0.8 g/cm^3 (1350 lbs/cy) (Hanson Professional Services INC, 2017). BAM typically has total porosity of about 35% and water holding capacity of about 10% by porosity. The permeability of BAM, as it is determined in laboratory, at maximum compaction should be greater than 25.4 mm/h (1 in/h) (Hanson Professional Services INC, 2017). BAM is installed in-

place according to FDOT Standard Specification Section 120, in which its compaction in dry condition is defined as 1280 to 1600 kg/m3 (~ 80 to 100 lbs/ft^3). Clean water may be added to the installed BAM to meet the compaction requirements. Local topsoil is used to cover the BAM media and preparation of side slope for planting. According to FDOT Standard Specification (2018), soil over grassed side slopes is not required to meet any specific density and should not be compacted to not impede plant growth. The grassed shoulder area must be loose to the depth of 15.24 cm (6 in) for seeding and plant operation (FDOT Standard Specification, 2018).

1.2.3 Stormwater management areas and risk of karst aquifer contamination

Stormwater management areas (retention basins) are type of BMP systems, which are designed to collect and store stormwater runoff temporarily, about 24 to 72 hours, and provide infiltration to recharge groundwater (Harper and Baker, 2007). They are a common type of stormwater management strategy in Florida for urbanized and commercial sites, as well as nearby roadways. As the function of dry retention basins primarily relies on infiltration, these stormwater management areas are designed and constructed in regions with permeable soil and adequate storage within the vadose zone (minimum 0.3 to 1 m of soil depth above the seasonal groundwater table) (Harper and., 2007). However, stormwater management areas are mostly designed hydraulically to collect runoff and intercept peak flows rather than effectively remove pollutants (Harper and., 2007). It is supposed that pretreatment of contaminants occurs through infiltration by physical, biological, and chemical processes, though nutrient uptake through biological process of plant surfaces and roots is expected to be limited since collected runoff should be infiltrated within a limited time, less than 72 hours (Harper and., 2007). Because collected runoff should be

infiltrated relatively fast, the configuration of the basin invert has an important role in protection of the aquifer. Potential risk of contaminant transport from surface to the groundwater aquifer is especially high where groundwater aquifers are karstic, as in some parts of Florida. Karst aquifers are highly prone to dissolution, sinkhole formation, and subsurface drainage features. For example, interconnection between a wastewater application facility and a first magnitude karst spring (Wakulla Sprig) was demonstrated through tracer experiments conducted by Kincaid et al. [2012] in Florida. Nutrients could transfer from surface to groundwater through infiltration into subsurface drainages and conduits and led to groundwater aquifer contamination and increase in the level of nutrients in the springs discharge point (Kincaid et al., 2012). These results justify the study of karst feature in stormwater basins as relatively littles research has addressed the potential risk of groundwater contamination from stormwater management areas (Stephenson et al., 1999; Moore and Beck, 2018).

The Floridan aquifer is a karstic aquifer and one of the important fresh water resources in the US (Stevanović, 2019). Karst aquifers are important water resources worldwide and supply drinking water for hundreds of millions of people, 40% in the US and roughly 20-25% in the world (Goldscheider, 2005; Ford and Williams, 2007; Ghasemizadeh et al., 2012). Due to the nature of karst systems with high groundwater velocity and dissolution of the rocks, they are highly susceptible to pollution. Karst development is typically through dissolution when limestone rocks come to contact with acidic water. Dissolution over time generates specific surface and subsurface karst features such as sinkhole, doline, polje, karst valley, cave and underground drainage streams, which makes groundwater aquifer more susceptible to surface contamination (Ford and Williams, 2007). For example, Silver Springs is one of the largest karst springs in the state of Florida, located

5 miles east of city of Ocala in Marion County and provides headwater to Silver River (Rosenau et al., 1977; Ghosh et al., 2016). Silver Springs is a tourist attraction spring because of significant water discharge, aquatic wildlife, and well-known glass bottom boats (Samek et al., 2004; King et al., 2004). Most impaired water in Silver Springs and Florida are associated to nitrogen and phosphorus loads, which impaired water quality parameters (Phelps et al., 2006). Since stormwater management areas are important BMPs where significant amount of runoff are infiltrated, care must be taken into account with respect to their performance to protect groundwater quality.

1.3 Dissertation structure

This dissertation is an assembly of three research studies developed with the common purpose of improving the management of nutrients in roadway runoff. In chapter 2, nutrient removal from roadway runoff is investigated within a novel design of BMP, a VFS containing engineered infiltration media sited within the roadway shoulder and embankment. The study is conducted by designing two physical models simulating roadway shoulder and vegetated embankment, one with engineered media and the other with common sandy topsoil in central Florida. The purpose of the study is to examine nutrient removal efficacy of engineered media in different rainfall-runoff event depths. In chapter 3, nutrient mass delivery is investigated within the runoff event scale to explore nutrient source and delivery mechanisms in variable runoff event types. This study may inform design of BMPs systematically by targeting effective runoff events in nutrient wash off over roadways. In chapter 4, the potential of nutrient transport from stormwater management areas near Silver Springs to and within surficial and karst groundwater aquifers are explored using

geophysical investigations and tracer experiments. In chapter 5, we include a summary of findings and conclusions of each chapter with suggestions for future studies.

1.4 References

Abdul-Aziz, O.I. and Al-Amin, S., 2016. Climate, land use and hydrologic sensitivities of stormwater quantity and quality in a complex coastal-urban watershed. Urban Water Journal, 13(3), 302-320. https://doi.org/10.1080/1573062X.2014.991328

Arias-Estévez, M., López-Periago, E., Martínez-Carballo, E., Simal-Gándara, J., Mejuto, J.C., García-Río, L., 2008. The mobility and degradation of pesticides in soils and the pollution of groundwater resources. Agriculture, Ecosystems & Environment 123(4), 247-260. https://doi.org/10.1016/j.agee.2007.07.011

Bach, P.M., McCarthy, D.T. and Deletic, A., 2010. Redefining the stormwater first flush phenomenon. Water Research, 44(8), 2487-2498. https://doi.org/10.1016/j.watres.2010.01.022

Badruzzaman, M., Pinzon, J., Oppenheimer, J. and Jacangelo, J.G., 2012. Sources of nutrients impacting surface waters in Florida: a review. Journal of environmental management, 109, 80-92. https://doi.org/10.1016/j.jenvman.2012.04.040

Barrett, M., Lantin, A., Austrheim-Smith, S., 2004. Storm water pollutant removal in roadside vegetated buffer strips. Transportation Research Record. 1890(1), 129-140. https://doi.org/10.3141%2F1890-16

Barrett, M.E., Walsh, P.M., Malina Jr, J.F., Charbeneau, R.J., 1998. Performance of vegetative controls for treating highway runoff. Journal of Environmental Engineering. 124(11), 1121-1128. https://doi.org/10.1061/(ASCE)0733-9372(1998)124:11(1121)

Bertrand-Krajewski, J.L., Chebbo, G. and Saget, A., 1998. Distribution of pollutant mass vs volume in stormwater discharges and the first flush phenomenon. Water Research, 32(8), 2341-2356. https://doi.org/10.1016/S0043-1354(97)00420-X

Boger, A.R., Ahiablame, L., Mosase, E., Beck, D., 2018. Effectiveness of roadside vegetated filter strips and swales at treating roadway runoff: a tutorial review. Environmental Science: Water Research & Technology. 4(4), 478-486. https://doi.org/10.1039/C7EW00230K

Booth, D.B., Jackson, C.R., 1997. Urbanization of aquatic systems: degradation thresholds, stormwater detection, and the limits of mitigation. JAWRA Journal of the American Water Resources Association 33(5), 1077-1090. https://doi.org/10.1111/j.1752-1688.1997.tb04126.x

Borris, M., Viklander, M., Gustafsson, A.M. and Marsalek, J., 2014. Modelling the effects of changes in rainfall event characteristics on TSS loads in urban runoff. Hydrological Processes, 28(4), 1787-1796. https://doi.org/10.1002/hyp.9729

Bouchard, D.C., Williams, M.K., Surampalli, R.Y., 1992. Nitrate contamination of groundwater: sources and potential health effects. Journal-American Water Works Association 84(9), 85-90. https://doi.org/10.1002/j.1551-8833.1992.tb07430.x

Carsel, R.F., Mulkey, L.A., Lorber, M.N., Baskin, L.B., 1985. The pesticide root zone model (PRZM): A procedure for evaluating pesticide leaching threats to groundwater. Ecological modelling 30(1-2), 49-69. https://doi.org/10.1016/0304-3800(85)90036-5

Chabaeva, A., Civco, D.L., Hurd, J.D., 2009. Assessment of impervious surface estimation techniques. Journal of Hydrologic Engineering 14(4), 377-387. https://doi.org/10.1061/(ASCE)1084-0699(2009)14:4(377)

Chai, L., Kayhanian, M., Givens, B., Harvey, J.T., Jones, D., 2012. Hydraulic performance of fully permeable highway shoulder for storm water runoff management. Journal of Environmental Engineering 138(7), 711-722. https://doi.org/10.1061/(ASCE)EE.1943-7870.0000523

Christian, L., Epps, T., Diab, G. and Hathaway, J., 2020. Pollutant Concentration Patterns of In-Stream Urban Stormwater Runoff. Water, 12(9), p.2534. https://doi.org/10.3390/w12092534

Dierkes, C., Lucke, T., Helmreich, B., 2015. General technical approvals for decentralized sustainable urban drainage systems (SUDS)—the current situation in Germany. Sustainability 7, 3031-3051. https://doi.org/10.3390/su7033031

Dingman, S.L., 2015. Physical Hydrology, 3rd Edition, Waveland Press, Long Grove, IL.

Ebrahimian, A., Wilson, B.N., Gulliver, J.S., 2016. Improved methods to estimate the effective impervious area in urban catchments using rainfall-runoff data. Journal of Hydrology 536, 109-118. https://doi.org/10.1016/j.jhydrol.2016.02.023

Eller, K.T. and Katz, B.G., 2017. Nitrogen Source Inventory and Loading Tool: An integrated approach toward restoration of water-quality impaired karst springs. Journal of environmental management, 196, 702-709. https://doi.org/10.1016/j.jenvman.2017.03.059

Feth, J.H., 1966. Nitrogen compounds in natural water—a review. Water Resources Research, 2(1), 41-58. https://doi.org/10.1029/WR002i001p00041

Florida Department of Transportation., 2018. Standard Specifications for Road and Bridge Construction. State of Florida Department of Transportation, 1221 p.

Ford, D., and Williams, P. 2007. Karst Hydrogeology and Geomorphology, John Wiley & Sons Ltd, West Sussex, England. DOI: 10.1002/9781118684986.

Galloway, J.N., Aber, J.D., Erisman, J.W., Seitzinger, S.P., Howarth, R.W., Cowling, E.B. and Cosby, B.J., 2003. The nitrogen cascade. Bioscience, 53(4), 341-356. https://doi.org/10.1641/0006-3568(2003)053[0341:TNC]2.0.CO;2

Garcia de la Serrana Lozano, M.D.C., 2017. Analysis of Infiltration and Overland Flow over Sloped Surfaces: Application to Roadside Swales. Doctoral dissertation, University of Minnesota, 243 p.

Gavrić, S., Leonhardt, G., Marsalek, J., Viklander, M., 2019. Processes improving urban stormwater quality in grass swales and filter strips: A review of research findings. Science of the Total Environment. 669, 431-447. https://doi.org/10.1016/j.scitotenv.2019.03.072

Ghasemizadeh, R., Hellweger, F., Butscher, C., Padilla, I., Vesper, D., Field, M., and Alshawabkeh, A. 2012. Review: Groundwater flow and transport modeling of karst aquifers, with particular reference to the North Coast Limestone aquifer system of Puerto Rico. Hydrogeol J, 20(8), 1441-1461. https://doi.org/10.1007/s10040-012-0897-4

Ghosh, D.K., Wang, D., Bilskie, M.V. and Hagen, S.C., 2016. Quantifying changes of effective springshed area and net recharge through recession analysis of spring flow. Hydrological Processes, 30(26), 5053-5062. https://doi.org/10.1002/hyp.10970

Goldscheider, N, 2005. Karst groundwater vulnerability mapping: application of a new method in the SwabianAlb, Germany. Hydrogeology Journal, 13(4), 555-564. https://doi.org/10.1007/s10040-003-0291-3

Hager, J., Hu, G., Hewage, K. and Sadiq, R., 2019. Performance of low-impact development best management practices: a critical review. Environmental Reviews, 27(1), 17-42. https://doi.org/10.1139/er-2018-0048

Hanson Professional Services INC., 2017. Design Documentation Report SR 15 (US 17) at SR 16 Intersction Improvement, Clay County Florida. Phase III Submittal to Florida Department of Transportation, Project ID 436118-1-52-01.

Harper, H.H., Baker, D.M., 2007. Evaluation of current stormwater design criteria within the state of Florida. Florida Department of Environmental Protection, 327 p.

Heffernan, J.B., Liebowitz, D.M., Frazer, T.K., Evans, J.M. and Cohen, M.J., 2010. Algal blooms and the nitrogen-enrichment hypothesis in Florida springs: evidence, alternatives,

and adaptive management. Ecological Applications, 20(3), 816-829. https://doi.org/10.1890/08-1362.1

Helmers, M.J., Eisenhauer, D.E., 2006. Overland flow modeling in a vegetative filter considering non-planar topography and spatial variability of soil hydraulic properties and vegetation density. Journal of Hydrology 328(1-2), 267-282. https://doi.org/10.1016/j.jhydrol.2005.12.026

Hicks, R. and Holland, K., 2012. Nutrient TMDL for Silver Springs, Silver Springs Group, and Upper Silver River (WBIDs 2772A, 2772C, and 2772E). Ground Water Management Section, Florida Department of Environmental Protection, Tallahassee, FL.

Hong, Y., Bonhomme, C., Le, M.H. and Chebbo, G., 2016. A new approach of monitoring and physically-based modelling to investigate urban wash-off process on a road catchment near Paris. Water Research, 102, 96-108. https://doi.org/10.1016/j.watres.2016.06.027

Horstmeyer, N., Huber, M., Drewes, J.E., Helmreich, B., 2016. Evaluation of site-specific factors influencing heavy metal contents in the topsoil of vegetated infiltration swales. Science of the Total Environment 560, 19-28. https://doi.org/10.1016/j.scitotenv.2016.04.051

Hu, D., Zhang, C., Ma, B., Liu, Z., Yang, X. and Yang, L., 2020. The characteristics of rainfall runoff pollution and its driving factors in Northwest semiarid region of China-A case study of Xi'an. Science of The Total Environment, p.138384. https://doi.org/10.1016/j.scitotenv.2020.138384

Jeong, H., Choi, J.Y., Lee, J., Lim, J. and Ra, K., 2020. Heavy metal pollution by road-deposited sediments and its contribution to total suspended solids in rainfall runoff from intensive industrial areas. Environmental Pollution, 265, p.115028. https://doi.org/10.1016/j.envpol.2020.115028

Jiang, R., Woli, K.P., Kuramochi, K., Hayakawa, A., Shimizu, M. and Hatano, R., 2010. Hydrological process controls on nitrogen export during storm events in an agricultural watershed. Soil Science & Plant Nutrition, 56(1), 72-85. https://doi.org/10.1111/j.1747-0765.2010.00456.x

Jones, M.J., 1971. The maintenance of soil organic matter under continuous cultivation at Samaru, Nigeria. The Journal of Agricultural Science 77(3), 473-482. DOI:10.1017/S0021859600064558

Kayhanian, M., Fruchtman, B.D., Gulliver, J.S., Montanaro, C., Ranieri, E., Wuertz, S., 2012. Review of highway runoff characteristics: Comparative analysis and universal implications. Water research 46(20), 6609-6624. https://doi.org/10.1016/j.watres.2012.07.026

Kibler, K.M., Chang, N.B., Wanielista, M.P., Wen, D., Shokri, M., Valencia, A., Lustoso-Alves Jr, E. and Rice, N., 2020. Optimal Design of Stormwater Basins With Bio-Sorption Activated Media (Bam) in Karst Environments–Phase II: Field Testing of BMPs. Florida Department of Transportation, 60 p.

Kincaid, T., Davies, G., Werner, C., DeHan, R., 2012. Demonstrating interconnection between a wastewater application facility and a first magnitude spring in a karstic watershed: Tracer

study of the Southeast Farm Wastewater Reuse Facility, Tallahassee, Florida. Florida Geological Survey, 192 p.

King, W.A., 2004. Through the looking glass of Silver Springs: tourism and the politics of vision. Americana 3(1).

Kirkby, M.J., 2014. Do not only connect: a model of infiltration-excess overland flow based on simulation. Earth Surface Processes and Landforms 39(7), 952-963. https://doi.org/10.1002/esp.3556

Koch, B.J., Febria, C.M., Cooke, R.M., Hosen, J.D., Baker, M.E., Colson, A.R., Filoso, S., Hayhoe, K., Loperfido, J.V., Stoner, A.M., Palmer, M.A., 2015. Suburban watershed nitrogen retention: Estimating the effectiveness of stormwater management structures. Elementa: Science of the Anthropocene, 3. https://doi.org/10.12952/journal.elementa.000063%20#sthash.rcQOPFkF.dpuf

Lapointe, B.E., Barile, P.J. and Matzie, W.R., 2004. Anthropogenic nutrient enrichment of seagrass and coral reef communities in the Lower Florida Keys: discrimination of local versus regional nitrogen sources. Journal of Experimental Marine Biology and Ecology, 308(1), 23-58. https://doi.org/10.1016/j.jembe.2004.01.019

Lee, J.H., Bang, K.W., Ketchum Jr, L.H., Choe, J.S. and Yu, M.J., 2002. First flush analysis of urban storm runoff. Science of the Total Environment, 293(1-3), 163-175. https://doi.org/10.1016/S0048-9697(02)00006-2

LeFevre, G.H., Paus, K.H., Natarajan, P., Gulliver, J.S., Novak, P.J., Hozalski, R.M., 2014. Review of dissolved pollutants in urban storm water and their removal and fate in

bioretention cells. Journal of Environmental Engineering 141(1), 04014050. https://doi.org/10.1061/(ASCE)EE.1943-7870.0000876

Liao, X., Nair, V.D., Canion, A., Dobberfuhl, D.R., Foster, D.K. and Inglett, P.W., 2019. Subsurface transport and potential risk of phosphorus to groundwater across different land uses in a karst springs basin, Florida, USA. Geoderma, 338, 97-106. https://doi.org/10.1016/j.geoderma.2018.11.005

Liu, A., Egodawatta, P., Guan, Y. and Goonetilleke, A., 2013. Influence of rainfall and catchment characteristics on urban stormwater quality. Science of the Total Environment, 444, 255-262. https://doi.org/10.1016/j.scitotenv.2012.11.053

Liu, Y., Engel, B.A., Flanagan, D.C., Gitau, M.W., McMillan, S.K., Chaubey, I., 2017. A review on effectiveness of best management practices in improving hydrology and water quality: needs and opportunities. Science of the Total Environment. 601, 580-593. https://doi.org/10.1016/j.scitotenv.2017.05.212

Loch, R.J., 2000. Effects of vegetation cover on runoff and erosion under simulated rain and overland flow on a rehabilitated site on the Meandu Mine, Tarong, Queensland. Soil Research 38(2), 299-312. https://doi.org/10.1071/SR99030

Mallin, M.A., Johnson, V.L., Ensign, S.H., 2009. Comparative impacts of stormwater runoff on water quality of an urban, a suburban, and a rural stream. Environmental Monitoring and Assessment 159(1), 475-491. https://doi.org/10.1007/s10661-008-0644-4

Martinez-Mena, M., Albaladejo, J., Castillo, V.M., 1998. Factors influencing surface runoff generation in a Mediterranean semi-arid environment: Chicamo watershed, SE Spain. Hydrological processes 12(5), 741-754. https://doi.org/10.1002/(SICI)1099-1085(19980430)12:5%3C741::AID-HYP622%3E3.0.CO;2-F

McKenzie, E.R., Money, J.E., Green, P.G., Young, T.M., 2009. Metals associated with stormwater-relevant brake and tire samples. Science of the total environment 407(22), 5855-5860. https://doi.org/10.1016/j.scitotenv.2009.07.018

Miguntanna, N.P., 2009. Nutrients build-up and wash-off processes in urban land uses (Doctoral dissertation, Queensland University of Technology).

Moore H, Beck B. 2018. Karst Terrane and Transportation Issues. In, R. A. Meyers (ed.), Encyclopedia of Sustainability Science and Technology, p.1-33, https://doi.org/10.1007/978-1-4939-2493-6_206-4.

Oms, M.T., Cerda, A., Cerda, T., 2000. Analysis of nitrates and nitrites. In: Nollet, L.M.L. (Ed.), Handbook of Water Analysis. Marcel Dekker, Inc., New York, USA.

Paerl, H.W., 1997. Coastal eutrophication and harmful algal blooms: Importance of atmospheric deposition and groundwater as "new" nitrogen and other nutrient sources. Limnology and oceanography, 42(5part2), 1154-1165. https://doi.org/10.4319/lo.1997.42.5_part_2.1154

Pappas, E.A., Smith, D.R., Huang, C., Shuster, W.D., Bonta, J.V., 2008. Impervious surface impacts to runoff and sediment discharge under laboratory rainfall simulation. Catena 72(1), 146-152. https://doi.org/10.1016/j.catena.2007.05.001

Phelps, G.G., 2004. Chemistry of ground water in the Silver Springs Basin, Florida, with an emphasis on nitrate. US Department of Interior, US Geological Survey, 54 p.

Phelps, G.G., Walsh, S.J., Gerwig, R.M. and Tate, W.B., 2006. Characterization of the Hydrology, Water Chemistry, and Aquatic Communities of Selected Springs in the St. Johns River Water Management District, Florida, 2004: U.S. Geological Survey Open-File Report 2006-1107, 51 p. https://doi.org/10.3133/ofr20061107

Pitt, R., Clark, S., Field, R., 1999. Groundwater contamination potential from stormwater infiltration practices. Urban Water 1(3), 217-236. https://doi.org/10.1016/S1462-0758(99)00014-X

Römkens, M.J.M. Prasad, S.N., 2006. Rain infiltration into swelling/shrinking/cracking soils. Agricultural water management 86(1-2), 196-205. https://doi.org/10.1016/j.agwat.2006.07.012

Rosenau JC, Faulkner GL, Hendry Jr, CW Hull, RW. 1977. Springs of Florida. Florida Department of Natural Resources, Bureau of Geology, Bulletin 31, 461. https://pubs.er.usgs.gov/publication/70039549

Samek, K., 2004. Unknown quantity: the bottled water industry and Florida's springs. Journal of Land Use & Environmental Law, 19(2), 569-595. https://ir.law.fsu.edu/jluel/vol19/iss2/16

Sansalone, J.J. and Buchberger, S.G., 1997. Partitioning and first flush of metals in urban roadway storm water. Journal of Environmental Engineering, 123(2), 134-143. https://doi.org/10.1061/(ASCE)0733-9372(1997)123:2(134)

Stagge, J.H., Davis, A.P., Jamil, E., Kim, H., 2012. Performance of grass swales for improving water quality from highway runoff. Water research, 46(20), 6731-6742. https://doi.org/10.1016/j.watres.2012.02.037

Stahre, P., Urbonas, B., 1990. Stormwater detention: for drainage, water quality, and CSO management. Prentice Hall. 338 p.

Stephenson, J.B., Zhou, W.F., Beck, B.F. and Green, T.S., 1999. Highway stormwater runoff in karst areas—preliminary results of baseline monitoring and design of a treatment system for a sinkhole in Knoxville, Tennessee. Engineering Geology, 52(1-2), 51-59. https://doi.org/10.1016/S0013-7952(98)00054-4

Stevanović, Z., 2019. Karst waters in potable water supply: a global scale overview. Environmental Earth Sciences, 78(23), 1-12. https://doi.org/10.1007/s12665-019-8670-9

Strock, J.S., Kleinman, P.J., King, K.W., Delgado, J.A., 2010. Drainage water management for water quality protection. Journal of soil and water conservation 65(6), 131-136. https://doi.org/10.2489/jswc.65.6.131A

Suthar, S., Bishnoi, P., Singh, S., Mutiyar, P.K., Nema, A.K., Patil, N.S., 2009. Nitrate contamination in groundwater of some rural areas of Rajasthan, India. Journal of Hazardous Materials 171(1), 189-199. https://doi.org/10.1016/j.jhazmat.2009.05.111

Taylor, G.D., Fletcher, T.D., Wong, T.H., Breen, P.F. and Duncan, H.P., 2005. Nitrogen composition in urban runoff—implications for stormwater management. Water Research, 39(10), 1982-1989. https://doi.org/10.1016/j.watres.2005.03.022

Tarboton, D.G., 2003. Rainfall-runoff processes. Online Workbook Published by the Utah State University. Logan, UT, USA.

Thompson, S.E., Katul, G.G., Porporato, A., 2010. Role of microtopography in rainfall-runoff partitioning: An analysis using idealized geometry. Water Resources Research, 46(7). https://doi.org/10.1029/2009WR008835

Trenouth, W.R. and Gharabaghi, B., 2016. Highway runoff quality models for the protection of environmentally sensitive areas. Journal of Hydrology, 542, 143-155. https://doi.org/10.1016/j.jhydrol.2016.08.058

Qin, Y., 2020. Urban flooding mitigation techniques: A systematic review and future studies. Water, 12(12), 3579. https://doi.org/10.3390/w12123579

Vahabi, J., Ghafouri, M., 2009. Determination of runoff threshold using rainfall simulator in the southern Alborz range foothill-Iran. Research Journal of Environmental Sciences 3(2), 193-201. DOI : 10.3923/rjes.2009.193.201

Wang, S., Zhao, M., Xing, J., Wu, Y., Zhou, Y., Lei, Y., He, K., Fu, L. and Hao, J., 2010. Quantifying the air pollutants emission reduction during the 2008 Olympic Games in Beijing. Environmental Science & Technology, 44(7), 2490-2496. https://doi.org/10.1021/es9028167

Wanielista, M., Yousel, Y., 1993. Stormwater Management. John Wiley and Sons, Inc., New York, NY, U.S.A., 579 p.

Wen, D., Valencia, A., Lustosa, E., Ordonez, D., Shokri, M., Gao, Y., Rice, N., Kibler, K., Chang, N.B. and Wanielista, M.P., 2020. Evaluation of Green Sorption Media Blanket Filters for Nitrogen Removal in a Stormwater Retention Basin at Varying Groundwater Conditions in a Karst Environment. Science of The Total Environment, p.134826. https://doi.org/10.1016/j.scitotenv.2019.134826

Winston, R.J., Hunt, W.F., 2016. Characterizing runoff from roads: Particle size distributions, nutrients, and gross solids. Journal of Environmental Engineering. 143(1), 04016074. https://doi.org/10.1061/(ASCE)EE.1943-7870.0001148

Winston, R.J., Hunt, W.F., Kennedy, S.G., Wright, J.D. Lauffer, M.S., 2011. Field evaluation of storm-water control measures for highway runoff treatment. Journal of Environmental Engineering 138(1), 101-111. https://doi.org/10.1061/(ASCE)EE.1943-7870.0000454

Yang, Y.Y., and Toor, G.S., 2017. Sources and mechanisms of nitrate and orthophosphate transport in urban stormwater runoff from residential catchments. Water Research, 112, 176-184. https://doi.org/10.1016/j.watres.2017.01.039

Yu, C., Duan, P., Yu, Z., Gao, B., 2019. Experimental and model investigations of vegetative filter strips for contaminant removal: A review. Ecological Engineering, 126, 25-36. https://doi.org/10.1016/j.ecoleng.2018.10.020

Zhao, S., Liu, S., Hou, X., Cheng, F., Wu, X., Dong, S. and Beazley, R., 2018. Temporal dynamics of SO_2 and NO_x pollution and contributions of driving forces in urban areas in China. Environmental Pollution, 242, 239-248. https://doi.org/10.1016/j.envpol.2018.06.085

CHAPTER 2 HYDRAULIC AND NUTRIENT REMOVAL PERFORMANCE OF VEGETATED FILTER STRIPS WITH ENGINEERED INFILTRATION MEDIA FOR TREATMENT OF ROADWAY RUNOFF

2.1 Preface

This chapter describes the application and efficacy of including engineered infiltration media as a subgrade to enhance nutrient removal within the configuration of VFS in road shoulders. The contents of this chapter have been submitted for publication to the Journal of Environmental Management[1] and are currently under revision.

2.2 Abstract

As a new strategy for treating excess nutrients in roadway runoff, a self-filtering roadway could be accomplished by including engineered infiltration media within a vegetated filter strip (VFS) located in the roadway shoulder. However, nutrient removal performance will depend on the design to effectively infiltrate roadway runoff and the capacity of subsurface media to sequester or remove nutrients from infiltrated runoff. The objective of this study is to test hydraulic and nutrient removal performance of a roadside VFS over varied rainfall-runoff event sizes and filter widths. Two identical 1:1 scale physical models of roadway shoulders and embankments, one containing engineered media (Treatment model) and the other without (Control model), were tested with simulated rainfall and runoff from 1- and 2-lane roadways. Overall, 32 paired hydraulic experiments and 28 paired nutrient removal experiments were completed to assess performance

[1] Shokri, M; Kibler, K.M., Hagglund, C, Corrado, A; Wang, D; Beazley, M; Wanielista, M., under-revision. Hydraulic and nutrient removal performance of vegetated filter strips with engineered infiltration media for treatment of roadway runoff. Journal of Environmental Management

across frequent and extreme rainfall-runoff events. The results indicate that scalability of performance with filter width varied by parameter. Runoff generation scaled predictably with filter width, as runoff generated close to the pavement and total infiltration increased with filter length. A 6 m-wide VFS containing the engineered media infiltrated all rainfall-runoff except during the most extreme storm events (one-hour storms of 76.2 mm and 50.8 mm), where respectively 35% and 22% of rainfall-runoff did not infiltrate and left the system as surface runoff. A majority of phosphorus was retained within a 1.5 m filter while nitrate removal was not observed until 6 m. The Treatment model strongly outperformed the Control model with respect to nitrate (arithmetic mean ± standard deviation of 94±6% reduction vs. 23±64% increase, $p < .001$) and total nitrogen removal (80±5% vs. 38±23% reduction, $p < .001$) due to higher rates of microbially-mediated denitrification in the Treatment model. The two models performed comparably with regard to phosphorus reduction (84±9% vs. 82±12% reduction). A minimum 6 m filter width is recommended to ensure sufficient infiltration of runoff and nitrogen removal. Results of this study address uncertainty regarding nutrient removal performance of VFS in urban runoff applications and highlight a potential strategy for standardizing VFS performance across varied soil properties by including engineered media within the filter.

Keywords: Vegetated filter strips, roadway runoff, nutrients, non-point source pollution, stormwater BMPs, engineered media

2.3 Introduction

Urbanization often has adverse effects to quantity and quality of water resources by generating more runoff, reducing groundwater recharge, and streamlining pathways of pollutants to water

bodies (Tedoldi et al. 2016; Chen et al. 2017; Fardel et al. 2020). Roadway runoff is a widespread non-point source of contaminants such as excess nutrients, heavy metals, sediments, toxic substances, and pesticides (Hu et al. 2020; Jeong et al. 2020). Excess nutrients can cause water quality degradation, eutrophication, and loss of biodiversity in receiving water bodies (Kayhanian et al. 2012; Trenouth and Gharabaghi, 2016; Liu et al. 2017; Chen et al. 2020). As a response, best management practices (BMPs) have been developed to reduce concentrations of pollutants in urban runoff, including excess nitrogen and phosphorus, before discharge to a receiving waterbody (Marsalek and Chocat, 2002; Clary et al. 2011; Li, 2015; Winston et al. 2019). Vegetated filter strips (VFS), also called buffer strips or grass strips (Lauvernet and Helbert, 2020), are BMPs applied to intercept and infiltrate runoff at the source and mitigate non-point source pollutants (Bhattarai et al. 2009; Yu et al. 2019). Despite wide implementation, variability in effectiveness of VFS is reported which may be attributed to variability in site-specific conditions (e.g. soil texture, precipitation and runoff generation processes) and seasonal variation (e.g. antecedent moisture) (Bhattarai et al. 2009; Stagge et al. 2012; Liu et al. 2017; Boger et al. 2018; Ekka et al. 2021). However, design failures have also been noted, including inappropriate scale and structure of design (e.g. width, slope, vegetation type and density), inadequate maintenance leading to performance degradation over time and accumulation of pollutants (Barrett et al. 1998; Barrett et al. 2004; Bhattarai et al. 2009; Koch et al. 2015; Liu et al. 2017; Yu et al. 2019).

VFS have been developed and tested in agricultural applications (Dillaha et al. 1989; Chaubey et al. 1994; Lim et al. 1998) and most rigorous research has focused on sediment transport processes (Meyer et al. 1995; Muñoz-Carpena et al. 1999; Abu-Zreig et al. 2001; Leguédois et al. 2008; Pan et al. 2017). However, VFS have more recently been proposed as an urban stormwater

solution, with the specific application of treating excess nutrients in roadway runoff (Winston et al. 2012; Stagge et al. 2012; Boger et al. 2018). To ensure adequate VFS performance for treating nutrients in roadway runoff, specific design criteria targeted to the urban roadway application should be based on reliable data regarding benefits to water quality, which require empirical experiments (Gavrić et al. 2019).

VFS nutrient removal performance within the right-of-way will depend on two processes: 1) the hydraulic performance of VFS to effectively infiltrate inflow runoff (Davis et al. 2012; Zhao et al. 2016; Rivers et al. 2021), and 2) the capacity of vegetation and subsurface media to effectively sequester or remove nutrients from infiltrated runoff (Boger et al. 2018; Gavrić et al. 2019). Vegetation morphology, density (cover), and canopy height provide first-order control to runoff and infiltration patterns. Hydraulic resistance tends to increase with vegetation cover and density (Spaan et al. 2005) as drag interaction with vegetation converts a portion of kinetic energy, causing flow velocity to decrease (Kibler et al. 2019). Greater infiltration rates within vegetation are a product of decrease in runoff velocity (Jin and Römkens, 2001; Zhao et al. 2016) and biologically-mediated changes to soil structure (Jones, 1971; Garcia de la Serrana Lozano, 2017; Gavrić et al. 2019). VFS hydraulic design requires understanding how climate, runoff generation and infiltration intersect at the site to optimize filter sizing. Larger rainfall events may form substantial runoff volumes that do not infiltrate entirely within the filter and therefore bypass the BMP as surface flow (Davis et al. 2012). Such bypass surface flows would not be fully treated within the BMP and can reach the receiving water body directly (Boger et al. 2018). Consequently, BMP design typically recommends capturing at least 70 to 90% of the annual runoff volume based on local relative frequency analysis of rainfall events (Roesner et al. 2011; Borris et al. 2014). The

design of the roadway VFS should be directed to the event sizes most likely to deliver the greatest pollutant loads. For instance, high-frequency (i.e. low magnitude) rainfall events may carry a substantial amount of the total annual pollutant loads to roadside shoulders (Dudley et al. 2001; Pappas et al. 2008).

There is a persistent uncertainty regarding nutrient removal effectiveness of VFS, especially for roadside applications (Boger et al. 2018; Gavrić et al. 2019; Hager et al. 2019). A review on this topic conducted by Hager et al. [2019] indicated high variation in removal of total nitrogen (TN, -26 to 69%), nitrate (NO_x-N, -25 to 71%), and total phosphorus (TP, -42 to 56%) from urban stormwater runoff by roadside VFSs. Another review (Boger et al. 2018) similarly concluded a broad range of performance in removals of TN (-26 to 86%), NO_3-N (-25 to 89%), and TP (-218 to 99%) from roadway runoff in roadside VFS and grassed swales. Both nitrate removal and generation within VFS are reported by Stagge et al. [2012], and VFS in California were found to have little to no effect in nitrogen and phosphorus removal from roadway runoff (Barrett et al. 2004). Such wide performance variations, including observations of negative removal (i.e. nutrient generation) are attributed to variation among soil properties, rainfall-runoff events, antecedent soil moisture, roadside condition (e.g. slope, filter width, vegetation type and density, and maintenance), and site history (e.g. nitrate retention from earlier smaller storm events) (Boger et al. 2018; Stagge et al. 2012).

The inconsistent performance of VFS regarding nutrient retention or removal as reported in the literature suggests the need for new strategies to enhance nutrient removal within the road shoulder. Soil type and its conductivity, slope, filter size, vegetation type, and vegetation cover are recognized as the main driving factors controlling water quality parameters through a VFS (Stagge

et al. 2012; Boger et al. 2018; Hager et al. 2019). However, roadway shoulders often are strictly managed in terms of soil type, compaction and surface slope, as well as vegetation type and maintenance (e.g. Florida Department of Transportation, 2018), thus roadway designs occupy a narrower set of boundary conditions that may influence performance as compared to agricultural or forestry VFS applications. Typical space limitations within road shoulders can also bound filter size. Including media that has been engineered to enhance both infiltration and nutrient removal as a filter in the subsurface of a roadway VFS may standardize and improve hydraulic and nutrient removal performance as a new strategy. For instance, bio-sorption activated media (BAM, BOLD & GOLD^{TM}) is an engineered porous media that has been developed for use in stormwater BMPs (O'Reilly et al. 2012; Wanielista et al. 2014; Wen et al. 2020b). Defined by specific ratios of sand, aluminum clays, and tire crumb, BAM is designed to promote drainage while enhancing nitrogen removal via denitrification within media biofilms and phosphorus retention via sorption to media components (O'Reilly et al. 2012). Laboratory column testing and batch studies of BAM (e.g. Chang et al. 2018a and b; Wen et al. 2018; Chang et al. 2019) suggest promising remediation of nutrients under varied physicochemical and biological conditions. However, the application of BAM or other engineered media within a VFS for the purpose of treating roadway runoff has not been studied. This novel engineering approach requires testing and validation to justify potential investments and inform design. For instance, understanding how nutrient transformation mechanisms within engineered media compare to native soils or scale with flowpath length and retention time within a VFS can inform the filter design that should be implemented for roadway applications.

The objective of this research is to test the application and efficacy of including engineered infiltration media as a subgrade to enhance nutrient removal within the configuration of road shoulders. For this purpose, we inspected 1) hydraulic and nutrient removal effectiveness of VFS equipped with engineered infiltration media when applied to shoulders of 1- and 2-lane roadways over varied rainfall-runoff event sizes, and 2) the appropriate scale of VFS filter width and certainty of performance for treating contaminated roadway runoff. Two identical 1:1 scale physical models of roadway shoulders and embankments were constructed, one containing engineered media (Treatment model) and the other without engineered media (Control model). The models were tested with identical simulated rainfall and runoff from 1- and 2-lane roadways. The hydraulic and nutrient removal performance of the Treatment VFS is compared to that of the Control, testing the hypothesis that infiltration and nutrient removal within the VFS containing engineered media exceeds that observed in the Control model. This is the first study to test infiltration and nutrient removal in a roadway VFS using engineered media, and novel experimental procedures were developed. Results can therefore provide important information on effectiveness of VFS and the design criteria to apply such BMPs in urbanized areas.

2.4 Materials and Methods

2.4.1 Study area

Two physical models (Treatment and Control) were constructed at 1:1 field scale to simulate 2.4 m lengths of roadways extending to a 9.0 m width along the roadway shoulder and embankment (Figure 2 and Figure 3). Water was able to drain freely from the bottom of the 1-m deep models, simulating infinite depth to the groundwater table such that any surface runoff generated was by

definition Hortonian (infiltration excess) overland flow (Woolhiser and Goodrich, 1988). The models were constructed in Orlando, Florida, at an outdoor research facility at the University of Central Florida (Figure 3). Central Florida has a humid subtropical climate. Much of the annual rainfall (mean 1300 mm) is delivered during the humid, warm season (May to October, mean high temperature of about 33 °C) while the rest of the year is mild and drier (mean low temperature of about 9 °C, Harper and Baker, 2007; NOAA, 2017). Warm water bodies around the state of Florida (e.g. Gulf of Mexico and Atlantic Ocean) are the main sources of natural precipitation (NOAA, 2017), which can be delivered in high-intensity bursts up to 94 mm/hr.

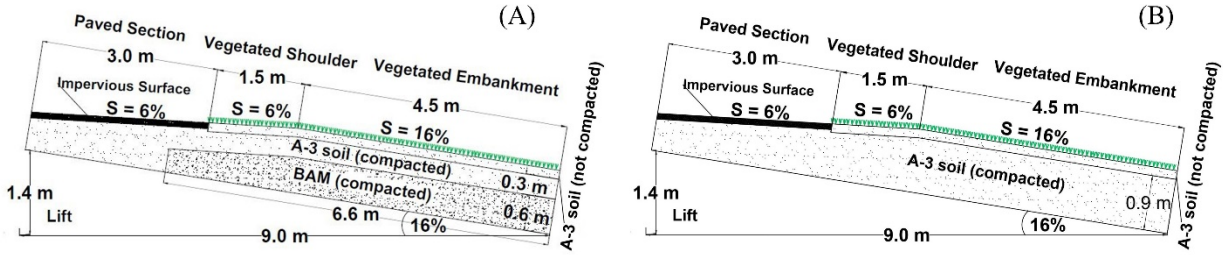

Figure 2. Physical models of roadside VFS containing (A) engineered media (Treatment) and (B) soil (Control).

Figure 3. Model construction and dimensions (A), filling with the media (B), compaction (C), final design with established vegetation (D), and hoisted calibrated rainfall simulator (E).

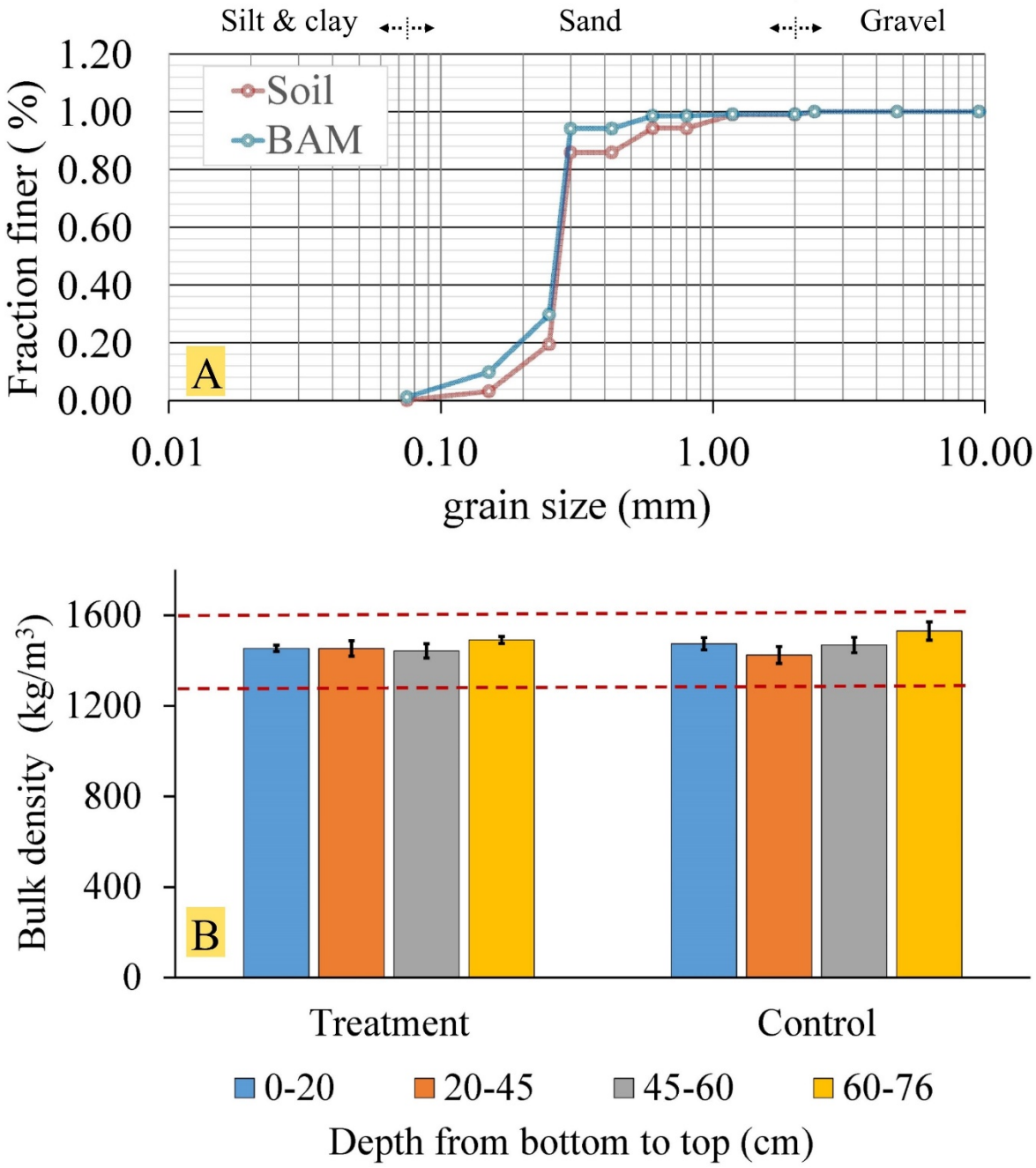

Figure 4. Particle size distributions of soil and BAM (A) and mean bulk density across depths of Treatment and Control models (B). Note: the red dashed lines in (B) indicate the range of standard compaction for roadside media specified in Florida.

2.5 Model design and construction

Two road shoulder models were constructed identically, following standard cross-section specifications for 1- and 2-lane roadways in Florida (Florida Department of Transportation, 2012). The only difference in the models was that the Treatment model contained a 0.6 m layer of engineered media (CTS BOLD & GOLD^{TM} BAM, by volume 85% sand, 10% tire crumb, and 5% clay). The engineered media filter was overlain by a 0.3 m layer of a locally-sourced sandy topsoil, including microbial community. The sandy topsoil (classified as sand by USDA textural classification) is typical of Central Florida topsoils (Figure 2). The Control model bed was filled to 0.9 m depth with the same sandy topsoil. Based on AASHTO classifications, both BAM and the topsoil were classified as A-3 soil type, characterized as a mixture of poorly-graded fine sands and a low percent of coarse sands and gravel (AASHTO, 2008). Particle size distributions determined for triplicate samples of BAM and soil using dry and wet sieve analyses (method ASTM C136/C136M-19) indicated similarity in particle size classes (Figure 4), with distributional differences by mass mainly occurring within the range of 160-420 μm. However, BAM contained a substantial volume of tire crumb in sizes larger than 250 μm, much in range of 1.18 to 2 mm (very coarse sand) which was not well represented in the mass analysis due to the lower particle density. All media were compacted to within the range of standard bulk density required for roadway shoulders in Florida (1280 to 1600 kg/m^3, FDOT Standard Specification, 2018), with the exception of the top 0.15 m to allow vegetation establishment (Figure 3). A 3.0 m impervious surface (6% slope) was poured at the upstream of each model to simulate a portion of the roadway and the paved shoulder (Figure 3). From the edge of the pavement, a 1.5 m vegetated shoulder (6% slope) was followed by 4.5 m of vegetated embankment (16.6% slope). The roadway shoulder and

embankment areas of both models were cultivated with *Paspalum notatum* Flüggé (Bahiagrass), a grass species commonly found along on roadways in Florida, using a standard seeding rate for vegetated roadside shoulders (Ferrell et al. 2012; Wasowska, 2014) (Figure 3 D). Bahiagrass vegetation was cultivated from seed over a period of 9 months to ensure a mature vegetative canopy and to allow development of microbial communities under similar conditions within the models before testing began. No fertilizers or chemicals were applied. Rainfall was simulated using a calibrated rainfall simulator (Figure 3 E) while roadway runoff was introduced upstream as a sheet flow dispersed over the concrete (Figure 5 A).

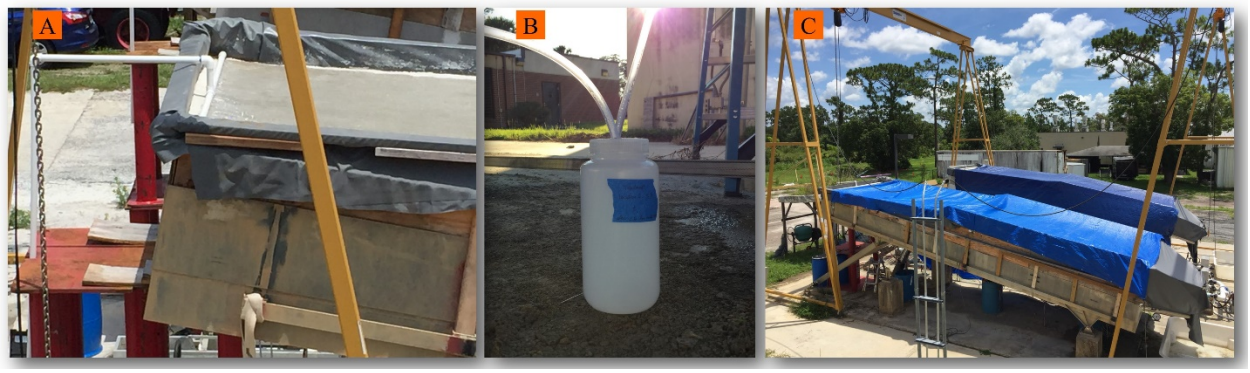

Figure 5. Roadway runoff delivered as sheet flow over pavement (A), collection of infiltrate samples (B), and models covered with waterproof tarpaulin to exclude natural rainfall (C).

2.6 Experimental procedure

Overall, 32 hydraulic experiments and 28 nutrient removal experiments were performed to test hydraulic and nutrient removal performance of the BAM VFS as compared to the Control model (Table 1). Each experiment consisted of identical testing in Treatment and Control models, and each tested design storm was replicated to simulate runoff from both 1- and 2-lane roadways. Parameters of design hyetographs (rainfall depth, duration, and pattern) were selected based on

frequency analysis of long-term (1984 - 2013) 15-min rainfall data gauged in north-central Florida (NOAA, 2017). Precipitation events were defined as periods of continuous precipitation separated by at least three hours (Harper and Baker, 2007). Events were categorized based on cumulative storm depth in order to calculate relative frequency of occurrence and return period. A second relative frequency analysis was completed considering rainfall duration within each categorized rainfall depth to detect the most frequent duration of events based on size. Finally, the most frequent within-event pattern was detected among storm depth-duration combinations, which was used to design storm hyetographs.

Testing under frequently-occurring storm conditions was undertaken to investigate hydraulic and nutrient removal performance during rainfall events likely to produce high cumulative loadings of nutrients to receiving water bodies (Table 1). Hydraulic performance was also tested under high-intensity rainfall conditions to indicate the maximum 1-hour storm intensities under which runoff was infiltrated. Partitioning of volumetric inflows (Q_{in}, consisting of precipitation and roadway runoff) into infiltrated water (Q_{inf}) and surface runoff (Q_{RO}) was accomplished using a water mass balance as Eq. 1.

$$Q_{in} = Q_{inf} + Q_{RO} + Q_E \quad (1)$$

where Q_{in} and Q_{RO} were measured and evapotranspiration (Q_E) was considered negligible at event scale. The length of overland flow over the vegetated section was measured from the pavement edge.

Table 1. Design rainfall-runoff events for hydraulic and nutrient removal experiments. Each was completed for both 1- and 2-lane roadways.

Experiment and event type		Cumulative rainfall depth (mm)	Duration (h)	Mean intensity (mm/h)	Return period (day or year)
Hydraulic experiments	Frequently-occurring storms	12.7	0.5	25.4	71 (d)
		19.1	0.75	25.4	114 (d)
		25.4	0.75	33.0	1.2 (y)
		38.1	3.75	10.16	2.6 (y)
	High-intensity testing	25.4	1.00	25.4	1.0 (y)
		38.1	1.00	38.1	7.0 (y)
		50.8	1.00	50.8	7.7 (y)
		76.2	1.00	76.2	62.5 (y)
Nutrient removal experiments		12.7	0.5	25.4	71 (d)
		19.1	0.75	25.4	114 (d)
		25.4	0.75	33.0	1.2 (y)
		25.4	0.75	33.0	1.2 (y)
		25.4	0.75	33.0	1.2 (y)
		38.1	3.75	10.16	2.6 (y)
		76.2	1.75	43.5	100 (y)

Runoff nutrient loads of nitrate, ammonia (NH_3-N), TN, and TP were designed based on review of literature citing event mean concentrations (EMC) of each constituent in roadway runoff (Table 2; Driscoll et al., 1990; Thomson et al., 1997; Barrett et al., 2004; Kayhanian et al., 2007; Harper and Baker, 2007; Winston et al. 2012; Winston and Hunt, 2016, Kibler et al., 2020), where EMC is defined as the mass per unit runoff volume (Sansalone and Buchberger, 1997). City tap water

was used for all experiments and its background nutrient concentrations were measured (Table 2). Standard solutions (Hach Company) of 1000 mg/L of nitrate (NO_3-N), ammonia, and phosphorus (as potassium phosphate) were added to base concentrations found in city water to achieve the target concentrations of nitrate, ammonia, and TP, respectively. Following the method applied by Caruso (2014), glycine ($C_2H_5NO_2$, 99% reagent) was used to create a stock solution of 1000 mg/L as an organic nitrogen source to bring TN concentrations in the mixed runoff solution into the target range (Table 2). The stock solutions were freshly prepared before each experiment. The ratio of nitrate:ammonia and TN:TP in the produced runoff were 5.3 to 1 and 8.3 to 1, respectively.

Table 2. Mean and range of reported roadway runoff nutrient loads as event mean concentrations (EMC) in Florida, Minnesota, California, and North Carolina and measured nutrient concentrations in tap water used in this study. Data are in (µg/L).

Nutrient species	NO_x-N	NH_3-N	TN	TP
Road runoff mean EMC	580	110	1750	210
Road runoff range of variation	230 – 1320	70 – 150	680 – 3200	70 – 560
UCF tap water	9 ± 2	2 ± 0	74 ± 4	100 ± 2

Each experiment was completed on Treatment and Control models on the same day, or in the case of long event durations, on consecutive days. Changes in water quality parameters were detected considering variation in time and location along the filter width. Runoff samples (1000 mL) were collected directly into plastic sampling bottles and samples of stormwater infiltrate (1000 mL) were collected in bottles from the bottoms of the models (Figure 5 B). Four hours after the start of rainfall-runoff, samples of infiltrate were taken along the filter at distances of 1.5 m, 3.0 m, and 6.0 m from the edge of pavement (Figure 2). Additional infiltrate samples were collected at the 6.0 m filter width at 20 hours from the start of the experiments, to assess the impact

of longer contact time with media. Dissolved oxygen (DO) and temperature were measured in triplicate samples directly after sampling. A YSI Pro 20i DO/Temperature meter was calibrated to the local DO saturation and then stirred into three 150 mL samples from each time/location. Specific conductivity (SC) and pH of water samples were also measured in triplicate within 24 hours of collection using a calibrated YSI Pro 1030 pH/ORP/conductivity/Temperature instrument. The SC and pH probes were calibrated before each use in standard calibration solutions (1413 and 10,000 µmoh/cm for SC and pH 4, 7, and 10 buffer solutions). The probes were washed with distilled water between each measurement. Using measured DO, water temperature, SC, and local air pressure, percent saturation of DO was calculated (Rounds et al. 2013).

After collection, 1000 mL samples were prepared for nutrient concentration testing. Samples were divided into three 60 mL bottles and three 100 ml bottles. Samples in the 60 mL bottles were preserved with H_2SO_4 until pH < 2. Samples were kept cool (T < 5°C) and delivered to a certified lab (Environmental Research & Design, Orlando, Florida) within 24 hours of collection. The samples were analyzed within 48 hours for ammonia, TN, and TP (preserved) and nitrate (filtered through 0.45 micron) concentrations. The species were determined through standard methods of NH_3-N (SM-22, Sec. 4500-NH_3 G, minimum detection limit (MDL) 10 µg/L), TN (SM-22, Sec4500-NC, MDL 25 µg/L), TP (SM-22, Sec. 4500 P F, MDL 1 µg/L), and NO_x-N (SM-22 Sec. 4500-NO_x F, MDL 2 µg/L). All nitrogen species were reported as µg/L N, to allow for comparison to TN. Percent nutrient removal was calculated at the sampling locations for each species considering the ratio of difference between nutrient concertation in runoff and infiltrate water to the runoff concentration times 100 (Strecker et al. 2001; Koch et al. 2015). Nutrient removal efficacy was then determined by calculating arithmetic mean and standard deviation of the

calculated percent removals considering all conducted 1- and 2-lane roadway experiments. Statistical analyses of independent-sample t-test (95% confidence intervals) were completed using SPSS for nutrient species and water chemistry parameters to test the significance of performance differences between the two models (Blanco-Canqui et al. 2004; Franco and Matamoros, 2016).

To ensure independence of experiments, at the conclusion of each test, all surfaces, vegetation, soils, and media of the models were flushed with at least 2000 L of water (approximately 40% of available pore volume). Flushing was completed exactly 90 hours before the start of each experiment, providing identical drainage time to ensure similar soil water content and dry vegetation at the start of each experiment. The models were covered when needed to exclude natural precipitation (Figure 5 C). The vegetation canopy height was maintained before each experiment (Ferrell et al. 2012) and vegetation density was monitored regularly *in situ* within 30 by 30 cm quadrats in seven randomly-selected locations of each model. Vegetation monitoring suggested that vegetation density was similar between the two models over the period of experimentation (Appendix A, Figure A.1).

2.7 Results and discussion

2.7.1 VFS hydraulic performance

As storms progressed, overland flow initially generated where roadway runoff flowed from the pavement to the vegetated section of models. Surface flows usually infiltrated further along the slope, however the length over which overland flow generated increased with storm intensity (Supplementary materials, Table A.1 and A.2) until the entire filter width generated overland flow. During identical storm events, overland flow was consistently generated at greater lengths in the

Treatment system as compared to the Control (Figure 6). Additionally, surface runoff was collected at the downstream of the Treatment model, but never in the Control model.

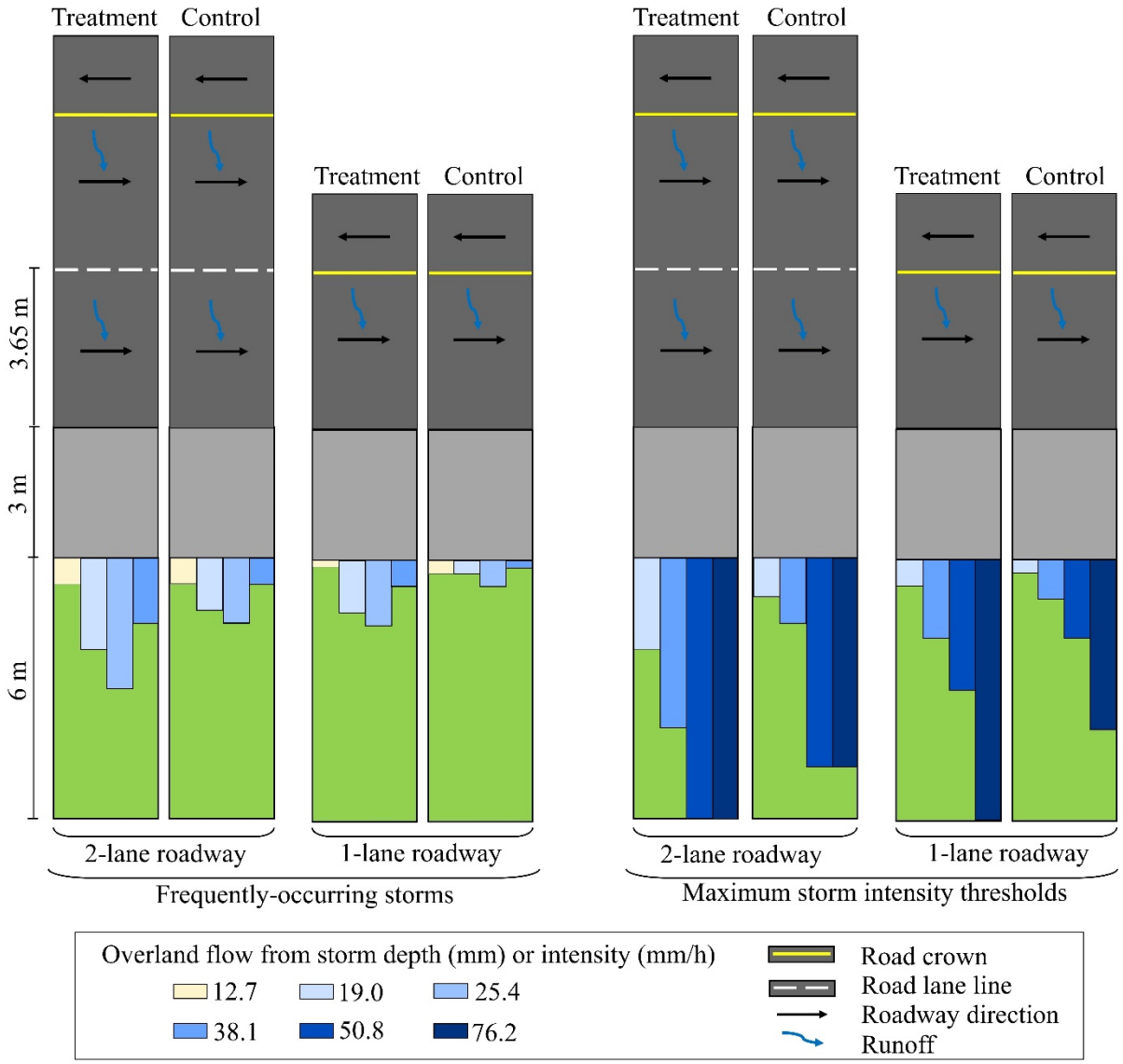

Figure 6. Hydraulic testing: overland flow generation length over Control and Treatment models during 1- and 2-lane simulations under typical and high-intensity storms.

Surface runoff generated to the end of the Treatment model during high rainfall intensities (Figure 6). All surface runoff recorded was generated as Hortonian overland flow, signifying that the infiltration rate into the Treatment model was lower than the water input rate. During 1-lane roadway simulations, surface runoff at the downstream of the Treatment model was recorded only during the highest intensity storm, 76.2 mm/h. Approximately 35% of inflow water did not infiltrate into the filter during this storm and left the Treatment system as Hortonian surface runoff. During simulations of a 2-lane roadway, respectively 22% and 35% of input water ran off as Hortonian flow at the downstream of the Treatment model during storm intensities of 50.8 mm/h and 76.2 mm/h (Figure 6). At an intensity of 50.8 mm/h, surface water runoff generated over the entire 6 m model approximately 30 min from the beginning of storm (Appendix A, Table A.2). This time decreased to about 20 min at the higher storm intensity of 76.2 mm/h.

By comparison, surface runoff was never recorded in the downstream of the Control model. For the same storm intensity, overland flow consistently infiltrated closer to pavement in the Control than the Treatment model (Figure 6). As vegetation density was similar in Treatment and Control models throughout the experiments (respective means of 6130±780 and 7230±1240 grass blades/m^2) (Appendix A, Figure A.1), observed differences in hydraulic performance are not likely attributed to different surface roughness conditions. The generally lower lengths of overland flow in the Control model and lack of Hortonian surface runoff at the downstream of the Control model suggests that infiltration rates through BAM were slightly lower relative to the sandy soil.

Hydraulic performance predictably scaled with filter length, such that more surface runoff was able to infiltrate into longer filter lengths. Despite the slightly lower infiltration rate relative to soils, it is likely that the hydraulic capacity of a 6 m wide VFS with BAM media would provide

infiltration capacity for most storm events, given sufficient depth to the groundwater table. The high-intensity hydraulic testing indicates that infiltration capacity is likely to be exceeded only rarely; for example, a 1-hour storm with mean intensity of 50.8 mm/h would have a recurrence interval in the study areas of about once every 7.7 years (Table 1). Runoff from more frequently-occurring storm events infiltrated completely within the 6 m filter width (Figure 6).

2.7.2 VFS nutrient removal performance

In comparisons of infiltrate to runoff, the Treatment filter strongly outperformed the Control in terms of nitrate and TN removal ($p < .001$, Figure 7, Table 3-Table 4). The most striking difference between Treatment and Control models was related to nitrate removal performance. Nitrate concentrations of infiltrate from the Control model increased relative to runoff concentration at every sampling location and time (Figure 7, Table 3). For instance, when considering mean response over all experiments, nitrate concentrations in Control infiltrate taken 3 m from the pavement increased more than threefold relative to runoff (arithmetic mean ± standard deviation of 220±196%) and remained elevated at 6 m from the pavement (by 23±64% at four hours and by 50±73% after 20 hours) (Table 3). However, in the Treatment model, though nitrate concentrations increased at 1.5 m and 3 m, nitrate had been all but removed from infiltrate by 6 m within four hours (94±6% removal) (Table 3). Conversion from ammonia to nitrate within the first 1.5 m of filter was evident in both Treatment and Control models, as ammonia concentrations decreased by 94±7% and 96±4% respectively (Figure 7 and Table 3-Table 4). The Treatment model also reduced TN more effectively than the Control ($p < .001$, Figure 7, Table 3-Table 4). Similar to nitrate, an increase in TN concentration was observed at 1.5 m in the Treatment

model and at 1.5 m and 3 m in the Control (Figure 7, Table 3). However, TN concentrations decreased in both models by 6 m. At 6 m, TN concentrations were reduced by a mean 80±5% in the Treatment model as compared to 38±23% in the Control (Table 3). With regard to phosphorous reduction, the Treatment and Control models performed similarly, respectively, reducing TP (84±9% vs. 82±12%) consistently within first 1.5 m of filter width (Figure 7 and Table 3-Table 4).

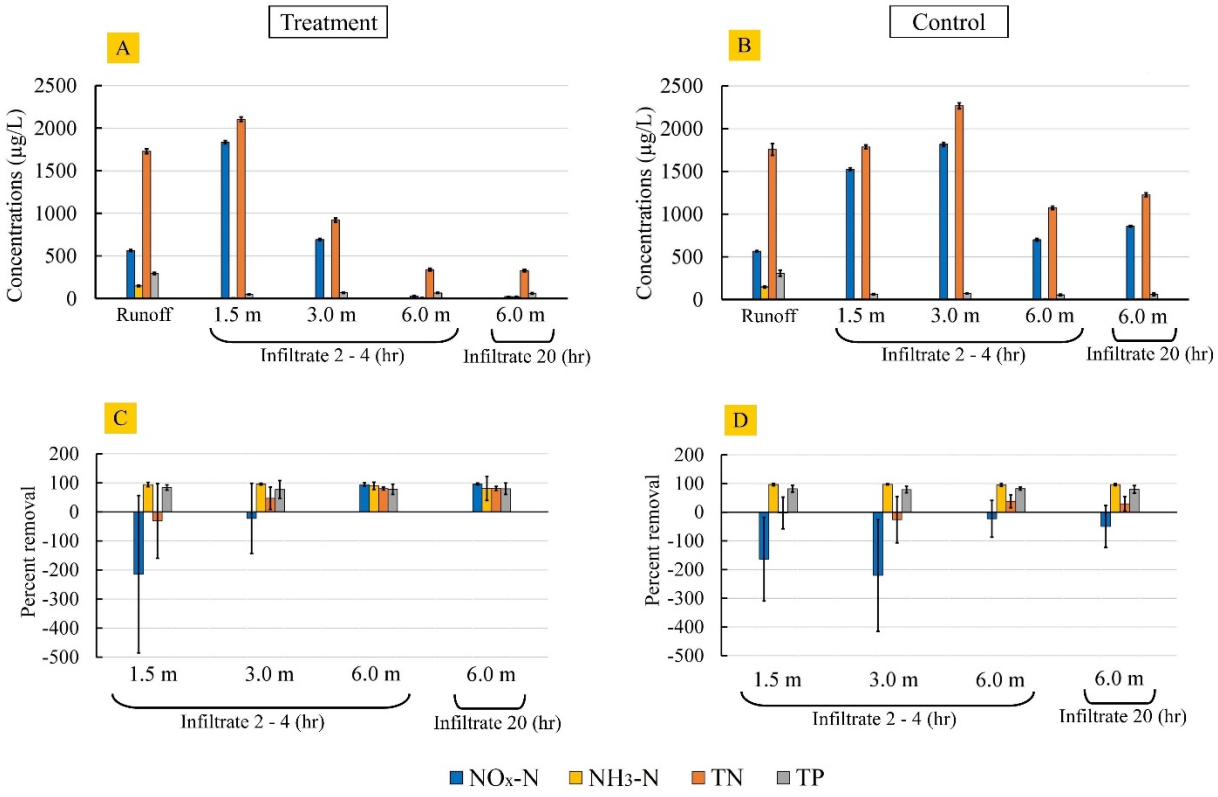

Figure 7. Arithmatic mean ± SD of nutrient concentrations in runoff and infiltrate samples at 1.5 m, 3.0 m, and 6.0 m along the filter width in Treatment (A) and Control (B) models. Mean percent removal ± SD of nutrients in infiltrate with respect to runoff in T(C) and Control (D) models.

Both pH and DO saturation decreased more strongly through the Treatment model than in the Control ($p < .05$, Tables 3-4). The larger drop in DO in the Treatment model indicates that oxygen was consumed at higher rates in the engineered media than in soil, likely through enhanced biological activities that also removed nitrate (O'Reilly et al. 2012; Wen et al. 2020a). Release of carbon dioxide by microbial activity led to carbonic acid production, causing the stronger observed decrease in pH in the Treatment model. Reduction in nitrogen concentrations through the filter can be attributed to conversion from ammonia to nitrate and removal of nitrate through denitrification. The rapid conversion of ammonia to nitrate is the likely mechanism that caused infiltrate ammonia concentrations to decrease at 1.5 m and nitrate concentrations to increase at 1.5 and 3 m, which was observed in both Treatment and Control models. However, denitrification processes varied between the models, with greater microbially-mediated denitrification in the Treatment model producing higher nitrate and TN removal rates. Phosphorus removal from the infiltrate in both models likely occurred via sorption to media particles (Liu et al. 2013; Hood et al. 2013).

Nitrogen removal performance was scaled to filter width. While nitrogen concentration behaviors at 1.5 m and 3 m filter widths varied from test to test, the strong decrease in nitrogen concentrations by 6 m in the Treatment model was highly consistent among experiments. Similar patterns of nutrient removal were observed across experiments of different storm depths, intensities, and roadway types (individual experiment results provided in supplementary materials, Tables A.3 to A.6 and Figures A.2 and A.3). The consistency of nutrient removal observed in the Treatment model across variable runoff events suggests that nutrient removal performance in roadway VFS is perhaps less affected by infiltration depth, but strongly related to subgrade media, filter width, and runoff nutrient concentration (a constant in this study). By contrast, the relatively

high standard deviations around nitrogen concentrations observed in infiltrate from the Control model indicate more variable performance of the local soils as compared to BAM. This is a reflection of the different microbial communities supported respectively by the sandy soils and BAM, potentially related to slight differences in water retention properties of the media. Nitrogen conversion and removal were observed relatively quickly within the biogeochemical conditions of the filter. Little difference in nitrate or TN concentration was seen when comparing samples with maximum stormwater-media contact times of 4 hours to 20 hours (Figure 7 and Table 3). Given the observed increase in nitrate and TN concentrations at 1.5 m and 3 m widths, a minimum VFS filter width of 6 m is recommended to ensure sufficient nutrient reduction performance (Figure 7 and Table 3-Table 4).

Table 3. Arithmetic mean ± standard deviation of water quality parameters and mean percent change relative to runoff.

		NO_x-N (µg/l)		NH_3-N (µg/l)		TN (µg/l)		TP (µg/l)		DO saturation (%)		SC (µS/cm)		pH	
		Treatment	Control	Treatment	Control	Treatment	Control	Treatment	Control	Treatment	Control	Treatment	Control	Treatment	Control
Arithmetic mean ± SD	Runoff	563±10	565±7	149±6	147±10	1729±27	1758±69	295±12	309±36	79±11	80±10	3±0	4±3	8.0±0	8.0±0
	Infiltrate 1.5 m (4hr)	1835±19	1526±17	6±1	4±1	2105±26	1788±22	48±4	63±6	94±7	95±10	4±0	4±3	7.4±0	7.9±0
	Infiltrate 3 m (4hr)	692±14	1816±23	4±1	3±0	919±25	2267±35	69±7	72±4	84±7	95±10	3±0	4±3	7.3±0	7.9±0
	Infiltrate 6 m (4hr)	32±4	700±14	10±1	6±1	339±16	1074±20	66±6	54±10	66±12	88±12	3±0	4±3	7.3±0	7.6±0
	Infiltrate 6 m (20hr)	23±3	859±9	16±11	4±1	329±12	1226±23	61±8	62±17	75±18	98±13	3±1	4±3	7.1±0	7.6±0
Mean percent change	Infiltrate 1.5 m (4hr)	214±271	164±146	-94±7	-96±4	31±129	3±55	-84±9	-82±12	22±17	20±19	1±4	-1±3	-8±1	-1±1
	Infiltrate 3 m (4hr)	22±121	220±196	-96±3	-97±2	-47±38	26±81	-78±31	-79±11	9±17	20±22	-4±9	-3±9	-9±2	-2±2
	Infiltrate 6 m (4hr)	-94±6	23±64	-90±12	-95±5	-80±5	-38±23	-78±18	-82±5	-15±21	10±20	-6±9	-1±4	-9±2	-5±2
	Infiltrate 6 m (20hr)	-96±3	50±73	-81±42	-96±4	-81±7	-29±26	-80±20	-80±13	-3±30	23±18	-15±14	-7±10	-11±3	-5±1

Table 4. Independent-sample *t*-test (95% confidence interval) for performance differences between Treatment and Control models at different sampling locations and times. Bolded and italic values are statistically significant.

		NO_x-N (µg/L)			NH_3-N (µg/L)			TN (µg/L)			TP (µg/L)			DO saturation (%)			SC (µS/cm)			pH		
		t	*df*	*p*	*t*	*df*	*p*	*t*	*df*	*p*	*t*	*df*	*p*	*t*	*df*	*p*	*t*	*df*	*p*	*t*	*df*	*p*
	Runoff	-0.19	26	.851	0.15	25	.884	-0.48	26	.637	-0.73	26	.471	-0.25	22	.803	-0.94	26	.358	1.13	26	.270
Infiltrate	1.5 m(4hr)	0.52	26	.609	0.98	25	.339	0.55	26	.589	-0.70	26	.489	-0.20	20	.845	-0.92	24	.365	-11.08	24	***.000***
	3 m(4hr)	-2.82	26	***.009***	1.37	25	.184	-2.45	26	***.021***	-0.08	26	.940	-3.00	20	***.007***	-0.97	24	.341	-9.25	24	***.000***
	6 m(4hr)	-6.28	26	***.000***	1.33	25	.195	-7.01	26	***.000***	0.76	26	.454	-4.29	22	***.000***	-1.10	26	.280	-5.86	26	***.000***
	6 m(20hr)	-6.70	26	***.000***	1.41	25	.170	-7.69	26	***.000***	0.33	26	.743	-3.53	22	***.002***	-0.18	26	.861	-7.44	26	***.000***

2.7.3 Design guidance for roadway VFS with engineered media

Results of the hydraulic and nutrient removal experiments suggest that road shoulder VFS containing engineered media may be effective BMPs for removing nitrogen from roadway runoff. In this study, the addition of engineered media was more effective than local soils at remediating nitrogen concentrations. While promising, the nitrogen reduction benefits of engineered media concluded in this study are strictly relative to the nutrient reduction performance of the Control soils tested in this experiment. Soil properties (e.g. texture, organic matter content) are naturally spatially heterogeneous and influence the microbial community and transformation of nitrogen through the soil profile. Therefore, nitrogen remediation that can be expected within unaltered soil profiles also varies from place to place. In some places, replacing the unaltered soil profile with a filtration media such as BAM may lead to greater reduction of nitrogen (as observed in this study); in other cases, the natural remediation of the unaltered soil profile may equal or exceed that of engineered media. Further study should be undertaken to understand where amendment of the local soil profile with engineered infiltration media will be likely to result in net improvement to stormwater quality.

High-intensity hydraulic testing confirmed that the capacity of 6 m wide VFS with sandy soil textures and/or BAM are unlikely to be exceeded during typical and even lower-frequency events. Although the infiltration rate through the BAM VFS was slightly lower than the Control sandy soils, the reduction in drainage rates in the BAM filter were not sufficient to produce surface runoff during event sizes that would occur with regularity. Again, given the spatial heterogeneity of soils, it should be understood that these results are partially controlled by the sandy soils tested. While

engineered media will behave similarly from place to place, soils used to overlay engineered media may vary with respect to properties that control drainage. When infiltration is not impeded by a shallow water table (Carluer et al. 2017; Fox et al. 2018), and when soil hydraulic conductivities are similar to those tested, hydraulic capacity is not necessarily a design limitation to nutrient remediation by a roadway shoulder VFS. The experimentation herein simulated areas with a relatively deep (> 1 m) vadose zone, such that surface infiltration into the VFS is not impeded by saturation from below by the groundwater table (Lauvernet and Helbert, 2020). Any surface runoff observed within the vegetated sections of the models in this research was generated as infiltration-excess (Hortonian) overland flow and was not saturation-excess overland flow. Therefore, the outcomes of these experiments cannot necessarily apply to situations when infiltration is impeded by groundwater table. In such situations, partitioning of runoff and infiltration will become site- and event-specific, and thus cannot be tested for generally. Prospective sites for VFS installation should be monitored to determine seasonal depth to the groundwater table. Since the filter cannot treat stormwater that does not infiltrate, calculation of potential annual nutrient removal benefit should consider whether reduced vadose zone capacity will limit stormwater infiltration and thus treatment.

Nitrogen removal observed through the BAM VFS in this study (80% lower TN concentrations in infiltrate as compared to runoff after 6 m of filter width) is similar to results of prior column and batch studies of BAM, which collectively indicate around a 70 to 78% decrease in TN (Chang et al. 2018a; Wen et al. 2018; Chang et al. 2019). Such performance similarity suggests that mechanisms observed in laboratory study of BAM may also apply within a roadway VFS configuration. With respect to TP removal, better performance was observed for the BAM VFS in

this study (84%) in comparison to the swale model (71%) and column experiments (60%) reported by Hood et al. (2013) for simulated highway runoff. In comparison to a VFS in North Carolina for treating nutrients in runoff from a 2-lane roadway (uncompacted fine sandy soil under 5.2% slope and 17.1 m filter width), the BAM VFS performed better with respect to nitrate (94% vs. 49%), TN (80% vs. 62%), and TP (84% vs. 48%) removals (Line and Hunt, 2009).

Nevertheless, further research should consider more detailed DO/redox analyses to better understand mechanisms of nutrient removal/retention or explore effects of variable carbon content or pH in runoff to more thoroughly characterize BAM performance in a VFS configuration. In particular, the observed local increase in nitrogen concentration within the first 3 m of filter from the edge of pavement can be a subject for future detailed research. Considering variable runoff nutrient concentrations and the impact of seasonal variations can also be beneficial.

2.8 Conclusion

This study compared hydraulic and nutrient removal performance of a road shoulder VFS in sandy soils equipped with an engineered media filter to that of an identical Control road shoulder containing only sandy soils. Rainfall-runoff events were simulated for both 1- and 2-lane roadways and across a range of typical and high-intensity events. With respect to nutrient removal, the VFS with engineered media outperformed the Control road shoulder, removing significantly more nitrate (94±6% reduction vs 23±64% increase, $p < .001$) and TN (80±5% vs. 38±23% reduction, $p < .001$) within a 6 m filter width. Changes detected to nitrogen speciation, pH and DO saturation along the length of the filters and through time indicate that rates of microbially-mediated denitrification were greater within the engineered media, leading to the strong nitrate removal

efficiency. Within the conditions of a roadway shoulder and embankment, rapid conversion of ammonia to nitrate within 1.5 m of the pavement was observed in both models, but soils in the Control model were unable to remove the nitrate effectively. Steeper gradients of pH due to carbonic acid production and DO depletion through the Treatment model highlight the role of enhanced microbial activity in engineered media to remove nitrate via denitrification. Both hydraulic and nutrient remediation performance scaled with filter width. Hydraulic testing indicated that a 6 m-wide VFS provided total infiltration for all but the highest-intensity storm events (76.2 mm/h and 50.8 mm/h for one-hour durations), where respectively 35% and 22% of precipitation and inflow runoff did not infiltrate. While most phosphorus was retained within 1.5 m of filter and nitrification of ammonia to nitrate occurred within 3 m of filter, nitrate removal via denitrification was not observed until infiltrate had passed through a 6 m-wide filter. To ensure hydraulic and nutrient reduction performance, a minimum 6 m filter width is recommended. The nitrogen removal performance of engineered media as compared to soils is likely to vary across different soil types, such that the clear nitrate removal benefit observed in this study may not be realized in all soil types. Further study is needed to understand where amendment of the local soil profile with engineered infiltration media will be likely to result in net improvement to stormwater quality.

2.9 Acknowledgement

This research was supported by the Florida Department of Transportation. The opinions, findings and conclusions expressed in this publication are those of the author(s) and not necessarily those of the Florida Department of Transportation or the U.S. Department of Transportation. The

authors would like to thank Erik Stuart, Gabriela Ford, Jordyn Washington, Olatoyin Olasimbo, Sam Maldonado, and Iris Peterson, who assisted in setting up the test models and running the experiments.

2.10 References

AASHTO, M., 145-91., 2008. Standard specification of soils and soil-aggregate mixtures for Highway Construction Purposes. American Association of State Highway and Transportation Official.

Abu-Zreig, M., Rudra, R.P. and Whiteley, H.R., 2001. Validation of a vegetated filter strip model (VFSMOD). Hydrological processes, 15(5), 729-742. https://doi.org/10.1002/hyp.101

Barrett, M., Lantin, A., Austrheim-Smith, S., 2004. Storm water pollutant removal in roadside vegetated buffer strips. Transportation Research Record. 1890(1), 129-140. https://doi.org/10.3141%2F1890-16

Barrett, M.E., Walsh, P.M., Malina Jr, J.F., Charbeneau, R.J., 1998. Performance of vegetative controls for treating highway runoff. Journal of Environmental Engineering. 124(11), 1121-1128. https://doi.org/10.1061/(ASCE)0733-9372(1998)124:11(1121)

Bhattarai, R., Kalita, P.K., Patel, M.K., 2009. Nutrient transport through a vegetative filter strip with subsurface drainage. Journal of Environmental Management. 90(5), 1868-1876. https://doi.org/10.1016/j.jenvman.2008.12.010

Blanco-Canqui, H., Gantzer, C.J., Anderson, S.H., Alberts, E.E., Thompson, A.L., 2004. Grass barrier and vegetative filter strip effectiveness in reducing runoff, sediment, nitrogen, and phosphorus loss. Soil Science Society of America Journal, 68(5), 1670-1678. https://doi.org/10.2136/sssaj2004.1670

Boger, A.R., Ahiablame, L., Mosase, E., Beck, D., 2018. Effectiveness of roadside vegetated filter strips and swales at treating roadway runoff: a tutorial review. Environmental Science: Water Research & Technology. 4(4), 478-486. https://doi.org/10.1039/C7EW00230K

Borris, M., Viklander, M., Gustafsson, A.M. and Marsalek, J., 2014. Modelling the effects of changes in rainfall event characteristics on TSS loads in urban runoff. Hydrological Processes, 28(4), 1787-1796. https://doi.org/10.1002/hyp.9729

Carluer, N., Lauvernet, C., Noll, D., Munoz-Carpena, R., 2017. Defining context-specific scenarios to design vegetated buffer zones that limit pesticide transfer via surface runoff. Science of The Total Environment. 575, 701-712. https://doi.org/10.1016/j.scitotenv.2016.09.105

Caruso, N.T., 2014. Biofiltration enhancement for the treatment of highway stormwater runoff. (MSc Thesis), Georgia Institute of Technology. http://hdl.handle.net/1853/53111

Chang, N.B., Wanielista, M.P., Wen, D., 2018a. Comparative Nitrogen and Pesticide Removal with Sorption Media in Linear Ditch for Groundwater and Stormwater Treatment. Florida Department of Transportation, Final report, 91 p.

Chang, N.B., Wen, D., Colona, W. and Wanielista, M.P., 2019. Comparison of Biological Nutrient Removal via Two Biosorption-Activated Media Between Laboratory-Scale and Field-Scale Linear Ditch for Stormwater and Groundwater Co-treatment. Water, Air, & Soil Pollution, 230(7), 1-19. https://doi.org/10.1007/s11270-019-4193-y

Chang, N.B., Wen, D., McKenna, A.M. and Wanielista, M.P., 2018b. The impact of carbon source as electron donor on composition and concentration of dissolved organic nitrogen in biosorption-activated media for stormwater and groundwater co-treatment. Environmental Science & Technology, 52(16), 9380-9390. https://doi.org/10.1021/acs.est.8b01788

Chaubey, I., Edwards, D.R., Daniel, T.C., Moore, P.A., Nichols, D.J., 1994. Effectiveness of vegetative filter strips in retaining surface-applied swine manure constituents. Transactions of the ASAE, 37(3), 845-850.

Chen, J., Theller, L., Gitau, M.W., Engel, B.A., Harbor, J.M., 2017. Urbanization impacts on surface runoff of the contiguous United States. Journal of Environmental Management. 100(187), 470-481. https://doi.org/10.1016/j.jenvman.2016.11.017

Chen, S.S., Tsang, D.C., He, M., Sun, Y., Lau, L.S., Leung, R.W., Lau, E.S., Hou, D., Liu, A. and Mohanty, S., 2020. Designing Sustainable Drainage Systems in Subtropical Cities: Challenges and Opportunities. Journal of Cleaner Production, 280(2), 124418. https://doi.org/10.1016/j.jclepro.2020.124418

Clary, J., Quigley, M., Poresky, A., Earles, A., Strecker, E., Leisenring, M., Jones, J., 2011. Integration of low-impact development into the international stormwater BMP database.

Journal of Irrigation and Drainage Engineering. 137(3), 190-198. https://doi.org/10.1061/(ASCE)IR.1943-4774.0000182

Davis, A.P., Stagge, J.H., Jamil, E., Kim, H., 2012. Hydraulic performance of grass swales for managing highway runoff. Water research, 46(20), 6775-6786. https://doi.org/10.1016/j.watres.2011.10.017

Dillaha, T.A., Reneau, R.B., Mostaghimi, S., Lee, D., 1989. Vegetative filter strips for agricultural nonpoint source pollution control. Transactions of the ASAE, 32(2), 513-0519.

Driscoll, E.D., Shelley, P.E., Strecker, E.W., 1990. Pollutant loadings and impacts from highway stormwater runoff. Volume I: Design Procedure (No. FHWA-RD-88-006).

Dudley, R.W., Hodgkins, G.A., Mann, A., Chisolm, J., 2001. Evaluation of the effects of development on peak-flow hydrographs for Collyer Brook, Maine. U.S. Geological Survey Water-Resources Investigations Report 2001-4156. https://doi.org/10.3133/wri20014156

Ekka, S.A., Rujner, H., Leonhardt, G., Blecken, G.T., Viklander, M. and Hunt, W.F., 2021. Next generation swale design for stormwater runoff treatment: A comprehensive approach. Journal of Environmental Management, 279, 111756. https://doi.org/10.1016/j.jenvman.2020.111756

Fardel, A., Peyneau, P.E., Béchet, B., Lakel, A., Rodriguez, F., 2020. Performance of two contrasting pilot swale designs for treating zinc, polycyclic aromatic hydrocarbons and glyphosate from stormwater runoff. Science of The Total Environment, 743, 140503. https://doi.org/10.1016/j.scitotenv.2020.140503

Ferrell, J., Unruh, B., Kruse, J., 2012. A guide for roadside vegetation management. Florida Department of Transportation, Tallahassee, Florida, p. 104.

Florida Department of Transportation., 2012. Plans Preparation Manual Volume 2: Plans Preparation and Assembly. Roadway Design Office, Tallahassee, Florida.

Florida Department of Transportation., 2018. Standard Specifications for Road and Bridge Construction. State of Florida Department of Transportation, p. 1221.

Fox, G.A., Muñoz-Carpena, R., Purvis, R.A., 2018. Controlled laboratory experiments and modeling of vegetative filter strips with shallow water tables. Journal of Hydrology. 556, 1-9. https://doi.org/10.1016/j.jhydrol.2017.10.069

Franco, J. and Matamoros, V., 2016. Mitigation of polar pesticides across a vegetative filter strip. A mesocosm study. Environmental Science and Pollution Research, 23(24), 25402-25411. https://doi.org/10.1007/s11356-016-7516-1

Garcia de la Serrana Lozano, M.D.C., 2017. Analysis of Infiltration and Overland Flow over Sloped Surfaces: Application to Roadside Swales. Retrieved from the University of Minnesota Digital Conservancy, 243 p. http://hdl.handle.net/11299/190570

Gavrić, S., Leonhardt, G., Marsalek, J., Viklander, M., 2019. Processes improving urban stormwater quality in grass swales and filter strips: A review of research findings. Science of the Total Environment. 669, 431-447. https://doi.org/10.1016/j.scitotenv.2019.03.072

Hager, J., Hu, G., Hewage, K. and Sadiq, R., 2019. Performance of low-impact development best management practices: a critical review. Environmental Reviews, 27(1), 17-42. https://doi.org/10.1139/er-2018-0048

Harper, H.H., Baker, D.M., 2007. Evaluation of current stormwater design criteria within the state of Florida. Florida Department of Environmental Protection, p. 327.

Hood, A., Chopra, M., Wanielista, M., 2013. Assessment of Biosorption Activated Media Under Roadside Swales for the Removal of Phosphorus from Stormwater. Water. 5(1), 53-66. https://doi.org/10.3390/w5010053

Jin, C.X., Römkens, M.J.M., 2001. Experimental studies of factors in determining sediment trapping in vegetative filter strips. Transactions of the ASAE. 44(2), 277.

Jones, M.J., 1971. The maintenance of soil organic matter under continuous cultivation at Samaru, Nigeria. The Journal of Agricultural Science. 77(3), 473-482. https://doi.org/10.1017/S0021859600064558

Kayhanian, M., Fruchtman, B.D., Gulliver, J.S., Montanaro, C., Ranieri, E., Wuertz, S., 2012. Review of highway runoff characteristics: Comparative analysis and universal implications. Water research. 46(20), 6609-6624. https://doi.org/10.1016/j.watres.2012.07.026

Kayhanian, M., Suverkropp, C., Ruby, A., Tsay, K., 2007. Characterization and prediction of highway runoff constituent event mean concentration. Journal of Environmental Management. 85(2), 279-295. https://doi.org/10.1016/j.jenvman.2006.09.024

Kibler, K.M., Chang, N.B., Wanielista, M.P., Wen, D., Shokri, M., Valencia, A., Lustoso-Alves, E., Rice, N., 2020. Optimal Design of Stormwater Basins with Bio-Sorption Activated Media (BAM) in Karst Environments – Phase II: Field Testing of BMPs. FDOT Final Report BDV24-977-20.

Kibler, K.M., Kitsikoudis, V., Donnelly, M., Spiering, D.W., Walters, L., 2019. Flow–vegetation interaction in a living shoreline restoration and potential effect to mangrove recruitment. Sustainability, 11(11), 3215. https://doi.org/10.3390/su11113215

Koch, B.J., Febria, C.M., Cooke, R.M., Hosen, J.D., Baker, M.E., Colson, A.R., Filoso, S., Hayhoe, K., Loperfido, J.V., Stoner, A.M., Palmer, M.A., 2015. Suburban watershed nitrogen retention: Estimating the effectiveness of stormwater management structures. Elementa: Science of the Anthropocene, 3. https://doi.org/10.12952/journal.elementa.000063%20#sthash.rcQOPFkF.dpuf

Lauvernet, C., Helbert, C., 2020. Metamodeling methods that incorporate qualitative variables for improved design of vegetative filter strips. Reliability Engineering & System Safety. p.107083. https://doi.org/10.1016/j.ress.2020.107083

Leguédois, S., Ellis, T.W., Hairsine, P.B., Tongway, D.J. 2008. Sediment trapping by a tree belt: processes and consequences for sediment delivery. Hydrological Processes: An International Journal, 22(17), 3523-3534. https://doi.org/10.1002/hyp.6957

Li, H., 2015. Green infrastructure for highway stormwater management: Field investigation for future design, maintenance, and management needs. Journal of Infrastructure Systems. 21(4), 05015001. https://doi.org/10.1061/(ASCE)IS.1943-555X.0000248

Lim, T.T., Edwards, D.R., Workman, S.R., Larson, B.T., Dunn, L., 1998. Vegetated filter strip removal of cattle manure constituents in runoff. Transactions of the ASAE, 41(5), 1375.

Line, D.E., Hunt, W.F., 2009. Performance of a bioretention area and a level spreader-grass filter strip at two highway sites in North Carolina. Journal of Irrigation and Drainage Engineering, 135(2), 217-224. https://doi.org/10.1061/(ASCE)0733-9437(2009)135:2(217)

Liu, A., Egodawatta, P., Guan, Y., Goonetilleke, A., 2013. Influence of rainfall and catchment characteristics on urban stormwater quality. Science of the Total Environment. 444, 255-262. https://doi.org/10.1016/j.scitotenv.2012.11.053

Liu, Y., Engel, B.A., Flanagan, D.C., Gitau, M.W., McMillan, S.K., Chaubey, I., 2017. A review on effectiveness of best management practices in improving hydrology and water quality: needs and opportunities. Science of the Total Environment. 601, 580-593. https://doi.org/10.1016/j.scitotenv.2017.05.212

Marsalek, J., Chocat, B., 2002. International report: stormwater management. Water Science and Technology, 46(6-7), 1-17. https://doi.org/10.2166/wst.2002.0657

Meyer, L.D., Dabney, S.M., Harmon, W.C., 1995. Sediment-trapping effectiveness of stiff-grass hedges. Transactions of the ASAE, 38(3), 809-815. https://doi.org/10.13031/2013.27895

Muñoz-Carpena, R., Parsons, J.E., Gilliam, J.W., 1999. Modeling hydrology and sediment transport in vegetative filter strips. Journal of Hydrology, 214(1-4), 111-129. https://doi.org/10.1016/S0022-1694(98)00272-8

NOAA.gov. 2017. National Centers for Environmental Information (NCEI) formerly known as National Climatic Data Center (NCDC) | NCEI offers access to the most significant archives of oceanic, atmospheric, geophysical and coastal data. [online] Available at: https://www.ncdc.noaa.gov/. [Accessed 15 October 2017]

O'Reilly, A.M., Wanielista, M.P., Chang, N.B., Xuan, Z., Harris, W.G., 2012. Nutrient removal using biosorption activated media: Preliminary biogeochemical assessment of an innovative stormwater infiltration basin. Science of the Total Environment, 432, 227-242. https://doi.org/10.1016/j.scitotenv.2012.05.083

Pan, D., Gao, X., Dyck, M., Song, Y., Wu, P. and Zhao, X., 2017. Dynamics of runoff and sediment trapping performance of vegetative filter strips: Run-on experiments and modeling. Science of the Total Environment, 593, 54-64. https://doi.org/10.1016/j.scitotenv.2017.03.158

Pappas, E.A., Smith, D.R., Huang, C., Shuster, W.D., Bonta, J.V., 2008. Impervious surface impacts to runoff and sediment discharge under laboratory rainfall simulation. Catena 72(1), 146-152. https://doi.org/10.1016/j.catena.2007.05.001

Rivers, E.N., Heitman, J.L., McLaughlin, R.A. and Howard, A.M., 2021. Reducing roadside runoff: Tillage and compost improve stormwater mitigation in urban soils. Journal of

Environmental Management, 280, 111732. https://doi.org/10.1016/j.jenvman.2020.111732

Roesner, L.A., Bledsoe, B.P. and Brashear, R.W., 2001. Are best-management-practice criteria really environmentally friendly?. Journal of Water Resources Planning and Management, 127(3), 150-154. https://doi.org/10.1061/(ASCE)0733-9496(2001)127:3(150)

Rounds, S.A., Wilde, F.D., Ritz, G.F., 2013, Dissolved oxygen (ver. 3.0): U.S. Geological Survey Techniques of Water-Resources Investigations, book 9, chap. A6.2. https://doi.org/10.3133/twri09A6.2

Sansalone, J.J. and Buchberger, S.G., 1997. Partitioning and first flush of metals in urban roadway storm water. Journal of Environmental Engineering, 123(2), 134-143. https://doi.org/10.1061/(ASCE)0733-9372(1997)123:2(134)

Spaan, W.P., Sikking, A.F.S., Hoogmoed, W.B., 2005. Vegetation barrier and tillage effects on runoff and sediment in an alley crop system on a Luvisol in Burkina Faso. Soil and Tillage Research, 83(2), 194-203. https://doi.org/10.1016/j.still.2004.07.016

Stagge, J.H., Davis, A.P., Jamil, E., Kim, H., 2012. Performance of grass swales for improving water quality from highway runoff. Water research, 46(20), 6731-6742. https://doi.org/10.1016/j.watres.2012.02.037

Strecker, E.W., Quigley, M.M., Urbonas, B.R., Jones, J.E., Clary, J.K., 2001. Determining urban storm water BMP effectiveness. Journal of Water Resources Planning and Management, 127(3), 144-149. https://doi.org/10.1061/(ASCE)0733-9496(2001)127:3(144)

Tedoldi, D., Chebbo, G., Pierlot, D., Kovacs, Y. and Gromaire, M.C., 2016. Impact of runoff infiltration on contaminant accumulation and transport in the soil/filter media of Sustainable Urban Drainage Systems: A literature review. Science of the Total Environment, 569, pp.904-926. https://doi.org/10.1016/j.scitotenv.2016.04.215

Trenouth, W.R., Gharabaghi, B., 2016. Highway runoff quality models for the protection of environmentally sensitive areas. Journal of Hydrology. 542, 143-155. https://doi.org/10.1016/j.jhydrol.2016.08.058

Thomson, N.R., McBean, E.A., Snodgrass, W., Monstrenko, I.B., 1997. Highway stormwater runoff quality: Development of surrogate parameter relationships. Water, Air, and Soil Pollution, 94(3-4), 307-347. https://doi.org/10.1007/BF02406066

Vahabi, J., Ghafouri, M., 2009. Determination of runoff threshold using rainfall simulator in the southern Alborz range foothill-Iran. Research Journal of Environmental Sciences 3(2), 193-201. http://dx.doi.org/10.3923/rjes.2009.193.201

Wanielista, M., Chang, N.B., Randall, A., Chopra, M., Hardin, M., Jones, J., Hood, A., Salamah, S., 2014. Demonstration Bio Media for Ultra-urban Stormwater Treatment (No. SMA 1660 7051). University of Central Florida.

Wasowska, Z., 2014. The Fate of Nitrogen and Phosphorus from a SImulated Highway Cross-Section. [Master thesis], University of Central Florida, p. 225.

Wen, D., Chang, N.B. and Wanielista, M.P., 2018. Comparative copper toxicity impact and enzymatic cascade effect on Biosorption Activated Media and woodchips for nutrient

removal in stormwater treatment. Chemosphere, 213, 403-413. https://doi.org/10.1016/j.chemosphere.2018.09.062

Wen, D., Ordonez, D., McKenna, A., Chang, N.B., 2020a. Fate and transport processes of nitrogen in biosorption activated media for stormwater treatment at varying field conditions of a roadside linear ditch. Environmental Research. 181, 108915. https://doi.org/10.1016/j.envres.2019.108915

Wen, D., Valencia, A., Lustosa, E., Ordonez, D., Shokri, M., Gao, Y., Rice, N., Kibler, K., Chang, N.B., Wanielista, M.P., 2020b. Evaluation of green sorption media blanket filters for nitrogen removal in a stormwater retention basin at varying groundwater conditions in a karst environment. Science of The Total Environment, 719, 134826. https://doi.org/10.1016/j.scitotenv.2019.134826

Winston, R.J., Hunt, W.F., 2016. Characterizing runoff from roads: Particle size distributions, nutrients, and gross solids. Journal of Environmental Engineering. 143(1), 04016074. https://doi.org/10.1061/(ASCE)EE.1943-7870.0001148

Winston, R.J., Hunt, W.F., Kennedy, S.G., Wright, J.D., Lauffer, M.S., 2012. Field evaluation of storm-water control measures for highway runoff treatment. Journal of Environmental Engineering. 138(1), 101-111. https://doi.org/10.1061/(ASCE)EE.1943-7870.0000454

Winston, R.J., Powell, J.T. and Hunt, W.F., 2019. Retrofitting a grass swale with rock check dams: Hydrologic impacts. Urban Water Journal, 16(6), 404-411. https://doi.org/10.1080/1573062X.2018.1455881

Woolhiser, D.A., Goodrich, D.C., 1988. Effect of storm rainfall intensity patterns on surface runoff. Journal of Hydrology, 102(1-4), 335-354. https://doi.org/10.1016/0022-1694(88)90106-0

Yu, C., Duan, P., Yu, Z., Gao, B., 2019. Experimental and model investigations of vegetative filter strips for contaminant removal: A review. Ecological Engineering, 126, 25-36. https://doi.org/10.1016/j.ecoleng.2018.10.020

Zhao, C.H., Gao, J.E., Zhang, M.J., Wang, F., Zhang, T., 2016. Sediment deposition and overland flow hydraulics in simulated vegetative filter strips under varying vegetation covers. Hydrological Processes. 30(2), 163-175. https://doi.org/10.1002/hyp.10556

CHAPTER 3 DYNAMICS OF NUTRIENT DELIVERY FROM ROADWAY RUNOFF OVER VARIED STORM EVENTS IN NORTH-CENTRAL FLORIDA

3.1 Preface

This chapter provides characterization of nutrient load and delivery within roadway runoff events under different rainfall-runoff conditions. The research reveal how nutrients may deliver differently under different runoff event types, helpful to design BMPs. The contents of this chapter are in preparation for submission to the Journal of Hydrology[2].

3.2 Abstract

Roadway runoff can be a major non-point source of nutrients entering surface and groundwater resources where runoff nutrient load and delivery dynamics can vary site to site, event by event, and within a single event, and their characterization is important for design of best management practices (BMPs). The objective of this novel research is to characterize runoff event types regarding nutrient load and delivery dynamics of total nitrogen (TN), ammonia nitrogen (NH_3-N), and nitrogen oxides (NO_x-N) at the event scales over varied storm events. Nine rainfall-runoff events in different range of rainfall depths, durations, and intensities were collected from two roadway segments near Silver Springs in Florida for this purpose. Runoff samples were collected over the events from runoff initiation to the end and then five samples were selected for chemical analysis representing nutrient dynamics across the events. Multivariate analysis techniques were

[2] Shokri, M; Kibler, K.M., Wang, D; Wanielista, M., under-submission. Dynamics of Nutrient Delivery from Roadway Runoff over Varied Storm Events in North-Central Florida. Journal of Hydrology

applied to get insight into correlation among influential factors affecting nutrient delivery. Antecedent dry period (ADP) prior to the events and runoff volume were identified respectively as the most influential factors on runoff nutrient supply and flux delivery. Accordingly, three runoff event types were discerned: type I (high nutrient supply and high flux delivery), type II (low nutrient supply but high flux delivery), and type III (low flux delivery). Non-parametric statistical analysis of nutrient mass delivery suggested a significant difference ($p < .05$) and greater mass first flush in type I than type II and III while type III events tend to end-flush nutrient delivery. The event type approach can resolve the inadequacies of traditional approaches and it is suggested to be considered for a cost-effectively design of BMP strategies.

Keywords: Roadway, runoff, nutrients, pollution, Silver Springs, Florida

3.3 Introduction

Roadway runoff is a widespread non-point source of contaminates such as nutrients, heavy metals, sediments, and toxic substances (Hu et al., 2020; Jeong et al., 2020). Degrading water quality in Florida's lakes, rivers, and springs such as Silver Springs in Central Florida have received widespread attentions because of excess nutrient pollution (Heffernan et al., 2010; Hicks and Holland, 2012; Liao et al., 2019; Gao et al., 2020). Excess nutrients can lead to algal bloom, ecosystem degradation, loss of biodiversity, and eutrophication in receiving water bodies (Bouchard et al., 1992; Pitt et al., 1999; Mallin et al., 2009; Suthar et al., 2009; Eller and Katz, 2017). Even though different sources of nutrients are documented including atmospheric deposition, septic tanks, fertilizers, livestock waste, and wastewater discharges (Badruzzaman et al., 2012; Eller and Katz, 2017), urban stormwater runoff is a potential source of excess nutrients

leading to degrading water quality in the state of Florida and the U.S (Abdul-Aziz and Al-Amin, 2016; Trenouth and Gharabaghi, 2016).

Nutrients from impervious road surfaces can be transported to road shoulders during rainfall-runoff events, typically in dissolved and particulate forms with dissolved as the dominant form of the transportation (Taylor et al., 2005; Wang et al., 2010; Winston and Hunt, 2016; Zhao et al., 2018). The process leading to runoff nutrient load and dynamic transport over event is complex because of many influential factors. Runoff nutrient load from roadways usually vary depend upon rainfall-runoff characteristics including rainfall depth, duration, intensity, antecedent dry period (ADP), runoff rate and volume and roadway properties (e.g. traffic lines, speed, average annual daily traffic (AADT), fuel type, and road design), and site specific conditions (e.g. proximate to traffic lights, stop signs, and nearby land uses) (Miguntanna, 2009; Borris et al., 2014; Horstmeyer et al., 2016; Trenouth and Gharabaghi, 2016). It is expected that nutrient load gradually increase from runoff initiation with rainfall depth, considering sufficient rainfall to generate overland flow (> 0.7 mm, Pappas et al., 2008) and finite nutrient supply (Trenouth and Gharabaghi, 2016). Higher storm intensity and greater transport capacity can proceed nutrient transportation (particulate form entrainments) while concentrations may decrease over time due to dilution (Borris et al., 2014). It is generally a consensus that ADP not only is positively (linearly or nonlinearly) correlated to runoff pollutant load (Kayhanian et al., 2003; Trenouth and Gharabaghi, 2016), but also documented as the dominant influential factor on nutrient load (Borris et al., 2014; Trenouth and Gharabaghi, 2016). However, an opposite correlation was also observed in collected runoff in some research (e.g. Li and Barrett, 2008) which was attributed to the role of curb structures at the

road shoulder. Higher pollutant levels were also related to higher annual average daily traffic (AADT) of roadways (Kayhanian et al., 2012).

Understanding nutrient delivery and dynamic over events is important as most BMPs are designed based on intercepting a percentile runoff volume (20 to 50%) which delivers the major pollutant mass (Stahre and Urbonas, 1990; Wanielista and Yousef, 1993; Bertrand-Krajewski et al., 1998). Such runoff volume with greatest pollutant mass is known as the first flush concept based on analyzing normalized cumulative pollutant mass and normalized cumulative runoff volume, so called as M(V) curves (Bertrand-Krajewski et al., 1998; Lee et al., 2002; Miguntanna, 2009; Jiang et al., 2010). However, first flush may not be observed in every runoff event, and nutrient delivery may vary event to event, site to site, or considered nutrient species or pollutant type. For example, a small storm event may just consist 20% of a larger event or a pollutant loud increase at the end of runoff event, so-called as end-flush, as reported for total nitrogen (TN) by Bach et al. [2010]. Therefore, the M(V) curve analysis, where all events were treated similarly, was not satisfactory because it disregards the impacts of runoff volume and pollutant type/source (Bach et al., 2010). A sliced-based approach is proposed by Bach et al. [2010] and endorsed by some researchers (e.g. Christian et al., 2020). However, the sliced-based approach requires collecting many continues water quality data (60 seconds), which may not be possible in every project. Thus, a new complementary procedure is needed to resolve treating and analyzing runoff events on the M(V) curve approach to systematically inspect nutrient delivery.

Runoff pollutant delivery over roadways depends on two main factors: 1) nutrient supply which is the sources of accumulating nutrient over surface of roadways, and 2) runoff flow (size and cumulative volume) to effectively wash off and transport nutrient to roadside, which depends

on rainfall characteristics including rainfall depth, duration, and intensity (Huber et al., 1988; Brodie and Egodawatta, 2011; Borris et al. 2014). Considering the two factors, Borris et al. [2014] specified two transport regimes for pollutant delivery. Transport-limited flow regime, which usually occur when runoff volume is low because of low rainfall depth and intensity and runoff may not effectively wash off and transport all available pollutant, leading to excess pollutant load within runoff volume. However, transport-limited flow regime may shift to a supply-limited flow regime when runoff volume increase by a certain threshold because of larger rainfall depth and intensity (Borris et al., 2014). Such transport or supply limited flow regimes were already and well knowingly applied for interpreting sediment transports in river systems as well (Lane, 1955; Grant et al., 2003). Defining transition from transport-limited flow regime to supply-limited flow regime may not be easy for roadway runoff events and require considering runoff, rainfall, and nutrient variation over events altogether to recognize similar runoff event-types in term of pollutant supply and flow regimes. Classifying runoff events in term of similar nutrient supply and flow regimes as a new strategy may fill the knowledge gaps reported to M(V) curve analysis and thus inspect first flush occurrences among different event types systematically. Accordingly, BMPs can be designed based on specific and frequent event types, which can wash off major nutrients within lower runoff volume. Given the complex and many influential factors, multivariate technique based on principal component analysis (PCA) can be used to detect interrelated correlations among influential factors on runoff pollutant load and transport conditions (e.g. Huang et al., 2007; Liu et al., 2013; Yang and Toor, 2017; Sun et al., 2018). Such techniques not only can provide the correlations, but also provide relative importance of different variables on the process in a graphically manner as the outcomes for the ease in interpretations.

The objective of this research is to evaluate dynamic nutrient delivery over roadway runoff events and inspect how first-flush or end-flush may occur within different runoff event types and nutrient species. For this purpose, we 1) discern correlations among event mean concentration (EMC) of nitrogen oxides (NO_x), ammonia (NH_3), and total nitrogen (TN) in event-scales with rainfall characteristics to detect the most influential factor(s) on runoff nutrient load, and 2) detect different runoff event types through a detail correlation analysis of the nutrient concentration delivery over runoff events with considering cumulative runoff and rainfall characteristics, and 3) inspect dynamic nutrient mass delivery and first flush or end-flush occurrences over different runoff event types. This study provides a new strategy and insightful information for analyzing nutrients delivery over roadway runoff events, an important information to transportation agencies and any organizations everywhere aimed mitigating impaired roadway runoff to protect water resources.

3.4 Methodology

3.4.1 Study area

The study area comprises of a section of State Road 40 (West Drainage Area) and State Road 35 (East Drainage Area) in Marion County, Florida, which drain runoff to a stormwater management basin (Basin 9b), that is located 550 m west of the main vents of Silver Springs (Figure 8). The climate of the area is humid subtropical with warm, humid summers and mild, dry winters (Knowles, 1996). Most precipitation (annual mean 1,295 to 1,321 mm) occurs during summer from June to September (Knowles, 1996; Shoemaker et al., 2004). Convective storms with frequent low rainfall depths are typical rainfall generation mechanism during summer season

in the area (Harper and Baker, 2007). The West road (a 340 m section of State Road 40) is a two-lane roadway and its approximate drainage area is 0.43 hectare. The East road (a 330 m section of State Road 35) is a two-way road with approximate drainage area of 0.41 hectare (Figure 8). Roadway runoff enters the basin into West and East runoff collection areas through West and East inlets in size of 45.7 cm and leaves the basin through infiltration into a shallow surficial aquifer (Figure 8, C). The West and East runoff collection areas were constructed each in 111.5 m^2 area with covering sidewalls by impermeable layer (Figure 8, D and E). Two monitoring wells were installed in West and East runoff collection areas (Well 1 and Well 3) to monitor water level changes by entering runoff volume (Figure 8, C). In addition, groundwater level was monitored continuously outside the runoff collection areas (Well 2) as a control site (Figure 8, C). More information on the structures and purpose of the collection areas can be obtained in Wen et al. (2020).

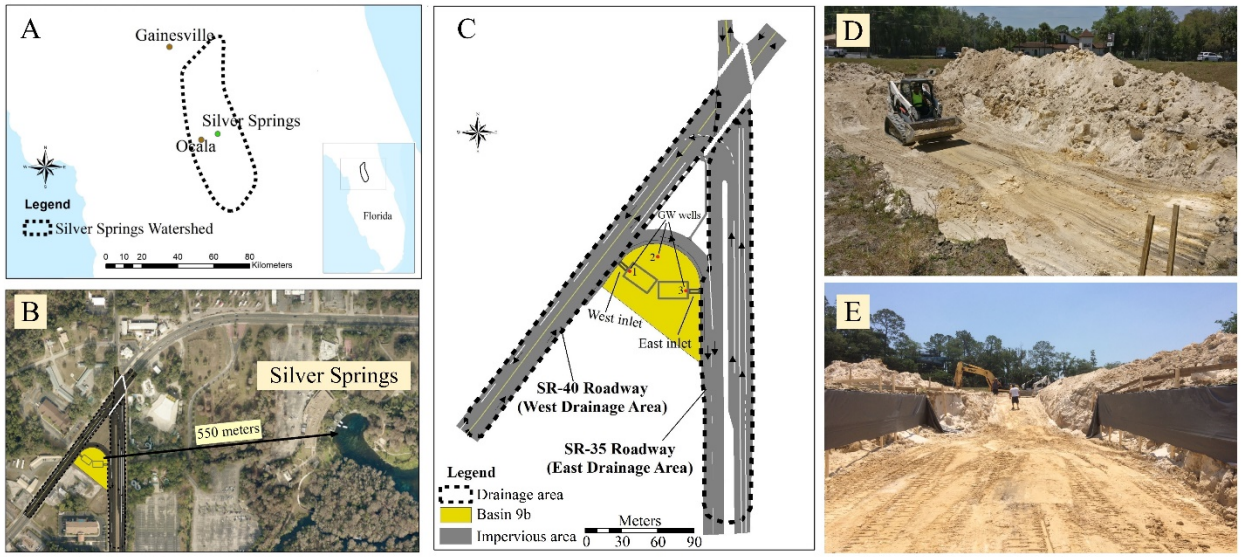

Figure 8. Study area: (A) Silver Springs springshed in Florida, (B) location of Basin 9b with respect to Silver Springs, (C) West and East Drainage Areas and their runoff collection areas with

including installed three monitoring groundwater wells, (D) construct of runoff collection areas, and (D) impervious sidewalls of runoff collection areas to prevent lateral flux movement and provide vertical infiltration.

3.5 Sampling

3.5.1 Runoff sampling, analysis, and event characteristics

Runoff entering the basin was measured and sampled at the West and East inlets over nine rainfall-runoff events (Figure 8). Runoff was sampled manually at 2-min intervals for the first 10 minutes of runoff, then from 5, 10 to 30 minutes intervals until runoff ended. Five samples from each event were selected for analysis to represent nutrient dynamics across the event. Non-filtered samples were acidified with H_2SO_4 to pH < 2 then analyzed for total nitrogen (TN) and ammonia (NH_3) following SM-21, Sec. 4500 N C and SM-21, Sec. 4500-NH_3 G methods, respectively. Filtered samples were passed through a 0.45 µm filter and analyzed for nitrogen oxides (NO_x) using SM-21, Sec. 4500-NO3 F method. All samples were delivered to the lab within 24 hours of collection and analyzed in triplicate by a certified laboratory (Environmental Research & Design, Inc.).

Discrete storm events were defined as a period of continuous rainfall that generates measurable runoff. Precipitation start and end times were recorded in the field and corresponding precipitation data were collected from the Silver Springs weather station (Station ID: KFLOCALA105), located about 1000 m southwest of Basin 9b. Mean rainfall intensity was calculated for each event by normalizing cumulative rainfall depth by rainfall duration and maximum rainfall intensity was calculated as well (Brezonik et al., 2002). In addition, 15-min rainfall data (resolution 2.54 mm) covering the last 30 to 40 years of precipitation were obtained from stations within or proximate

to the Silver Springs Springshed from NOAA National Center for Environmental Information. After quality checking the data, relative frequency analysis of long-term data was complete and cumulative depth of frequency and mean annual number of occurrence based on cumulative depth were determined for the sampled storm events.

Runoff depths were recorded at 15-min intervals by pressure transducers (TE Connectivity TruBlue 555 Vented Level Data Logger, 0 – 300 psi, accuracy 0.05%) installed in the monitoring wells near the West and East inlets in the runoff collection areas (Figure 8 C, Well 1 and Well 3). Volumes of direct precipitation and evapotranspiration over storm events into/out of collection areas were small relative to runoff volumes and are thus neglected (Eq. 2 and Eq. 3). Lateral subsurface outflows from the collection areas are also neglected, given that the impervious sidewalls precluded lateral flow out of the collection areas. Thus, net vertical groundwater flux through the media could be calculated using Darcy equation. We apply a mass balance model over the collection areas, where changes in recorded water level over time (Δh) reflect inflows (runoff into collection areas) minus outflows (vertical flux) (Eq. 4). Therefore, total volumes of runoff entering the collection areas (Q_t) are estimated as the sum of volume change calculated by Δh over the collection area in a given time period and volume of vertical flux over the same time period (Eq. 5). Vertical outflows were calculated using Darcy Law following the vertical hydraulic gradient pressure head at each recorded data point with respect to recorded groundwater table measured in Well 2 by ONSET HOBO Water Level Data Loggers (Eq. 6 and Figure 8 C). Hydraulic conductivity of the media during the storm events (K) were determined by the water level recession rate recorded at the end of runoff. However, during long duration of an event (Event 2 in result section), media could be saturated and led to overestimating vertical flux rate. Thus, we

applied mean calculated rate of events which occurred quickly as presenting unsaturated hydraulic conductivity of media during that event.

$$\int_0^t Q_{in}\, dt = A.(P + R) \tag{2}$$

$$\int_0^t Q_{out}\, dt = A.(ET + V) \tag{3}$$

$$\int_0^t Q_{in} - \int_0^t Q_{out} = \sum_{n=1}^{m} A.\Delta h \tag{4}$$

$$\int_0^t Q_t\, dt = \sum_{n=1}^{m} A\Delta h + A\int_0^t (V)dt \tag{5}$$

$$V = K\frac{\Delta\varphi}{\Delta l} \tag{6}$$

Where $Q_{in}(L^3)$ is the estimated runoff inflow, A (L^2) is the area within the systems, P is the direct rainfall depth (L), R is the runoff depth measured by pressure transducers (L), ET is the direct evapotranspiration depth in from the systems (L), V is the vertical groundwater flux rate through media (LT^{-1}), Δh (L) is the positive water level changes (L), and n is the first time interval and m is the last time interval of runoff inflow over the event, K is the hydraulic conductivity of media (LT^{-1}), and $\frac{\Delta\varphi}{\Delta l}$ is the vertical hydraulic gradient measured from local water level in the system with respect to groundwater level (dimensionless).

3.5.2 Runoff nutrient load analysis

Event mean concentrations (EMC) of each nutrient parameter was computed following Eq. 7 (Sansalone et al., 1997). Pollutant concentrations were assumed to change linearly between collected samples (Bach et al., 2010) and the synoptic runoff samples were applied to represent chemical concentrations of corresponding portions of the runoff hydrograph. Consequently, runoff

volumes correspond to each nutrient mass sample portion were determined and EMC were calculated for the nutrient parameters.

$$EMC = \frac{M}{V} = \frac{\int_0^{tr} c(t)\, q(t)\, dt}{\int_0^{tr} q(t)\, dt} \quad (7)$$

Where *M* presents cumulative event mass (M), *V* is the total volume of flow during event (L^3), c(t) is the mean flow weighted concentration of element (M/L^3), q(t) is the flow which varies over the event period (L^3/T).

To provide insight into influential processes in nutrient delivery dynamics over storm events, multi-criteria analysis (using PROMETHEE and GAIA software, Khalil et al., 2004) was undertaken at two timescales. At the event scale, event-mean storm characteristics including rainfall depth, intensity, and ADP as actions and mean of EMC of NO_x, NH_3, and TN for West and East drainage areas were considered as criteria to understand the relative influence of storm driving factors on event nutrient EMCs. In the second analysis within events, coupled cumulative runoff flux and instantaneous concentration measurements were analyzed along with storm intensity and ADP to more intensively evaluate dynamic processes related to nutrient wash-off and transport within events. In MCDM analysis, the actions attributed to each criteria in a provided matrix are pairwise compared and then ranked from the best to the worst action through computing their different preference flows: positive flow (φ^+), negative flow (φ^-), and net flow (φ) (Khalil et al., 2004; Liu et al., 2013). The positive flow presents how much an action preferred in comparison to other actions in criteria while negative flow provides how much the other actions preferred to that specified action and the net flow is the different between positive and negative flow of the actions. The relationships are graphically presented following PCA describing the

correlation among criteria and actions, a way to provide insight into detecting major physical components on nutrient supply and transport capacity of runoff events. In the PCA result, the vectors with acute angle present correlated variables while in an orthogonal angle indicates uncorrelated and with an obtuse angle means opposite correlation. To get insight into the behavior of runoff events with respect to nutrient transport, dynamic nutrient mass delivery with respect to runoff volume were analyzed through M(V) curve analysis (Lee et al. 2002; Jiang et al., 2010). The two procedures could provide categorization of runoff event types considering relatively similar nutrient content and transport. The relative tendency of nutrient delivery in event types was inspected as nutrient mass first-flush ratio (MFF_n) delivered in the first 30% (MFF_{30}) and 50% (MFF_{50}) of runoff volume (Eq. 8) (Bertrand-Krajewski et al., 1998; Hathaway and Hunt, 2011; Li et al., 2015; Christian et al., 2020). Where V is the runoff volume (m^3) in any defined n percentile of the total runoff volume (V_{tot}) (m^3).

$$MFF_n = \sum_{V=0}^{V=n\%\,(V_{tot})} P_v \tag{8}$$

Non-parametric statistical analyses of independent-sample t-test using the Wilcoxon rank sum test, considering 95% confidence intervals, were completed using SPSS to compare nutrient mass first-flush ratio at 30% and 50% of runoff volumes between different runoff event types (Christian et al., 2020). These runoff volume thresholds were considered in accordance to many recent studies (Stahre and Urbonas, 1990; Bertrand-Krajewski et al., 1998; Bach et al., 2010; Christian et al., 2020).

3.6 Results

The sampled storms capture behavior across a range of rainfall-runoff characteristics with cumulative rainfall depths ranging from 0.2 mm to 22 mm, durations from 5 to 566 minutes, mean intensities of the events from 0.9 to 73.0 mm/h, and peak intensity from 2.54 to 121.9 mm/h (Table 5). Estimated annual occurrences based on cumulative depth are in range of 3 to 33 times per year (Table 5). In general, shorter storms produced shorter runoff durations. The ADPs vary in range of 0.8 to 20.5 days where six of the events have ADP less than 5 days and the rest have longer ADP preceding the event (Table 5). In general, events with longer ADP produced higher nutrient EMC and runoff mass load (Table 5 and Table 6). However, there is an event with short ADP (Event3) which generated low mass but characterized as large nutrient EMCs. In general, West Drainage Area produced larger EMC and nutrient mass than the East Drainage Area (Table 6).

Table 5. Rainfall-runoff storm events with estimated runoff volumes from West and East drainage roads to the Basin 9b during the collected events.

Event ID	Date	Rainfall depth (mm)	Rainfall period (h)	Average Rainfall intensity (mm/h)	Peak rainfall intensity (mm/h)	Mean annual occurrence (times/year)	Antecedent dry period (days prior)	SR 40 (West road)		SR 35 (East road)	
								Runoff volume (m^3)	Runoff duration (min)	Runoff volume (m^3)	Runoff duration (min)
Event1	Apr 15, 18	22.30	5.03	4.43	121.9	3	5.5	84.4	215	89.9	215
Event2	May 14, 18	8.63	9.43	0.92	3.04	8	20.5	126.7	565	162.3	565
Event3	Jun 21, 18	0.25	0.08	3.13	3.04	33	1.7	0.14	15	0.14	22
Event4	Jul 4, 18	0.76	0.08	9.50	3.04	33	1.3	0.14	15	0.13	20
Event5	Jul 08, 18	1.06	0.50	2.12	2.54	33	0.8	0.70	42	11.6	42
Event6	Jul 18, 18	7.87	0.57	13.81	33.5	8	1.4	50.6	50	34.2	50
Event7	Sep 03, 18	2.79	0.20	13.95	25.4	33	1.0	36.9	34	27.0	34
Event8	Sep 16, 18	6.09	0.08	73.13	60.9	11	2.5	55.3	31	47.9	31
Event9	Sep 26, 18	8.12	1.30	6.25	21.3	8	8.0	55.2	39	49.9	40

Table 6. EMC values for the analyzed nutrient components over collected storm events from SR40 and SR35 drainage area to the Basin 9b. Unit is mg/L.

	EMC - SR40 Road			EMC - SR35 Road			Ratio (SR40 to SR35)		
	NO_x	NH_3	TN	NO_x	NH_3	TN	NO_x	NH_3	TN
Event 1	0.22	0.16	1.46	0.15	0.16	0.68	1.5	1.1	2.2
Event 2	0.59	0.35	2.13	0.47	0.10	1.64	1.3	3.5	1.3
Event 3	0.60	0.31	2.75	1.02	0.08	2.31	0.6	4.2	1.2
Event 4	0.35	0.10	0.81	0.05	0.06	0.42	7.7	1.5	1.9
Event 5	0.43	0.09	0.82	0.05	0.05	0.37	9.0	1.7	2.2
Event 6	0.24	0.01	0.57	0.12	0.01	0.43	2.0	1.7	1.3
Event 7	0.06	0.03	0.54	0.01	0.04	0.44	5.4	0.8	1.2
Event 8	0.20	0.08	0.88	0.12	0.08	0.70	1.6	1.0	1.3
Event 9	0.15	0.20	1.73	0.12	0.06	0.93	1.3	3.5	1.8
Mean	0.32	0.15	1.30	0.23	0.07	0.88	1.4	2.1	1.5

3.6.1 Correlation analysis of storm and runoff water quality

The results of PCA analysis on runoff event-scale indicated that events can be classified into two categories considering nutrient supply, designated as the orientation of nutrient vectors (Figure 9). Events with positive scores on PC1 have relatively higher nutrient contents while events with negative scores on PC1 have relatively lower nutrient contents (Figure 9). Strong correlations among different nutrient species can be inferred, indicated as acute angles among their vectors. However, correlation between TN and NH_3 are nearly complete positive and they are correlated with ADP and rainfall depth, suggesting ADP and rainfall depth as influential factors on nutrient supplies and wash off (Figure 9). Though there are correlation among nutrient species, NO_x is uncorrelated with ADP, indicated as an orthogonal angle between their vectors, and likely suggesting additional source of its supply. Yet, π decision axis is more associated to TN and NH_3 rather than NO_x, which they are the more influential criterion on overall runoff nutrient loads. Hitherto, nutrient vectors are negatively correlated with rainfall intensity which suggests decrease in nutrient load by increase in storm intensity. The data variance (Δ) more than 80% presents that most of information is incorporated in the analysis (Figure 9). Similar patterns as Figure 8 are obtained for each individual watershed, which are not shown here.

To discern the impact of ADP on storm nutrient load, concentrations of nutrients in the collected samples were plotted against instantaneous flow rates (Figure 10). Storm runoff following longer ADP (e.g. Event2, Event1, and Event9) resulted in high concentrations of TN (> 1.6 mg/L) during high flow rates (> 1 L/s) while storms with shorter ADP (e.g. Event7 and Event6) resulted in lower concentrations of TN (< 0.7 mg/L) during the same range of flow rates

(Figure 10 and Table 5). Same as TN, the highest and lowest concentrations of NH_3 and NO_x were observed during storms with longest and shortest ADP (Figure 10). These results confirm ADP as a nutrient mass supply; however, the role of runoff as a flux transport capacity must be explored further. The background nutrient concentrations of roadways may be considered as potentially any concentrations <0.7 mg/L with respect to TN, and <0.1 mg/L for NH_3 and NO_x species inferred from boxplot concentration distributions (Figure 10).

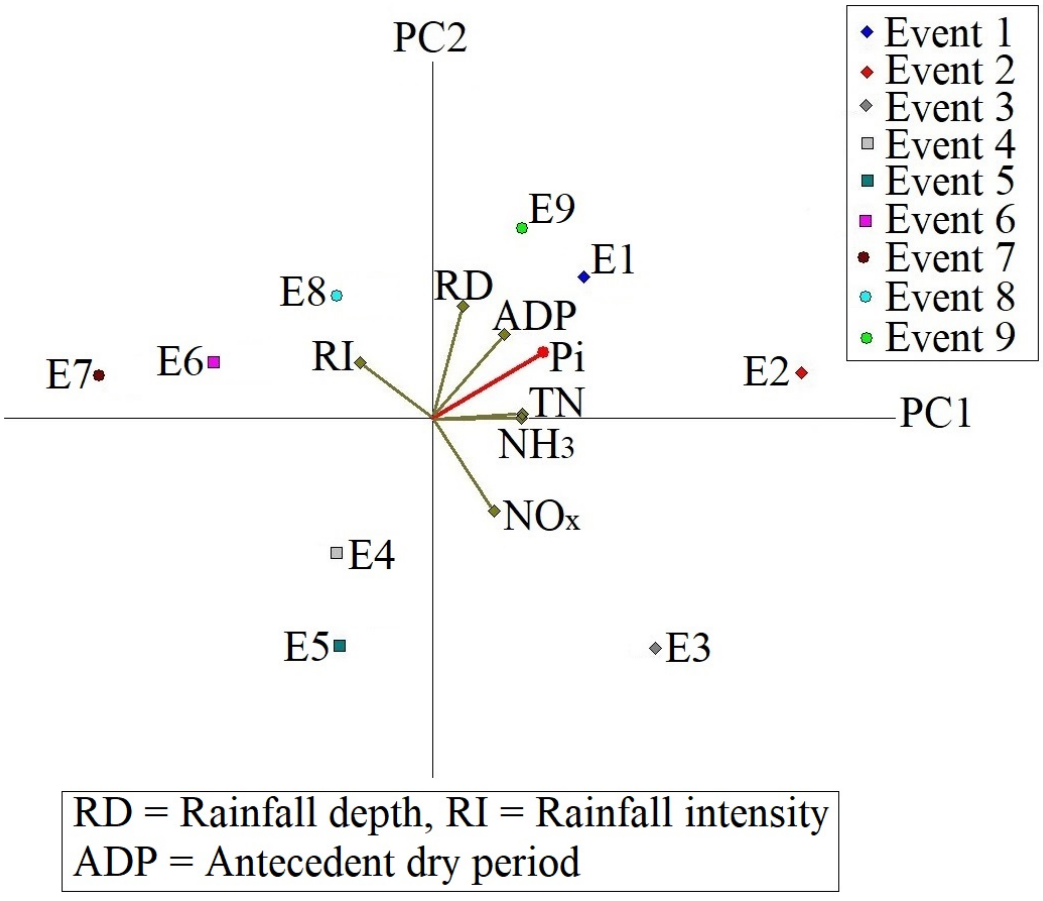

Figure 9. GAIA biplot presenting correlation among mean nutrient EMCs of West and east drainage roads and rainfall characteristics (Δ = 86 %) over collected storm events.

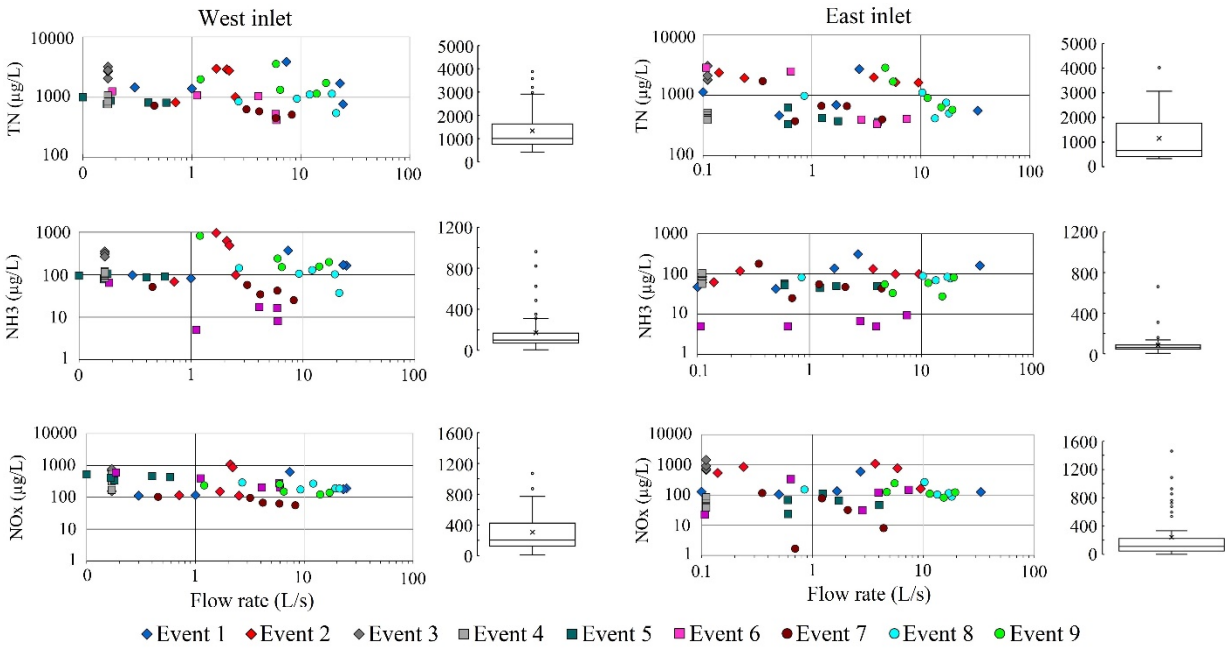

Figure 10. Concentrations of TN, NH_3, and NO_x in collected runoff samples against estimated instant flow rate from the West and East inlets and boxplot of concentration variation among all events. Note: the same color points are the synoptic runoff samples within a same event.

3.6.2 Runoff nutrient concentrations with correlation to runoff flux and storm properties

To discern the impacts of transport capacity (indicated by runoff volume) on runoff nutrient delivery, coupled cumulative runoff flux and instantaneous concentration measurements along with rainfall properties were considered for multi-criteria analysis. For this purpose, criteria were defined as concentrations of NO_x, NH_3, and TN of the samples specified as number 1 (runoff initial) to 5 (runoff tail) with estimated cumulative runoff, rainfall intensity, and ADP. Runoff events are classified according to nutrient load regime (Figure 11). As presented in GAIA biplot, positive correlation can be observed among nutrient vectors and they correlate with ADP, similar as PCA analysis in section 3.1. Projected data on the positive PC1 axis indicates higher nutrient concentrations while positive score on PC2 indicates increase in runoff volume. Correlation

between TN and NH_3 is higher and while NO_x and other two nutrient species are correlated with ADP in East drainage road, it is not correlated well with ADP in West drainage road (Figure 11). There is negative correlations among nutrient vectors with cumulative runoff and rainfall intensity, indicating decrease in nutrient concentrations with increase in stormwater runoff and rainfall intensity. A decreasing trend in nutrient concentrations from runoff initial to runoff tail can be concluded for some events (for example, Event1, Event2, and Event9) as imply by large distances between first and last actions and position of actions with respect to nutrient and flux vectors (Figure 11). However, nutrient concentration variation through runoff event was insignificant in limited runoff flux events (for example, Event3, Event4, and Event5) as designated by clustering actions on negative PC2 axis (Figure 11). This result suggest variation in nutrient delivery regime in different types of runoff events under the control of available nutrient supply and transport condition.

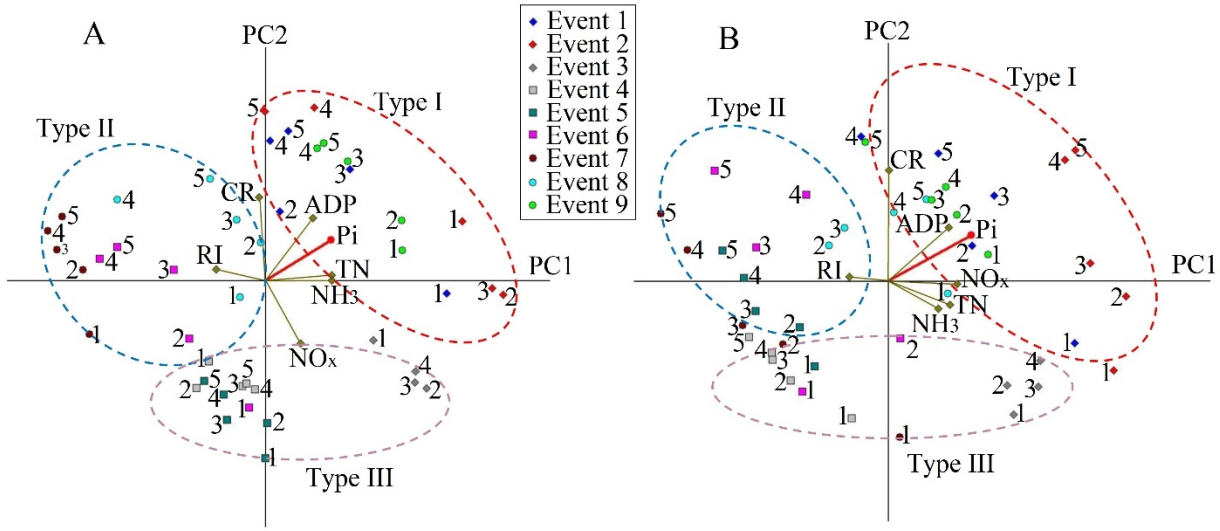

CR= Cumulative runoff, RI= Rainfall intensity, ADP= Antecedent dry period

Figure 11. GAIA biplot of the correlation among concentrations of TN, NH3, and NOx in collected runoff samples indicated as number 1 (initial runoff) to number 5 (runoff tail) considering estimated cumulative runoff (CR), average rainfall intensity (RI), and antecedent dry

period (ADP) from the SR40 (A) (Δ = 72.8) and the SR35 (B) (Δ = 67.1). Note: Event 3 has four analyzed samples.

The role of transport capacity may be more illustrated by comparing nitrogen delivery patterns in events with similar nutrient supply (similar ADP) but different transport capacity. For example, though Event1 and Event9 had similarly moderately high nutrient loads and high transport capacities, the peak flow rate of Event1 was roughly double that of Event9, and maximum rainfall intensity was approximately five times that of Event9, suggesting that Event1 had more capacity to mobilize and transport different forms of nitrogen (e.g. organic and inorganic nitrogen, dissolve and particulate loads). Both Event1 and Event9 had similar moderately high ADP, suggesting similar available nutrient loads for transport. While actual nutrient concentrations are not appreciably different, the two events present different nutrient delivery patterns with respect to different nitrogen species. For example, percent variation in concentrations of NO_x (filtered) and NH_3 (unfiltered) over runoff transport varied with same pattern and similarly over high intense runoff of Event1 while that varied antithetical in smaller runoff and lower intense storm of Event9 (Figure 12).

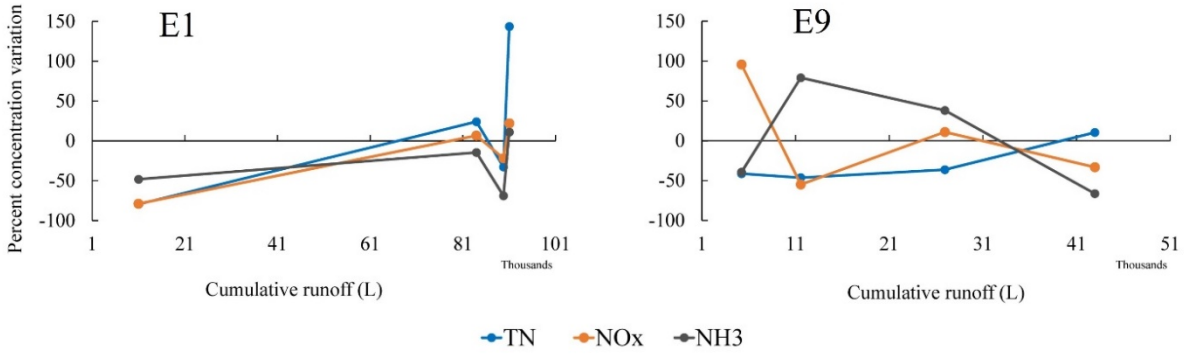

Figure 12. Percent variation in nutrient concentrations of collected samples over cumulated runoff in Event1 and Event9. Note: percent variation is calculated at each sampling based on concentrations of previous sample and so it could not be calculated for the first sample.

3.6.3 Runoff event type

Three runoff event types are discerned considering dominant physical components regulating nutrient load: nutrient supply and capacity of storm runoff flux to transport (Figure 13). Type I events which have relatively high nutrient supply and high transport capacity, type II events that have relatively low nutrient supply but high transport capacity, and type III events which have low transport capacity (either high or low nutrient supply) (Figure 13). The type I events are characterized by long ADP (> 5.5 days) and high runoff volume (> 50 m^3) while type II and III are characterized by short ADP (< 2.5 days) but higher runoff volume in type II (27 < R < ~50 m^3) than type III (< 11 m^3) (Table 5).

This presented runoff event type model is obtained from the PCA results that could discern relatively similar runoff events in terms of available nutrient supply and flux transport capacity with revealing similarity or difference of supply source for different nutrient species (Figure 11). This event type approach can resolve the problem associated to the traditional M(V) curve approach which disregarded the impacts of runoff volume and availability of nutrient supply (Bach et al., 2010). Since the runoff event type approach here confirms the major similarity of supply source for the considered nutrient species, M(V) curve analysis can be done for the species together in each runoff event type.

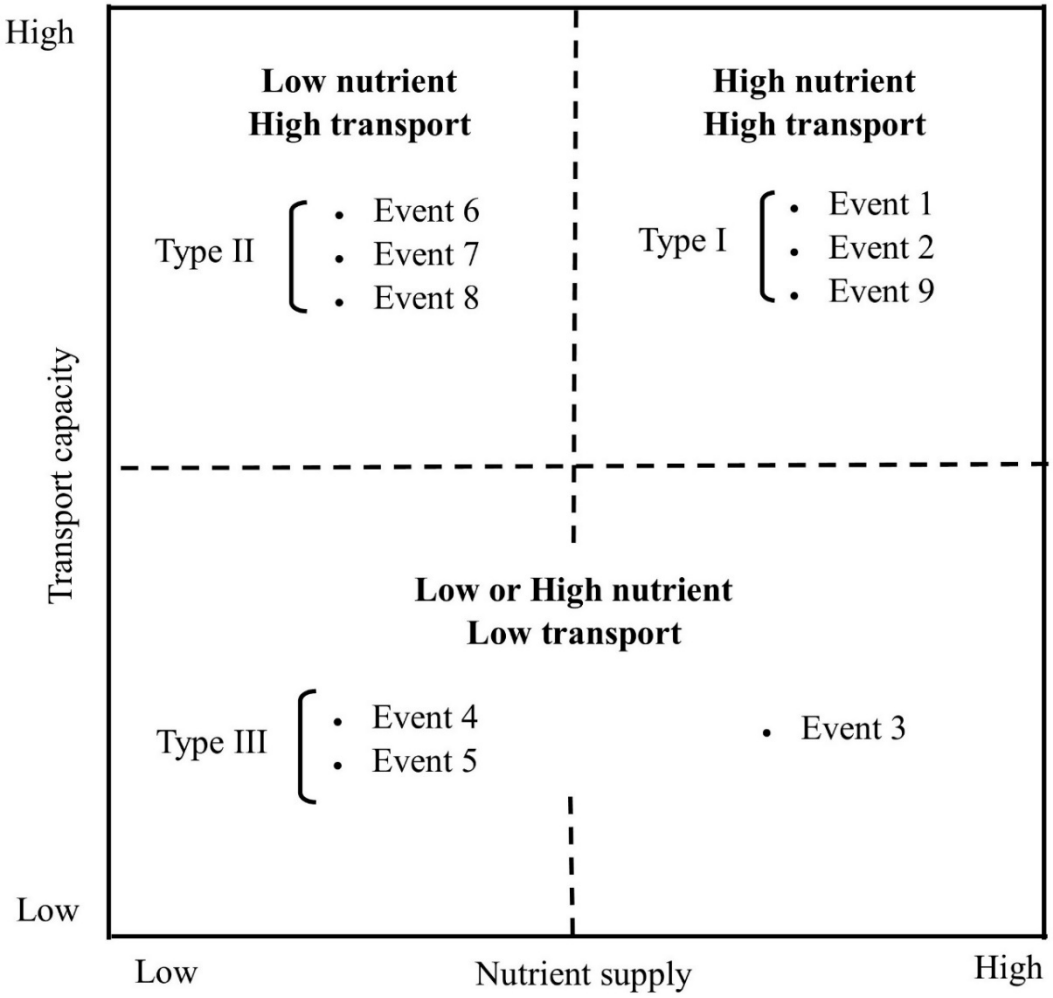

Figure 13. Different types of runoff event in term of nutrient supply and flux delivery conditions from roadways.

3.6.4 Mass nutrient and runoff volume event

The M(V) curves analyses indicated nutrient mass exceedance to runoff volume mostly over type I events rather than types II and III (Figure 14). Nutrient mass first-flush ratio is greater in the order of type I > type II > type III (Figure 14). For example, 50% of runoff volume in type I events can approximately deliver 0.50 to 0.70% of nutrient mass supply while that is about 0.43 to 0.60%

in type II events (regardless of observed unusual NO_x) and only about 0.37 to 0.63% in low transport capacity of type III events (Figure 14 and Table 7). The Wilcoxon rank sum test indicated a significant difference and greater first flush at MFF_{30} in type I than type II ($Z = -2.26$, $p < 0.05$) and type III ($Z = -3.25$, $p < 0.001$) (Table 8). Similarly, there is a significant difference and more nutrient mass delivery in type I rather than type II and III at MFF_{50}. However, there is not a statistically difference in nutrient delivery between type II and III (Table 8).

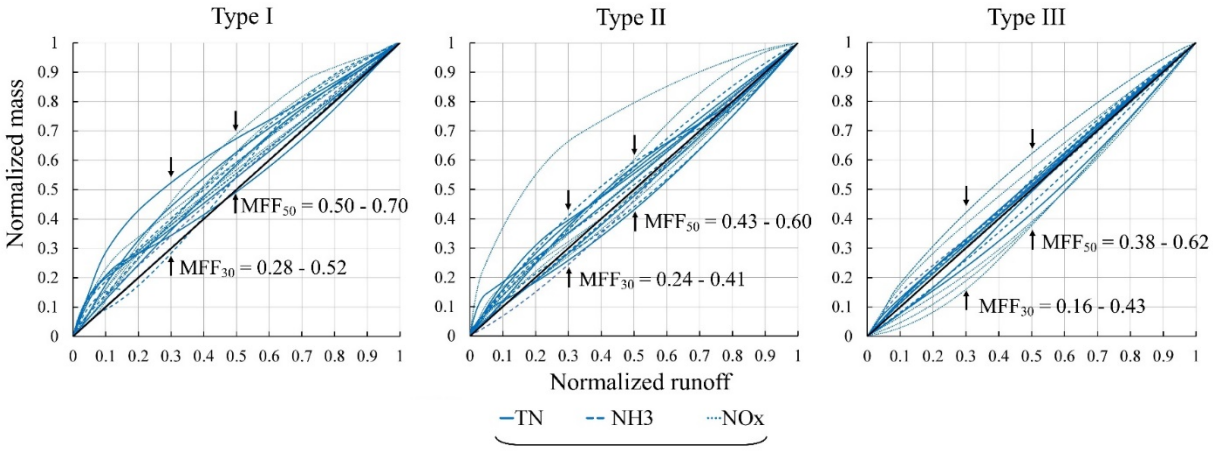

Figure 14. Normalized cumulative mass against normalized cumulative runoff of nutrients over different roadway runoff event types.

Table 7. Summary statistics of nutrient delivery considering MFF30 and MFF50 including maximum, minimum, mean, median, and percent relative standard deviation (RSD) of the event types.

	MFF_{30}			MFF_{50}		
	Type I	Type II	Type III	Type I	Type II	Type III
Max	0.52	0.41	0.43	0.69	0.60	0.62
Min	0.28	0.24	0.16	0.49	0.43	0.38
Mean	0.38	0.33	0.29	0.57	0.51	0.49
Median	0.38	0.35	0.31	0.58	0.51	0.51
RSD (%)	16.2	16.1	21.9	10.3	10.6	13.2

Table 8. Independent-sample t-test (95% confidence interval) for nutrient mass first-flush ratio at 30% (MFF30) and 50% (MFF50) between different runoff event types. Bolded and italic values are statistically significant.

	MFF_{30}		MFF_{50}	
	p	*Z*	*p*	*Z*
Type I vs. Type II	***.023***	-2.267	***.008***	-2.648
Type I vs. Type III	***.001***	-3.250	***.001***	-3.313
Type II vs. Type III	.098	-1.653	.380	-0.878

3.7 Discussion

BMP nutrient removal strategies can be designed cost-effectively based on a specific runoff event types that can wash off nutrient and decrease concentrations to a background level. Among the detected event types, type I events provide the most reliable information for designing remediation strategies. Nutrient exceedance to runoff volume in type I events indicated first flush occurrences (Lee et al., 2002), and deliver nutrient over early part of runoff events. However, type II events with low ADP, and most likely low nutrient mass over road surfaces than typical runoff events, may not be appropriate to be considered for BMP remediation strategy designs. The type III events with low transport capacity, regardless of ADP condition for low or high nutrient mass supply, may not potentially be capable of washing off available nutrient mass from surface of roadways. Due to low transport capacity, type III events, may deliver a greater nutrient mass over runoff tail and thus present end-flush occurrences. This phenomenon by nature confirms the weakness of runoff flux to wash off nutrients and thus treatment systems should not be designed based on such a type of events. As type III events are mostly observed with low runoff volume and

short runoff duration, which is in agreement with the detected storm events (Table 5) (Lee et al., 2002).

The calculated mean EMC for TN in West (1.3 mg/L) and East (0.88 mg/L) drainage roadways in this research are comparable and in agreement with reported mean EMC of TN for many roadways in Florida (1.56 mg/L) by Harper et al. (2007). Mean EMC of TN is also in agreement with that reported for many roadways in North Carolina, California, and Minnesota (Driscoll et al., 1990; Thomson et al., 1997; Barret et al., 2004; Kayhanian et al., 2007; Winston et al., 2012; Winston and Hunt, 2016). However, mean EMC of NO_x (0.28 mg/L) hereby is lower than mean NO_x concentrations (0.62 mg/L) reported for same roadways in the mentioned states. The observed high EMC of nutrients in low transport capacity of Event3 is in agreement with the statement provided by Bach et al. (2010) where low transport capacity events may present constant contaminant concentrations with high EMC.

ADP was detected as the most influential factor of runoff nutrient supply based on the PCA analysis. The detected strong correlation between ADP and runoff nutrient load is in agreement with analyzed roadway runoff in Colleague Station in Texas reported by Li and Barrett, (2008) which indicated ADP as the most significant predictor of runoff pollutant loads and positively correlated with AADT as well. However, uncorrelated relationship between ADP and runoff nutrient load is also reported for some collected roadway runoff (e.g. Irish et al., 1998; Liu et al., 2013). The higher ratio of nutrient EMCs and mass delivery in West drainage road than that in the East drainage road (Table 6) are in correlation with the higher AADT of the West road (mean 20,570 ± 514 for 2013-17) to that for the East road (mean 13,500 ± 770 for 2013-17). These findings are in agreement with the observed general increase in runoff nutrient contents with an

increase in the level of AADT in California roadways (Kayhanian et al., 2003). These observations suggest that ADP and AADT have important roles in roadway runoff nutrient load and with increase in both, higher background nutrient over surface of roadways should be expected that most be considered in analysis from site to sites.

The impact of rainfall intensity on runoff nutrient load may be more complex to be explored only by the PCA analysis. For example, no relationship was observed between rainfall depth and intensity with nutrient transport from street runoff catchments in Tampa Bay, Florida (Yang and Toor, 2017). However, a strong positive correlation was observed between rainfall intensity and TN load in the work of Liu et al. (2013). In another research, Egodawatta et al., (2007) pointed out a step-wise function based on rainfall intensity threshold between rainfall intensity and nutrient transport and Liu et al., (2013) stated rainfall intensity larger than 20 mm/h can transport more nutrients due to their relatively higher kinetic energy. However, research conducted by Miguntanna (2009) indicated higher nutrient transport in lower intensity rainfalls than higher intensity ones. These variations suggest the complex role of rainfall intensity on runoff nutrient load and further research may be needed.

It must be noted that in addition to nutrient supply and flow conditions, other factors (e.g. preferential transport way and rainfall intensity) may influence on nutrient delivery at a lower level. For example, TN and NH_3 behave similarly as the highest and lowest mass delivery were detected, respectively, during high nutrient and high flux of Event2 (type I) and low nutrient and high flux of Event6 (type II), while NO_x exhibits a different behavior (Figure 10). The concentrations of NO_x in Event6 was greater as compared to NH_3 and TN among the events (Figure 10). The observed difference may be associated to differential transport pathways of different

nitrogen species. Non-filtered samples (TN and NH_3) will include nutrients sorbed to sediment particles while filtered samples (NO_x) will reflect only dissolved constituents. The different transport with including likely spatial variation may be the reason for the observed larger ratio of EMC for NO_x in the West drainage area than the East drainage area during small frequent storms of Event4, Event5, and Event 7 (Table 6). The deviation of behavior was also evident in the PCA analysis, indicated as a stronger correlation between TN and NH_3 in the West drainage area and not correlated well with the NOx subspecies in comparison to the East drainage area (Figure 9). Moreover, the observed stronger first flush during Event9 but faster occurrences over Event1 may suggest the impact of rainfall intensity and likely tendency to deliver nutrient components sorbed to particulate forms (TN and NH_3) over higher rainfall intensity of Event9 than delivery in dissolved form over lower rainfall intensities of Event1.

Even though drainage areas leading to West and East inlets were similar in size and land cover, events of similar rainfall magnitude often produced different runoff responses. For example, while cumulative rainfall depth is comparable between storms in Event2 and Event6, peak intensity was much greater during Event6 (11 mm/h) as compared to Event2 (1.6 mm/h), producing very different runoff signatures. Despite similar recorded rainfalls, these two events produced very different cumulative runoff volumes (Table 5). This discrepancy here indicates the great uncertainty in extrapolating precipitation estimates based on point measurements to watershed scales, especially during small-scale convective storms. The high spatial variability of precipitation is also evident in storm on Event5, as much greater runoff is produced from the East drainage area (11.6 m^3) as compared to the West drainage area (0.7 m^3), despite similar watershed areas.

Nevertheless, further research should consider collecting more runoff events in different locations for comparison. Analyzing frequency of runoff event types should be conducted by collecting more runoff events before design of BMPs. Detailed analysis considering particulate form of nutrient delivery related to temporal variation of rainfall intensity and runoff flow conditions would be help to get further insight into dissolved and particulate form of delivery. Next research may consider analyzing initial background nutrient concentrations and concentrations after storms to ensure sufficient wash off by runoff events. Detailed DO/redox analysis and pH variation over storm events provide better understanding of the mechanism of nutrient delivery variation over events.

3.8 Conclusion

This research-field study characterized roadway runoff nutrient delivery in event-scale over different storm events. In overall, 18 rainfall-runoff events were collected from two roadway catchment areas, which deliver roadway runoff to a stormwater basin near Silver Springs, Florida. Each rainfall-runoff event was monitored through analyzing dynamic nutrient delivery of NH_3-N, NO_x-N, and TN concentrations using five synoptic water samples from runoff initiation to the end. Multivariate analyses considering rainfall characteristics, runoff volume and rate, and dynamic nutrient concentrations indicated that storms following long dry periods produced greater concentrations of nitrogen, reflecting greater mass loads on the roadways. Runoff events with greater volume (> 50 m3) could wash off and decrease nutrient concentrations to an estimated background concentration, identified as high transport flux capacities. Three types of runoff event were discerned considering dominant physical components on runoff nutrient loads: ADP and

transport capacity. Runoff events with high ADP (> 5.5 days) and high transport capacities (type I) presented greater mass first flush than runoff events with either low ADP (<2.5 days) and high transport capacity (type II) or low transport capacity events (< 11 m3) (type III). The presented runoff event type approach could resolve the inadequacies of traditional approach of analyzing nutrient mass delivery. While this research can be improved through collecting low temporal resolution runoff quality data, it is suggested that runoff event type approach to be considered for design of remediation strategies.

3.9 Acknowledgement

This research was supported by the Florida Department of Transportation. The opinions, findings and conclusions expressed in this publication are those of the author(s) and not necessarily those of the Florida Department of Transportation or the U.S. Department of Transportation. The authors would like to thank Dr. Dan Wen, Dr. Yuan Gao, Andrea Valencia, Eranildo Lustosa, Diana Ordonez, and Nyle Rice, who assisted in collecting runoff samples.

3.10 References

Abdul-Aziz, O.I. and Al-Amin, S., 2016. Climate, land use and hydrologic sensitivities of stormwater quantity and quality in a complex coastal-urban watershed. Urban Water Journal, 13(3), 302-320. https://doi.org/10.1080/1573062X.2014.991328

Bach, P.M., McCarthy, D.T. and Deletic, A., 2010. Redefining the stormwater first flush phenomenon. Water Research, 44(8), 2487-2498. https://doi.org/10.1016/j.watres.2010.01.022

Badruzzaman, M., Pinzon, J., Oppenheimer, J. and Jacangelo, J.G., 2012. Sources of nutrients impacting surface waters in Florida: a review. Journal of Environmental Management, 109, 80-92. https://doi.org/10.1016/j.jenvman.2012.04.040

Bertrand-Krajewski, J.L., Chebbo, G. and Saget, A., 1998. Distribution of pollutant mass vs volume in stormwater discharges and the first flush phenomenon. Water Research, 32(8), 2341-2356. https://doi.org/10.1016/S0043-1354(97)00420-X

Blanco-Canqui, H., Gantzer, C.J., Anderson, S.H., Alberts, E.E., Thompson, A.L., 2004. Grass barrier and vegetative filter strip effectiveness in reducing runoff, sediment, nitrogen, and phosphorus loss. Soil Science Society of America Journal, 68(5), 1670-1678. https://doi.org/10.2136/sssaj2004.1670

Boger, A.R., Ahiablame, L., Mosase, E. and Beck, D., 2018. Effectiveness of roadside vegetated filter strips and swales at treating roadway runoff: A tutorial review. Environmental Science: Water Research & Technology, 4(4), pp.478-486. https://doi.org/10.1039/D1EW00235J

Borris, M., Viklander, M., Gustafsson, A.M. and Marsalek, J., 2014. Modelling the effects of changes in rainfall event characteristics on TSS loads in urban runoff. Hydrological Processes, 28(4), 1787-1796. https://doi.org/10.1002/hyp.9729

Bouchard, D.C., Williams, M.K., Surampalli, R.Y., 1992. Nitrate contamination of groundwater: sources and potential health effects. Journal-American Water Works Association 84(9), 85-90. https://doi.org/10.1002/j.1551-8833.1992.tb07430.x

Brezonik, P.L. and Stadelmann, T.H., 2002. Analysis and predictive models of stormwater runoff volumes, loads, and pollutant concentrations from watersheds in the Twin Cities metropolitan area, Minnesota, USA. Water Research, 36(7), 1743-1757. https://doi.org/10.1016/S0043-1354(01)00375-X

Brodie, I.M. and Egodawatta, P., 2011. Relationships between rainfall intensity, duration and suspended particle washoff from an urban road surface. Hydrology Research, 42(4), 239-249. https://doi.org/10.2166/nh.2011.117

Christian, L., Epps, T., Diab, G. and Hathaway, J., 2020. Pollutant Concentration Patterns of In-Stream Urban Stormwater Runoff. Water, 12(9), p.2534. https://doi.org/10.3390/w12092534

Eller, K.T. and Katz, B.G., 2017. Nitrogen Source Inventory and Loading Tool: An integrated approach toward restoration of water-quality impaired karst springs. Journal of Environmental Management, 196, 702-709. https://doi.org/10.1016/j.jenvman.2017.03.059

Florida Traffic Online., 2017. Florida Department of Transportation. An online data source (https://tdaappsprod.dot.state.fl.us/fto/), Accessed: Nov, 14, 2018.

Franco, J. and Matamoros, V., 2016. Mitigation of polar pesticides across a vegetative filter strip. A mesocosm study. Environmental Science and Pollution Research, 23(24), 25402-25411. https://doi.org/10.1007/s11356-016-7516-1

Grant, G.E., Schmidt, J.C. and Lewis, S.L., 2003. A geological framework for interpreting downstream effects of dams on rivers. Water Science and Application, 7, 209-225. https://doi.org/10.1029/007WS13

Harper, H.H., Baker, D.M., 2007. Evaluation of current stormwater design criteria within the state of Florida. Florida Department of Environmental Protection, p. 327.

Hathaway, J.M. and Hunt, W.F., 2011. Evaluation of first flush for indicator bacteria and total suspended solids in urban stormwater runoff. Water, Air, & Soil Pollution, 217(1-4), 135-147.

Heffernan, J.B., Liebowitz, D.M., Frazer, T.K., Evans, J.M. and Cohen, M.J., 2010. Algal blooms and the nitrogen-enrichment hypothesis in Florida springs: evidence, alternatives, and adaptive management. Ecological Applications, 20(3), 816-829. https://doi.org/10.1890/08-1362.1

Hicks, R. and Holland, K., 2012. Nutrient TMDL for Silver Springs, Silver Springs Group, and Upper Silver River (WBIDs 2772A, 2772C, and 2772E). Ground Water Management Section, Florida Department of Environmental Protection, Tallahassee, FL.

Horstmeyer, N., Huber, M., Drewes, J.E., Helmreich, B., 2016. Evaluation of site-specific factors influencing heavy metal contents in the topsoil of vegetated infiltration swales. Science of the Total Environment 560, 19-28. https://doi.org/10.1016/j.scitotenv.2016.04.051

Huang, J., Du, P., Ao, C., Ho, M., Lei, M., Zhao, D. and Wang, Z., 2007. Multivariate analysis for stormwater quality characteristics identification from different urban surface types in

Macau. Bulletin of Environmental Contamination and Toxicology, 79(6), 650-654. https://doi.org/10.1007/s00128-007-9297-1

Hu, D., Zhang, C., Ma, B., Liu, Z., Yang, X. and Yang, L., 2020. The characteristics of rainfall runoff pollution and its driving factors in Northwest semiarid region of China-A case study of Xi'an. Science of The Total Environment, p.138384. https://doi.org/10.1016/j.scitotenv.2020.138384

Huber, W.C., Dickinson, R.E., Barnwell Jr, T.O. and Branch, A., 1988. Storm water management model; version 4. Part A. User's Manual. U.S. Environmental Research Agency. Office of Research and Development: Washington, DC.

Irish Jr, L.B., Barrett, M.E., Malina Jr, J.F. and Charbeneau, R.J., 1998. Use of regression models for analyzing highway storm-water loads. Journal of Environmental Engineering, 124(10), 987-993. https://doi.org/10.1061/(ASCE)0733-9372(1998)124:10(987)

Jeong, H., Choi, J.Y., Lee, J., Lim, J. and Ra, K., 2020. Heavy metal pollution by road-deposited sediments and its contribution to total suspended solids in rainfall runoff from intensive industrial areas. Environmental Pollution, 265, p.115028. https://doi.org/10.1016/j.envpol.2020.115028

Jiang, R., Woli, K.P., Kuramochi, K., Hayakawa, A., Shimizu, M. and Hatano, R., 2010. Hydrological process controls on nitrogen export during storm events in an agricultural watershed. Soil Science & Plant Nutrition, 56(1), 72-85. https://doi.org/10.1111/j.1747-0765.2010.00456.x

Kayhanian, M., Fruchtman, B.D., Gulliver, J.S., Montanaro, C., Ranieri, E., Wuertz, S., 2012. Review of highway runoff characteristics: Comparative analysis and universal implications. Water Research 46(20), 6609-6624. https://doi.org/10.1016/j.watres.2012.07.026

Kayhanian, M., Singh, A., Suverkropp, C. and Borroum, S., 2003. Impact of annual average daily traffic on highway runoff pollutant concentrations. Journal of environmental engineering, 129(11), 975-990. https://doi.org/10.1061/(ASCE)0733-9372(2003)129:11(975)

Khalil, W.A.S., Goonetilleke, A., Kokot, S. and Carroll, S., 2004. Use of chemometrics methods and multicriteria decision-making for site selection for sustainable on-site sewage effluent disposal. Analytica Chimica Acta, 506(1), 41-56. https://doi.org/10.1016/j.aca.2003.11.003

Kleinman, P.J., Srinivasan, M.S., Dell, C.J., Schmidt, J.P., Sharpley, A.N. and Bryant, R.B., 2006. Role of rainfall intensity and hydrology in nutrient transport via surface runoff. Journal of Environmental Quality, 35(4), 1248-1259. https://doi.org/10.2134/jeq2006.0015

Lapointe, B.E., Barile, P.J. and Matzie, W.R., 2004. Anthropogenic nutrient enrichment of seagrass and coral reef communities in the Lower Florida Keys: discrimination of local versus regional nitrogen sources. Journal of Experimental Marine Biology and Ecology, 308(1), 23-58. https://doi.org/10.1016/j.jembe.2004.01.019

Lee, J.H., Bang, K.W., Ketchum Jr, L.H., Choe, J.S. and Yu, M.J., 2002. First flush analysis of urban storm runoff. Science of the Total Environment, 293(1-3), 163-175. https://doi.org/10.1016/S0048-9697(02)00006-2

Li, D., Wan, J., Ma, Y., Wang, Y., Huang, M. and Chen, Y., 2015. Stormwater runoff pollutant loading distributions and their correlation with rainfall and catchment characteristics in a rapidly industrialized city. PloS one, 10(3), p.e0118776. https://doi.org/10.1371/journal.pone.0118776

Liao, X., Nair, V.D., Canion, A., Dobberfuhl, D.R., Foster, D.K. and Inglett, P.W., 2019. Subsurface transport and potential risk of phosphorus to groundwater across different land uses in a karst springs basin, Florida, USA. Geoderma, 338, 97-106. https://doi.org/10.1016/j.geoderma.2018.11.005

Liu, A., Egodawatta, P., Guan, Y. and Goonetilleke, A., 2013. Influence of rainfall and catchment characteristics on urban stormwater quality. Science of the Total Environment, 444, 255-262. https://doi.org/10.1016/j.scitotenv.2012.11.053

Liu, S., Chen, F.L. and Xue, J., 2017. Evaluation of traffic density parameters as an indicator of vehicle emission-related near-road air pollution: A case study with NEXUS measurement data on black carbon. International Journal of Environmental Research and Public Health, 14(12), p.1581. https://doi.org/10.3390/ijerph14121581

Mahbub, P., Ayoko, G.A., Goonetilleke, A., Egodawatta, P. and Kokot, S., 2010. Impacts of traffic and rainfall characteristics on heavy metals build-up and wash-off from urban roads.

Environmental Science & Technology, 44(23), 8904-8910. https://doi.org/10.1021/es1012565

Mallin, M.A., Johnson, V.L., Ensign, S.H., 2009. Comparative impacts of stormwater runoff on water quality of an urban, a suburban, and a rural stream. Environmental Monitoring and Assessment 159(1), 475-491. https://doi.org/10.1007/s10661-008-0644-4

Miguntanna, N.P., 2009. Nutrients build-up and wash-off processes in urban land uses (Doctoral dissertation, Queensland University of Technology).

Paerl, H.W., 1997. Coastal eutrophication and harmful algal blooms: Importance of atmospheric deposition and groundwater as "new" nitrogen and other nutrient sources. Limnology and Oceanography, 42(5part2), 1154-1165. https://doi.org/10.4319/lo.1997.42.5_part_2.1154

Pappas, E.A., Smith, D.R., Huang, C., Shuster, W.D., Bonta, J.V., 2008. Impervious surface impacts to runoff and sediment discharge under laboratory rainfall simulation. Catena 72(1), 146-152. https://doi.org/10.1016/j.catena.2007.05.001

Phelps, G.G., 2004. Chemistry of ground water in the Silver Springs Basin, Florida, with an emphasis on nitrate (p. 54). US Department of Interior, US Geological Survey.

Phelps, G.G., Walsh, S.J., Gerwig, R.M. and Tate, W.B., 2006. Characterization of the hydrology, water chemistry, and aquatic communities of selected springs in the St. Johns River Water Management District, Florida, 2004 (No. 2006-1107, pp. 0-0).

Pitt, R., Clark, S., Field, R., 1999. Groundwater contamination potential from stormwater infiltration practices. Urban Water 1(3), 217-236. https://doi.org/10.1016/S1462-0758(99)00014-X

Sansalone, J.J. and Buchberger, S.G., 1997. Partitioning and first flush of metals in urban roadway storm water. Journal of Environmental Engineering, 123(2), 134-143. https://doi.org/10.1061/(ASCE)0733-9372(1997)123:2(134)

Shoemaker, W.B., O'Reilly, A.M., Sepúlveda, N., Williams, S.A., Motz, L.H. and Sun, Q., 2004. Comparison of estimated areas contributing recharge to selected springs in north-central Florida by using multiple ground-water flow models. Tallahassee, FL.

Sun, Z., Brittain, J.E., Sokolova, E., Thygesen, H., Saltveit, S.J., Rauch, S. and Meland, S., 2018. Aquatic biodiversity in sedimentation ponds receiving road runoff–What are the key drivers?. Science of The Total Environment, 610, 1527-1535. https://doi.org/10.1016/j.scitotenv.2017.06.080

Suthar, S., Bishnoi, P., Singh, S., Mutiyar, P.K., Nema, A.K., Patil, N.S., 2009. Nitrate contamination in groundwater of some rural areas of Rajasthan, India. Journal of Hazardous Materials 171(1), 189-199. https://doi.org/10.1016/j.jhazmat.2009.05.111

Trenouth, W.R. and Gharabaghi, B., 2016. Highway runoff quality models for the protection of environmentally sensitive areas. Journal of Hydrology, 542, 143-155. https://doi.org/10.1016/j.jhydrol.2016.08.058

Valtanen, M., Sillanpää, N. and Setälä, H., 2014. The effects of urbanization on runoff pollutant concentrations, loadings and their seasonal patterns under cold climate. Water, Air, & Soil Pollution, 225(6), p.1977. https://doi.org/10.1007/s11270-014-1977-y

Wanielista, M., and Yousef, Y., 1993. Stormwater management. John Wiley & Sons, Inc., New York, N.Y., 1-579

Wang, S., Zhao, M., Xing, J., Wu, Y., Zhou, Y., Lei, Y., He, K., Fu, L. and Hao, J., 2010. Quantifying the air pollutants emission reduction during the 2008 Olympic Games in Beijing. Environmental Science & Technology, 44(7), 2490-2496. https://doi.org/10.1021/es9028167

Wen, D., Valencia, A., Lustosa, E., Ordonez, D., Shokri, M., Gao, Y., Rice, N., Kibler, K., Chang, N.B. and Wanielista, M.P., 2020. Evaluation of green sorption media blanket filters for nitrogen removal in a stormwater retention basin at varying groundwater conditions in a karst environment. Science of The Total Environment, 719, p.134826. https://doi.org/10.1016/j.scitotenv.2019.134826

Winston, R.J. and Hunt, W.F., 2016. Characterizing runoff from roads: Particle size distributions, nutrients, and gross solids. Journal of Environmental Engineering, 143(1), p.04016074. https://doi.org/10.1061/(ASCE)EE.1943-7870.0001148

Wu, J.S., Allan, C.J., Saunders, W.L. and Evett, J.B., 1998. Characterization and pollutant loading estimation for highway runoff. Journal of Environmental Engineering, 124(7), 584-592. https://doi.org/10.1061/(ASCE)0733-9372(1998)124:7(584)

Yang, Y.Y., and Toor, G.S., 2017. Sources and mechanisms of nitrate and orthophosphate transport in urban stormwater runoff from residential catchments. Water Research, 112, 176-184. https://doi.org/10.1016/j.watres.2017.01.039

Zhao, S., Liu, S., Hou, X., Cheng, F., Wu, X., Dong, S. and Beazley, R., 2018. Temporal dynamics of SO_2 and NO_x pollution and contributions of driving forces in urban areas in China. Environmental Pollution, 242, 239-248. https://doi.org/10.1016/j.envpol.2018.06.085

CHAPTER 4 CONTAMINANT TRANSPORT FROM STORMWATER MANAGEMENT AREA TO A FREASHWATER KARST SPRING IN FLORIDA: RESULTS OF NEAR-SURFACE GEOPHYSICAL INVESTIGATION AND TRACER EXPERIMENTS

4.1 Preface

This chapter describes the configuration of karst condition under stormwater management areas and how potentially contaminated stormwater may move from stormwater management area to and within karst aquifers near Silver Springs. The contents of this chapter are under review at the Journal of Hydrology: Regional Studies[3].

4.2 Abstract

Silver Springs is a karst spring in north-central Florida. As landuses in the springshed have urbanized in recent decades, concentrations of contaminants, including nitrate, have increased in spring water, causing environmental concerns. Pathways of groundwater movement from stormwater management areas to Silver Springs were investigated using ground-based geophysical surveys (ground penetrating radar and frequency domain electromagnetics) accompanied by tracer tests in the Upper Floridan Aquifer (UFA) and surficial aquifer. Results indicated heterogeneous near-surface and deep karst conditions, where stormwater runoff may be transported quickly through groundwater to the spring. A wide range of groundwater velocities (10^{-6} to 10^{-3} ms^{-1}) were observed in the surficial aquifer, where faster flow speeds were associated with subsurface

[3] Shokri, M.; Gao, Y., Kibler, K.M., Wang, D; Wanielista, M., Wightman, M.J., Rice, N., under-revision. Contaminant transport from stormwater management areas to a freshwater karst spring in Florida: results of near-surface geophysical investigations and tracer experiments. Journal of Hydrology: Regional Studies.

anomalies and preferential flow. However, tracer injected into the UFA was observed in the spring hours later, suggesting possible maximum groundwater velocities on the order of 10^{-1} ms^{-1} in the karst aquifer. Series of tracer pulses in the spring highlight the complexity of flow pathways to Silver Springs. Aquifer dispersivity was estimated to be 1.8 m. The rapid transport of tracer from stormwater basins to Silver Springs suggests that stormwater infiltration basins may be hotspots for potential aquifer and spring contamination in karst areas. Development of stormwater best management practices (BMPs) that integrate heterogeneous karst transport processes may enhance spring and groundwater quality in Silver Springs and other karst regions.

4.3 Introduction

Karst aquifers are important resources of fresh water characterized by specific geologic and hydrogeologic conditions (Ford and Williams, 2013; Ficco and Sasowsky, 2018; Goldscheider et al., 2020). Within karst aquifers, surface and underground openings (e.g. sinkholes and conduits) are formed by the dissolution of karstic rocks (limestone and dolomite) and groundwater flows within a heterogeneous system governed by the combination of matrix porosity, fracture porosity, and conduit porosity (Shuster and White, 1971; White, 1998; Bakalowicz, 2005; Hartmann et al., 2014; Yang et al., 2019). The rock dissolution and flow heterogeneity can render groundwater susceptible to surface contamination, particularly where karst features are exposed at the surface, or where surface soils are thin and the groundwater table is shallow (Stephenson et al., 1999; Katz, 2001; Zhou and Beck, 2005; Shokri et al., 2016; Katz, 2019). For example, since the 1960s nitrogen concentrations have steadily increased in Silver Springs, a first-magnitude karst spring in north-central Florida discharging water from the Floridan aquifer system (FDEP, 2006, 2012;

Hicks and Holland, 2012). The increase in nitrogen concentration has been attributed to increases in urban, residential, and agricultural land uses in the springshed (Heffernan et al., 2010; Yang et al., 2019; Gao et al., 2020). Increase in nitrogen concentration can cause water quality degradation, algal blooms, and eutrophication (Eller and Katz, 2017; Glibert, 2017).

Given the unique hydrogeology of karst areas, where groundwater flows may be orders of magnitude higher than in alluvial aquifers (Kačaroğlu, 1999), contaminant transport from the surface to and within karst aquifers may be rapid (Worthington and Ford, 2009; Husic et al., 2020a and b). For example, average groundwater velocity in Dinaric karst was measured in the range of 1.7 to 47,500 m/d (Milanovic, 1981; Kačaroğlu, 1999) and as 5,280 m/d in a travertine karst aquifer in Antalya, Turkey (Günay and Ekmekçi, 1997). By contrast, groundwater velocity is typically less than 1 m/d in alluvial aquifers (Matthess and Pekdeger, 1985; Essouayed et al., 2019). High groundwater velocities in karst systems may influence subsurface biogeochemical processes by limiting opportunity for biogeochemical transformation and nutrient uptake, producing high nutrient concentrations at discharge points (Puckett and Cowdery, 2002; Dubrovsky et al., 2010). Conservative tracers can provide information about hydraulic connections between injection and monitoring points, allowing for estimation of aquifer characteristics and residence time (Kačaroğlu, 1999, Corbett et al., 2000; Flury and Wai, 2003; Worthington and Soley, 2017; Aley, 2019, Lauber et al., 2014). Analysis of breakthrough tracer curves can also provide knowledge about potential dispersivity of contaminants in an aquifer (ex. Geyer et al., 2007; Massei et al., 2006; Morales et al., 2007; Goldscheider et al., 2008). Further, ground-based geophysical techniques including ground penetrating radar (GPR) and electromagnetic (EM) response can detect subsurface preferential flow paths in karst regions (Militzer et al., 1979; Smith, 1986; Butler,

1984; Doolittle and Collins, 1998; Ahmed and Carpenter, 2003; Jardani et al., 2007; Zhu et al., 2011; Chalikakis et al., 2011).

While management of non-point source contamination in karst aquifers requires a basinwide approach, stormwater infiltration areas may be locations of particular vulnerability, as diffuse pollutants are concentrated to these locations during runoff events (Weiss et al., 2008; Moore and Beck, 2018). The typically thin surface soils found in epikarst of well-developed karst areas may allow contaminated surface water, such as urban stormwater runoff, to discharge into groundwater through open sinkholes or infiltrate relatively quickly through subsurface karst features and fractures, potentially limiting the effectiveness of stormwater management basins in attenuating contaminants (Byle, 2001; Behroozi, 2019). For example, stormwater management basins are typical stormwater best management practices (BMPs) applied in karst areas of Florida and must be permitted as meeting specific design and performance standards to guarantee water quality and quantity requirements of the stormwater management system (e.g. Harper and Baker, 2007; ERP, 2013). However, even though geometric designs, minimum infiltration rates and vadose zone capacities are specified (e.g. retention basins should infiltrate runoff within 24 to 72 hours of event, should have minimum unsaturated subsurface storage 0.3 to 1 m above the seasonal groundwater table, and side-slopes should not be steeper than 3:1), the presence of subsurface anomalies and sinkholes may increase expected infiltration rates and negatively influence treatment performance. A better understanding of how stormwater management basins function within karst areas can help establish better strategies for stormwater management, groundwater protection, and water quality restoration. To address these research gaps and provide guidance for stormwater runoff management, the objective of this research is to characterize subsurface conditions in stormwater

management basins within the Silver Springs springshed and to observe travel times of shallow and deep groundwater flow from stormwater management basins to surface discharge in Silver Springs. This study is one of the first to directly investigate how stormwater may be transported to and within karst aquifers, which is important information for water resources managers aiming to protect or remediate water quality in karst regions.

4.4 Methodology

4.4.1 Study area

The Silver Springs springshed (approximately 2,362 km^2) discharges groundwater to Silver Springs, one of the largest karst springs in Florida (Knowles et al., 2010; German 2010) (Figure 15). Silver Springs is located 10 km east of the city of Ocala and forms the headwaters of the Silver River, where flow gauged at the Silver River monitoring station (USGS 02239501) represents combined discharge from multiple spring vents. The climate of north-central Florida is humid subtropical with warm, rainy summers (June to September) and mild, dry winters with mean annual precipitation and temperature of about 1,520 mm and 22 °C, respectively (NOAA, 2017). The mean annual groundwater discharge (1933–2007) from Silver Springs is about 22.7 m^3/s, mainly supplied by the Upper Floridan Aquifer (UFA), which is a sequence of thick (300 – 460 m) eogenetic karst (Phelps, 2004; Phelps et al., 2006; Knowles et al., 2010). The majority of groundwater flow in the UFA (about 86%) occurs in the top 30 m of the aquifer, which is a granular limestone and the dolomite formation of Ocala Limestone (Upper Eocene) (Faulkner, 1970; Knowles et al., 2010). The UFA is separated from a perched surficial aquifer (Pliocene to Holocene) by a semi-confining unit of interbedded quartz, sand, silt, and clay of the Hawthorn

Group (Miocene) (Knowles et al., 2002; Phelps, 2004). The surficial aquifer consists of sand, silty sand, to clay sediments of varied thickness and may be locally absent where carbonate rocks are exposed (Phelps, 2004; Knowles, 1996). Geomorphologically, the Silver Springs springshed has a low gradient (55 m of relief), and the lowest elevation corresponds to the location of main Silver Springs vents, forming a local base level for groundwater. The dissolution of karst rocks has resulted in numerous shallow sinkholes, depressions and fractures distributed around Silver Springs (Faulkner, 1970; Phelps, 2004).

Three study areas (Basins 1-3) within the Silver Springs springshed were chosen, forming a transect across the springshed in the direction of expected prevalent groundwater flow (west to east, Figure 15, Table 9). The study areas are all dry stormwater management basins where stormwater runoff from surrounding roadways drains into the basins and infiltrates to recharge the groundwater system through basin soils. Basin 1 (29º12’55” N and 82º03’30” W) is owned and managed by Florida Department of Transportation and Basins 2 (29º12’06” N and 82º05’01” W) and 3 (29º11’57” N and 82º05’53” W) are managed by the City of Ocala. Bore-hole data obtained in the basins indicated the existence of a surficial aquifer consisting of unconsolidated sand and silty sandy soil from the surface to about 3 m depth, a consolidated semi-confining unit of quartz, sand, silt, and clay of from 3 to 6 m depth, and limestone below 6 m (Kibler et al., 2020). Several sinkholes had been reported in Basins 2 (eleven) and 3 (fourteen) (Florida Department of Transportation, 2019) (Figure 1 B). The presence of these known sinkholes indicates that these basins may be potential hotspots for groundwater contamination. Basin 1 was chosen for study due to its proximity to the main vents of Silver Springs. During initial field surveys, three sinkholes

were observed in Basin 2 (including a large open sinkhole) and two sinkholes were observed in Basin 3, including a large collapsed sinkhole and a deep small soil pipe (Figure 16).

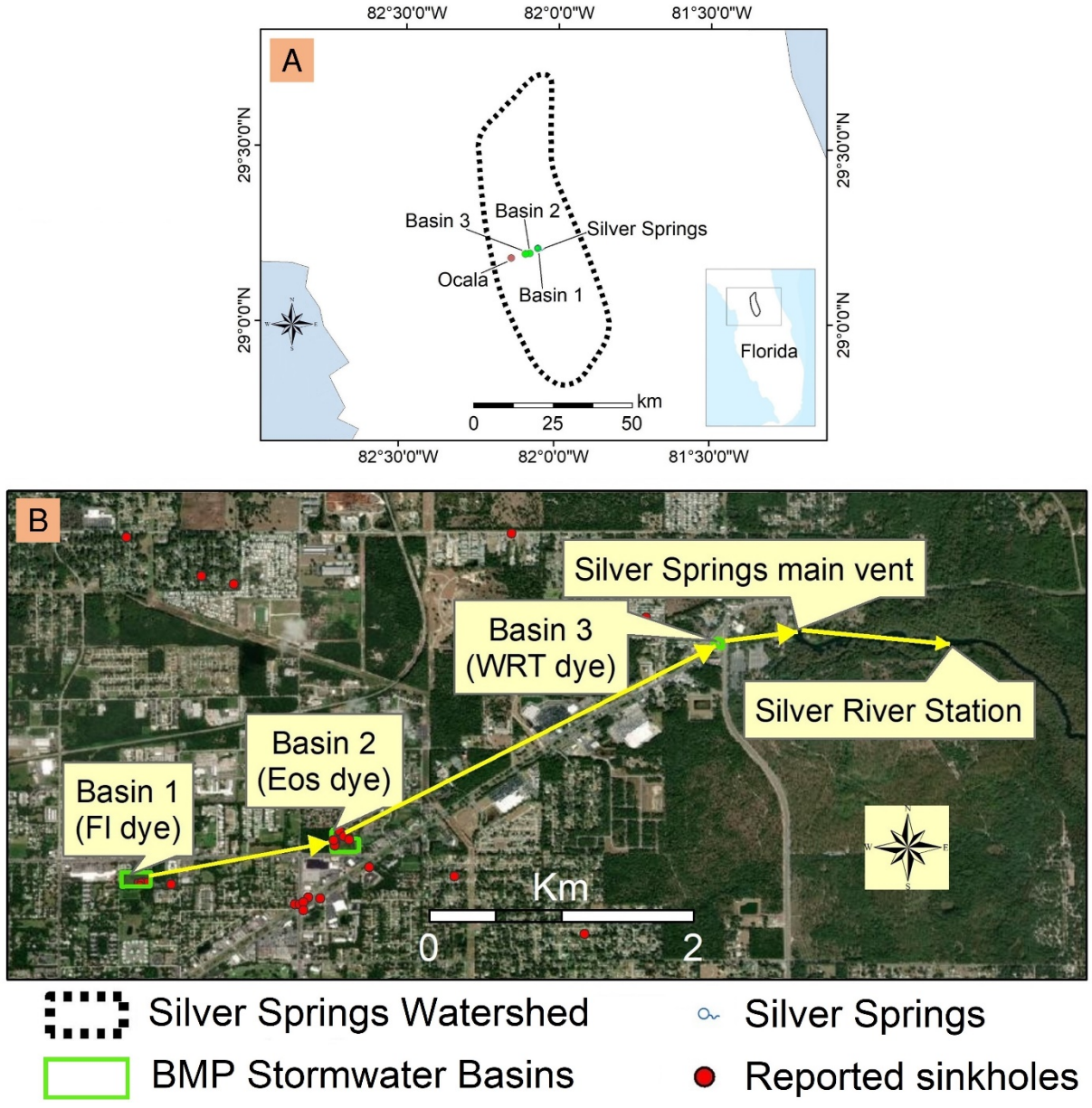

Figure 15. Silver Springs location in Florida (A), stormwater retention basins investigated with respect to the Silver Springs main vent and Silver River monitoring station (B).

Table 9. Study basin characteristics and near-surface anomalies detected by GPR survey.

	Basin 1	Basin 2	Basin 3
Latitude and longitude	29º12’55” N 82º03’30” W	29º12’06”N 82º05’01”W	29º11’57” N 82º05’53” W
Elevation at bottom of basin (m a.m.s.l)	13.0	13.4	17.0
Basin area (ha)	1.56	2.45	1.56
Distance to Silver River station (m)	1600	4100	5800
Number of anomalies detected	53	1	64
Anomaly depth (m)	0.5 to 6.7	6	0.6 to 6

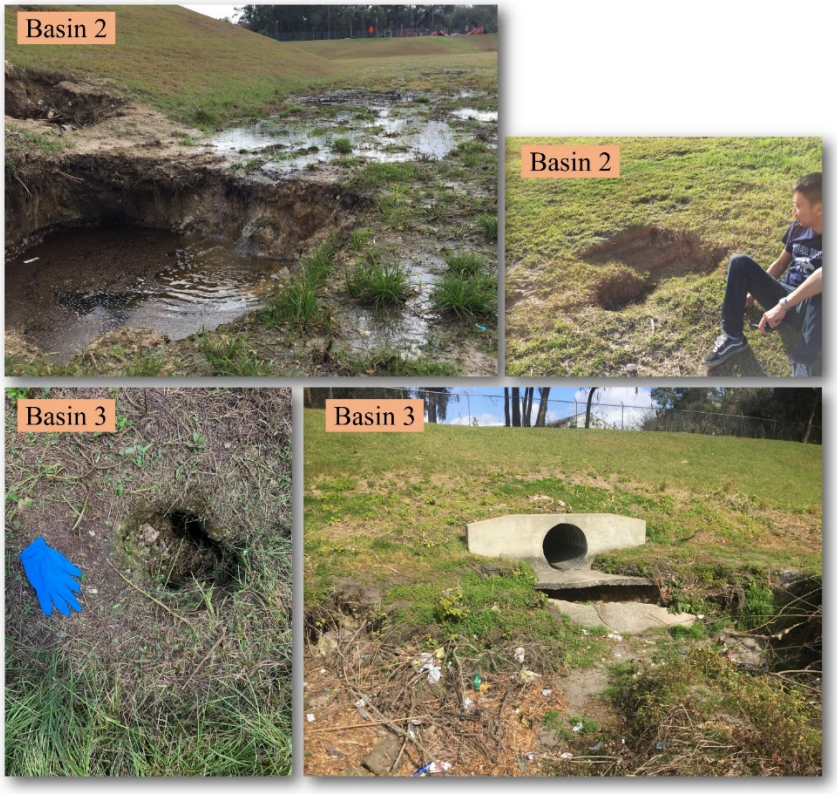

Figure 16. Open and collapsed sinkholes in Basins 2 and 3, observed during field surveys. Runoff was observed directly discharging into the local surficial aquifer through the open sinkhole in Basin 2. Photos were taken in Feb 2019 by Mohammad Shokri.

4.4.2 Experimental procedure

4.4.2.1 Geophysical surveys

The subsurface of study areas was characterized to a maximum depth of 15 m below surface using two geophysical methods, GPR and EM. GPR was performed using a GSSI SIR 3000 with a 270 mega-Hertz (MHz) antenna using 512 samples per scan. The GPR was used to detect subsurface geological features (anomalies) to depths of 6 to 6.7 m that could be related to development of buried karst features. GPR data were collected on 3-m grids across each site using a time range setting of 110 nano-seconds (ns) for Basin 1 and 150 ns for Basins 2 and 3. EM data were collected over 6 m transects using a Geonics EM34-3 with a 10 m coil separation. The EM responses were used to understand the spatial variation of subsurface conductivity across the basins, where areas of low signal conductivity typically represent higher hydraulic conductivities (Chalikakis et al., 2011). The EM data were collected using both a vertical coplanar (horizontal dipole) and horizontal coplanar (vertical dipole) coil configurations, providing an effective exploration range of 7.5 m and 15 m, respectively (McNeill, 1980).

Based on results from the GPR survey and severe anomalies, a transect of monitoring wells was established across 5 km of the springshed, establishing one well in each Basin 1 to 3. The 10 cm diameter wells were installed to depths that allowed tracer injection directly into the UFA (6.0 m in Basin 1 and 7.6 m in Basins 2 and 3, Figure 15 and Figure 17). In addition to the monitoring wells installed in the UFA (hereafter ‘deep’ wells), a network of 12 relatively shallow (3.0 m depth) monitoring wells (hereafter ‘shallow’ wells) was installed within the surficial aquifer of Basin 1 (Figures 1 and 3). Groundwater level was monitored continuously (15 min interval) in the surficial aquifer of Basin 1 in well 7 over the first tracer experiment using pressure sensors

(ONSET HOBO U20 and U20L) installed at the ground surface and at a depth of 3 m. Groundwater level was measured in the deep wells at the start of the second tracer test. Inflow runoff volumes from the roadway into Basin 1 were determined from pressure transducers installed in stilling wells near runoff inlets (Wen et al., 2020). Groundwater discharge at Silver Springs was obtained from the USGS Silver River monitoring station.

4.4.2.2 Tracer tests

Tracer experiments were undertaken under natural flow field conditions to evaluate groundwater flow in the surface aquifer in the vicinity of Silver Springs and in the UFA across a section of the Silver Springs basin. To characterize shallow groundwater flows in the vicinity of Silver Springs, approximately 7.0 kg of Rhodamine WT (RWT) was injected on July 25, 2017 into the surficial aquifer from Well 0 in Basin 1 (Figure 17), followed by 1,420 L of water at a rate of 0.25 Ls^{-1}. RWT tracer was monitored within the shallow well network in Basin 1 and at the Silver River station, located approximately 1.7 km from the injection point and 1.1 km from the main Silver Springs discharge vent (Figure 15). The tracer was assumed to travel from the injection point to the main Silver Springs vent (Mammoth Spring) and then flow in the Silver River as open channel flow to the Silver River station. Groundwater from the wells and spring water samples (200 mL) were collected with hand pumps and portable pump samplers (Sigma 900Max) and tested in triplicate for mean tracer concentration over a period of 9 months following tracer injection. Water samples were collected at short intervals (every 1 – 2 hours) immediately after tracer injection and gradually increased (to once a day and once a week) as time progressed from the time of injection.

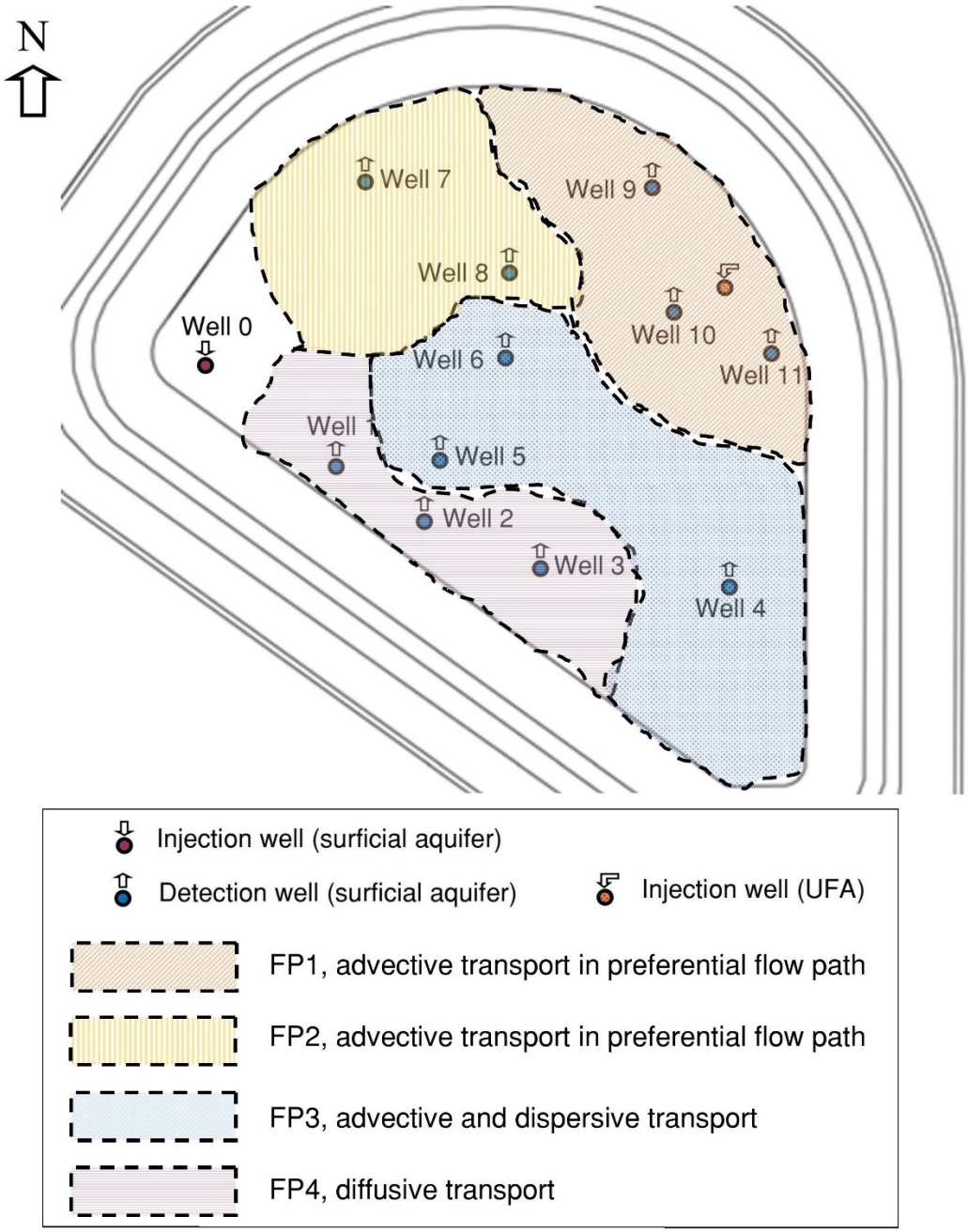

Figure 17. Locations of tracer injection and monitoring wells established in surficial aquifer in Basin 1.

When RWT was no longer detectable in Silver Springs (nearly 2 years after first tracer injection), a second tracer test was undertaken at the springshed scale. Three tracer dyes with distinctive emittance, RWT, Eosine (Eos), and Fluorescein (Fl) (OZARK Underground Lab, Inc.), were injected into the UFA through the deep monitoring wells (Figure 15). Tracers (11.3 kg of RWT, 13.6 kg of Eos, and 11.3 kg of Fl) were diluted with water (1:5) before simultaneous injection into deep wells in Basins 1, Basin 2, and Basin 3 on May 22, 2019, followed by flushing with 1,130 L water (Figure 15). Groundwater and spring water samples were collected regularly from deep wells in Basins 1 and 2 and from the Silver River monitoring station and tested for tracer concentration over a period of 9 months from tracer injection. Sampling started at 1 h intervals at the time of tracer injection and increased to 3.5, 10, and 24 hr intervals.

All tracer samples were kept in dark cool conditions (< 5 °C) and tracer concentration was measured in triplicate after filtration through a 0.2 micron nylon membrane. Concentrations of RWT and Fl were measured using two absorbance channels of an AquaFlour handheld fluorimeter while Eos concentrations were measured using a RF 5000 spectrofluorophotometer (Farmer and Blew, 2010; Aley and Beeman, 2015; Aley, 2019). All readings were converted to ppb equivalents using calibration curves created using standard solutions of known concentration for each tracer.

4.4.2.3 Analysis methods

GPR data were processed using Radan 7 software and adjustments were made to remove air-ground contacts in order to provide an accurate estimation of the depth to GPR signal reflectors. A dielectric constant of 6 was chosen for the analysis, which is appropriate for semi-saturated sandy sediments in Florida. GPR anomalies were identified based upon the localized increase in

penetration depth and amplitude of the GPR signal at depth relative to the surrounding areas. EM transects were interpolated to contour maps of conductivity using Kriging geospatial methods. The GPR and EM results were compared qualitatively to detect convergence in conductivity gradients and locations of subsurface anomalies, which guided the placement of monitoring wells.

Maximum and average pulse groundwater velocities were estimated, based respectively on the first arrival time of tracer after injection (Knochenmus, 1967; Taylor and Greene, 2008; McGurk et al., 2012) or the time of peak tracer concentration (Knochenmus, 1967; McGurk et al., 2012; Yang et al., 2019). Groundwater velocity was estimated considering the straight-line distance between injection and monitoring points (L), and the time (t) elapsed from tracer injection to the detection of tracer above background (to estimate maximum velocity, v_{max}) or the time of peak concentration (to estimate average pulse velocity, v). Hydraulic gradient was estimated considering the water table elevation difference and distance between monitoring wells and the local base flow level in Silver Springs main vent. Using the maximum observed groundwater velocity, Reynolds number (R_e) was estimated (Equation 9) (Czachor, 2011), where ρ [M L^{-3}] and μ [M L^{-1} T^{-1}] are the density and dynamic viscosity of water, v_{max} [L T^{-1}] is the maximum observed groundwater velocity, d and θ are the pore diameter [L] and porosity [L L^{-1}] (respectively 0.5 mm and 0.3 for sandy soil).

$$R_e = \frac{\rho v_{max} d}{\mu(1-\theta)} \quad (9)$$

The breakthrough curve of RWT in the Silver River station indicated a positive skewness which could possibly be a result of non-equilibrium effects created by immobile-fluid regions

(Field and Pinsky, 2000; Goldscheider, 2008). To estimate dispersivity in such a case, a two-region non-equilibrium transport model was fit to the RWT breakthrough curve (Equations 10 and 11).

$$\boldsymbol{\beta R \frac{\partial C_1}{\partial t} = \frac{D}{vL}\frac{\partial^2 C_1}{\partial Z} - \frac{\partial C_1}{\partial Z} - \omega(C_1 - C_2) - \mu_1 C_1} \quad (10)$$

$$\boldsymbol{(1-\beta) R \frac{\partial C_2}{t'} = \omega(C_1 - C_2) - \mu_2 C_2} \quad (11)$$

where, D [$L^2\ T^{-1}$] is longitudinal dispersion coefficient, v [$L\ T^{-1}$] is the pulse velocity, estimated from the timing of tracer peaks, C_1[Dimensionless] and C_2 [Dimensionless] represent volume-averaged solute concentrations in the flowing and stagnant regions, respectively, and μ_1 and μ_2 refer to dimensionless solute decay in equilibrium and non-equilibrium regions, respectively (Field and Pinsky, 2000). t' and Z are dimensionless time and space variables, respectively. The partition coefficient β describes the proportion of mobile water ($0 < \beta < 1$), where high values indicate a high proportion of mobile water affecting solute transport and R is adjustable model parameter (Field and Pinsky, 2000). The mass transfer coefficient ω describes exchange between the two fluid regions ($\omega > 0$), where high values mean intense mass transfer between two fluid regions. Equations 2 and 3 were solved numerically using the QTRACER2 program and the model was fitted following Toride et al., (1999) and EPA, (2002). For this estimation, 297 data points were applied.

4.5 Results

4.5.1 Geophysical surveys

GPR data detected many subsurface anomalies at depths ranging from 0.5 to 6.7 m below the local surface in the basins (Table 9). Respectively 53 and 64 near-surface anomalies (potential

karst features) were detected in Basins 1 and 3 (detailed locations can be obtained in supplementary kml file). The GPR profiles suggest wide and relatively deep anomalies, potentially due to sediment depression in surficial aquifer due to water percolation (Figure 18). The spatial distribution of detected anomalies in Basin 3 correlated well with the locations of the reported and observed sinkholes (Figure 15 and Figure 19). Despite the presence of reported and observed sinkholes in Basin 2, only one minor near-surface anomaly was detected by GPR (Figure 19 C and D and Table 9). Observed sinkholes and GPR anomalies were found within regions characterized by low EM signal conductivity (Figure 15 and Figure 19), which is associated with areas of low clay content, greater hydraulic conductivity and subsurface groundwater drainage routes (Kovalevsky et al., 2004). Despite the higher sensitivity of the vertical dipole mode to geological anomalies (Nobes, 1999; Caminha-Maciel and Figueiredo, 2013), data taken from the horizontal dipole mode provided a better correlation with observed sinkhole locations (Figure 19). In Basin 1, the EM data were spurious, potentially due to interference from surrounding utilities.

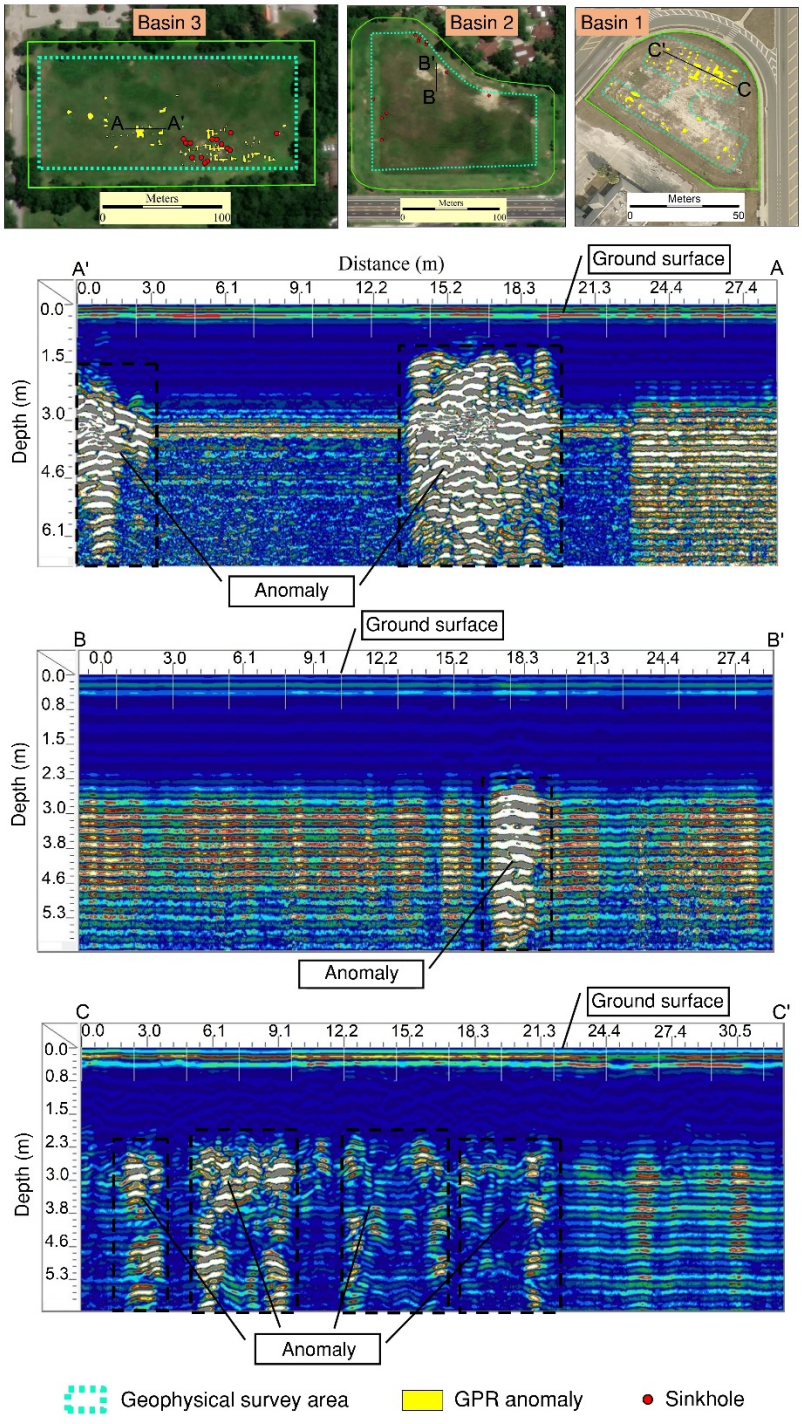

Figure 18. Example of GPR profiles and location of detected anomalies and sinkhole data.

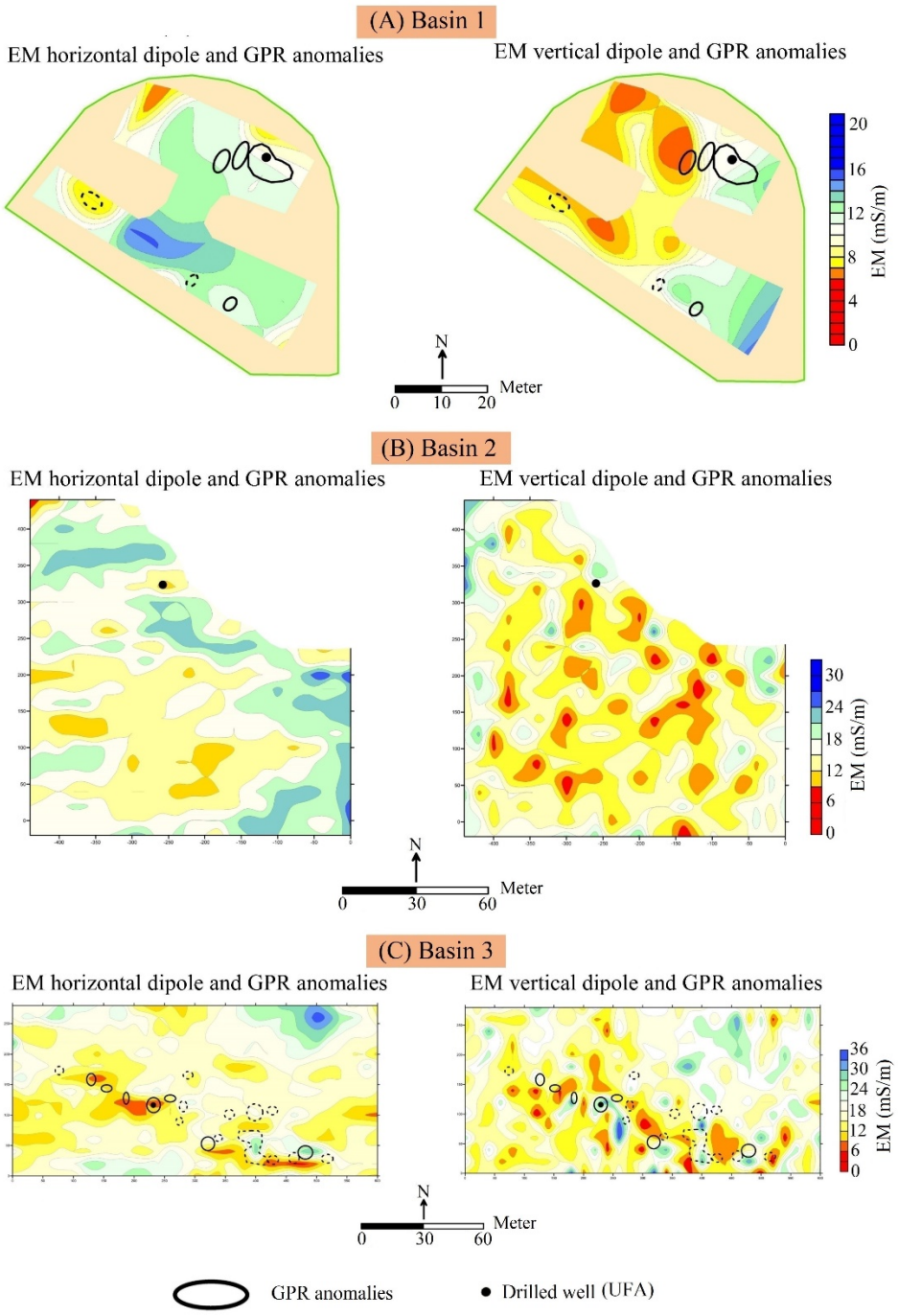

Figure 19. Spatial variation of EM conductivity in the horizontal (7.5 m depth) and vertical (15 m depth) dipole and locations of likely karst features based on GPR anomalies in Basin 1 (A), Basin 2 (B), and Basin 3 (C). Well location is the site of wells for tracer injection into UFA.

4.5.2 Solute transport in surficial aquifer

After RWT was introduced into the surficial aquifer of Basin 1 near Silver Springs, the range of observed maximum horizontal groundwater flow speeds (10^{-3} to 10^{-6} m/s, Table 10) estimated based on first instances of tracer detection in the wellfield suggests variable flowpaths and transport mechanisms of shallow groundwater in the spring vicinity. Tracer movement revealed four distinctive patterns of groundwater flow behavior that varied according to location relative to the tracer injection site (Figure 17 and Table 10). The first flow pattern (FP1) with the fastest travel time (9.2 to 438.7 m/d, R_e from 0.04 to 1.9) was seen in wells 9 to 11, located northeast of the injection site along the predominant direction of the regional groundwater flow (towards Silver Springs) and within a region where severe subsurface anomalies were detected by GPR (Figure 17, Figure 18, Figure 19, and Figure 20 A). Tracer was detected almost immediately after injection (less than one hour in wells 10 and 11) (Table 10). The second flow pattern (FP2) was observed in wells 7 and 8 with velocity in range of 1.2 to 1.4 m/d (R_e from 7.6×10^{-3} to 8.8×10^{-3}, Figure 17 and Figure 20 B). Tracer was detected after 13 days in wells 7 and 8, following a heavy rainfall that discharged approximately 182 m^3 of stormwater runoff to the basin (R_1) (Figure 20). Infiltration of the stormwater runoff led to local increase in elevation of the groundwater table, which may have accelerated transport of the tracer.

The third flow pattern (FP3) was characterized by a lower groundwater velocity (0.3 to 0.8 m/d, R_e from 2.1×10^{-3} to 5.2×10^{-3}) observed in wells 1–3, which were located southeast of the injection site (Table 10). Tracer was detected in wells 1-3 about 35 days after injection (Figure 20 C). A rainfall event occurred 21 days after the injection, discharging approximately 148 m^3 stormwater runoff (R_2) to the basin that could have likely driven the tracer movement;

simultaneous tracer pulses associated within this runoff event are detected in wells 7-11 (Figure 20 A and B). The fourth flow pattern (FP4) with the lowest maximum groundwater velocity (0.2 to 0.4 m/d, R_e from 1.2×10^{-3} to 2.5×10^{-3}) was seen in wells 4 - 6 after about 107 to 128 days from the injection (Figure 17, Figure 20 D, and Table 10). The tropical Hurricane Irma (R_3) occurred on day 48 following tracer injection (Figure 20). This event discharged about 1,907 m^3 stormwater runoff to the basin and increased groundwater levels for weeks, presumably opening up new subsurface flowpaths. Despite this, tracer did not appear in wells 4 to 6 until 59 days after the storm (Figure 20 D).

RWT was first detected at the Silver River monitoring station 3.5 hours after injection into well 0 in Basin 1, suggesting a maximum velocity of about 10,900 m/d (0.13 m/s) between the surficial aquifer and the monitoring point in Silver River (Figure 20 E, Table 10). The hydraulic gradient was estimated during this time as 4.7×10^{-3}. The breakthrough curve in Silver River indicated four distinct concentration pulses, the first peaking at 53.1 ppb, 42 days after tracer injection (Figure 20 E). The second, third, and fourth peak concentrations ranged from 26.1 – 39.5 ppb and were observed respectively 115, 177, and 246 days after injection. Based upon these tracer pulses, pulse groundwater velocities between the surficial aquifer in Basin 1 and Silver Springs are estimated in the range of 2.3 to 13.5 m/d (Table 11). Groundwater flow discharge in Silver Springs increased from 11.6 to 20.3 m^3/s over the monitoring period with a relatively sharp increase after Hurricane Irma (R_3), which closely followed the first observed peak concentration (Figure 20 E). The hydraulic gradient from the surficial aquifer to the spring increased from 3.9×10^{-3} to 4.2×10^{-3} following the hurricane. It is likely that the elevated groundwater table and

spring discharge that lasted weeks after the hurricane had an influence to the delivery of tracer following the first observed peak.

Table 10. Maximum groundwater velocities in surficial aquifer and UFA estimated by time of first tracer detection.

Tracer test	Injection point and tracer	Detection point		Distance from injection (m)	Time to first detection (days)	Maximum velocity (m/d)	Maximum velocity (m/s)
Surficial aquifer	Basin 1, well 0 RWT	FP1	Well 10	35.1	0.1	440.0	5.1×10^{-3}
			Well 11	42.7	0.6	68.0	7.8×10^{-4}
			Well 9	36.6	4.0	9.2	1.1×10^{-4}
		FP2	Well 8	24.4	17.0	1.4	1.6×10^{-5}
			Well 7	18.3	15.2	1.2	1.4×10^{-5}
		FP3	Well 3	29.0	35.0	0.8	9.6×10^{-6}
			Well 2	20.5	35.0	0.6	6.7×10^{-6}
			Well 1	12.5	35.0	0.3	3.9×10^{-6}
		FP4	Well 4	42.7	107.0	0.4	4.6×10^{-6}
			Well 5	21.4	107.0	0.2	2.3×10^{-6}
			Well 6	24.4	128.0	0.2	2.2×10^{-6}
		Silver River		1600	0.2	10,900.0	1.3×10^{-1}
UFA	Basin 1, deep well RWT	Silver River		1600	0.08	19,200.0	2.2×10^{-1}
	Basin 2 Eos	Basin 1		2900	NA	NA	NA
		Silver River		4100	NA	NA	NA
	Basin 3 Fl	Basin 2		1400	6.0	230.0	2.7×10^{-3}
		Basin 1		4300	NA	NA	NA
		Silver River		5800	NA	NA	NA

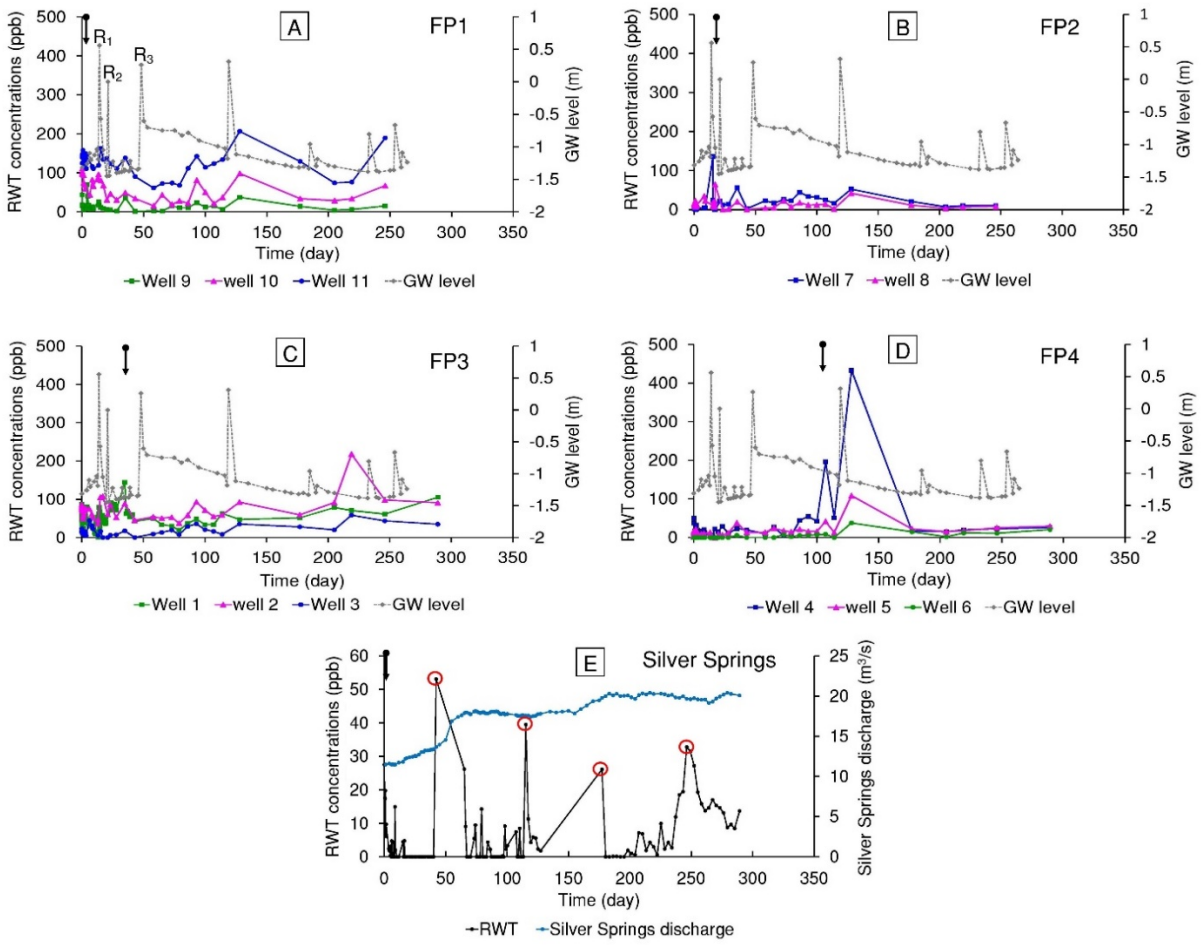

Figure 20. Tracer (RWT) concentrations observed in shallow wells of Basin 1 (A-D) and in Silver River (E) after tracer injection to the surficial aquifer. Groundwater table elevations relative to local ground surface and Silver Springs discharge are shown. Black arrows indicate the approximate time of first tracer detection in the well groups.

4.5.3 Solute transport in Upper Floridan Aquifer

The RWT injected into the UFA from Basin 1 was detected above background at the Silver River station about two hours, indicating a maximum UFA groundwater velocity of 19,200 m/d (0.22 m/s) in the vicinity of Silver Springs (Figure 21 A, Table 10) while the hydraulic gradient was estimated as about 4.7×10^{-3}. Reynolds number of the observed maximum groundwater velocities (71 and 121, calculated assuming flow through porous media, Eq 1) indicates turbulent flow condition. It is therefore unlikely that this flow was sustained through a homogenous porous medium, but instead was transported through conduit flow. Following the first detection, tracer concentrations remained low for several days but began to increase steadily after about 8 days and reached a peak concentration of 4.6 ppb after about 70 days (Figure 21 A). Concentrations returned to near baseline by around 140 days and then increased again in a lower, more diffuse peak about 245 days from the injection (Figure 21 A). Pulse groundwater velocities based on timing of these tracer peaks were about 2.3 to 7.9 m/d (Table 11). The breakthrough curve indicated that most detected tracer traveled to the spring within about 100 days after the injection (Figure 21 A). and that the bulk of this mass was captured from 8 to 100 days after injection. A two-region non-equilibrium model fitted to the main breakthrough curve suggests that the dispersivity of the aquifer is about 1.8 meters.

Neither Eos from Basin 2 nor Fl from Basin 3 injected into the UFA were observed at the Silver River monitoring station (Table 10). Eos was never observed in any monitoring location. The hydraulic gradient between Basin 2 and Silver Springs and Basin 3 and Silver Springs was estimated as 3.5×10^{-4} and 2.3×10^{-4}, respectively. However, Fl was detected in the UFA below

Basin 2 approximately 6 days after injection in Basin 3, suggesting a maximum groundwater velocity between Basins 3 and 2 of 233 m/d (Figure 21 B, Table 10) under a hydraulic gradient of about 2.2×10^{-4}. The observed Fl concentration increased slowly after detection from 0.08 to 1.9 ppb (by around 61 days), then increased rapidly to 18.3 ppb by 86 days (Figure 21 B). From 86 to around 200 days, Fl concentrations remained largely at a steady state, varying between 18.3 and 22.7 ppb. Concentrations began to increase again after 214 days and continued to increase through the cessation of monitoring (Figure 21 B).

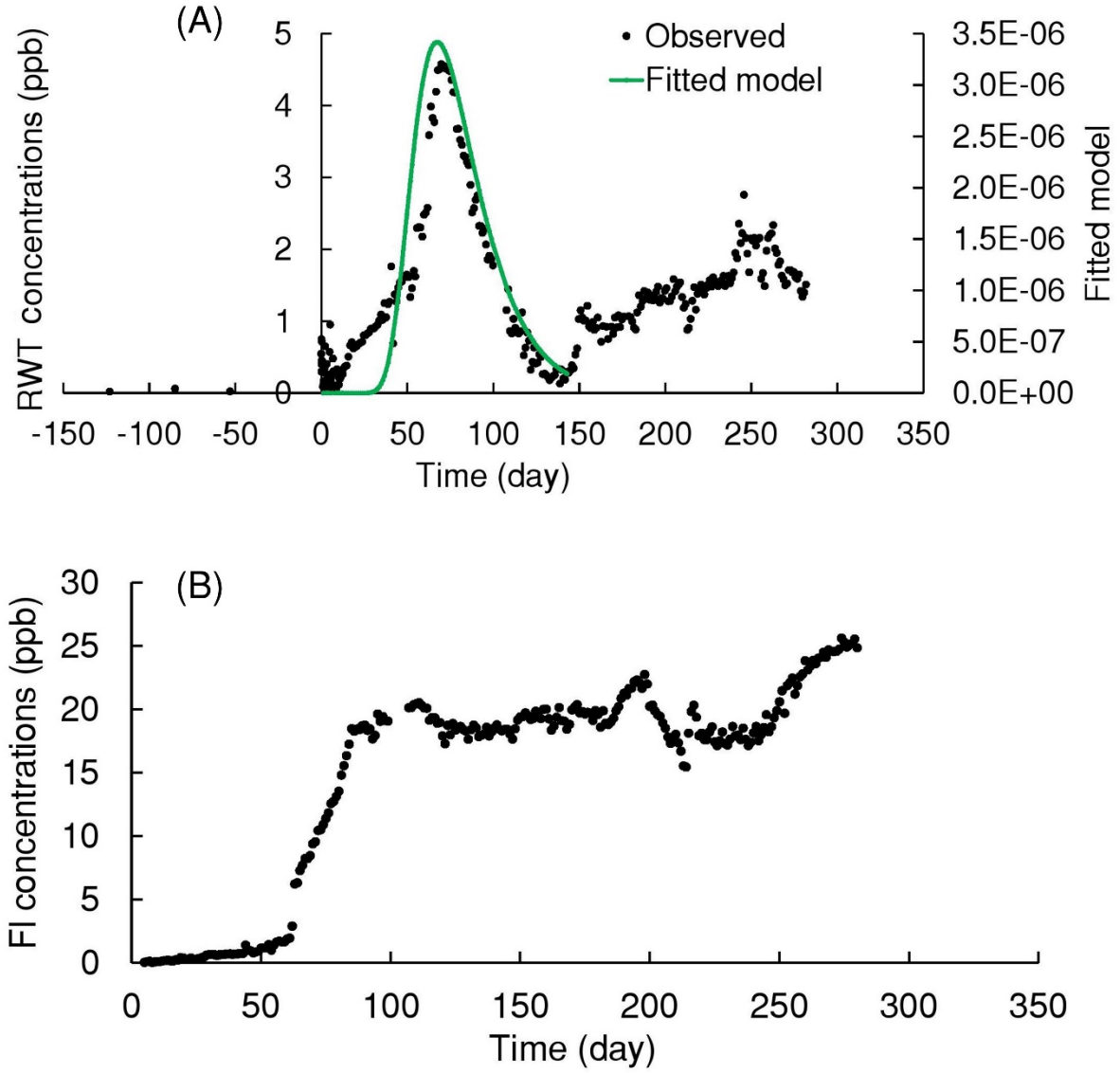

Figure 21. Tracer concentrations observed after injection into UFA: RWT (injected at Basin 1) concentration observed at Silver River station (A) and Fl (injected at Basin 3) concentrations observed in Basin 2 (B). Time at zero is the tracer injection time and measured background concentrations in Silver Springs are presented in the months before tracer injection.

Table 11. Average pulse groundwater velocities in surficial aquifer and UFA estimated by time of peak tracer concentrations observed at Silver River Station.

Tracer test	Injection point and tracer	Peak	Time to peak (days)	Pulse velocity (m/d)	Pulse velocity (m/s)
Surficial aquifer	Basin 1, well 0 RWT	Pulse 1	42.0	13.5	1.6×10^{-4}
		Pulse 2	115.0	4.9	5.7×10^{-5}
		Pulse 3	177.0	3.2	3.7×10^{-5}
		Pulse 4	246.0	2.3	2.7×10^{-5}
UFA	Basin 1, deep well RWT	Pulse 1	72.0	7.9	9.2×10^{-5}
		Pulse 2	245.0	2.3	2.7×10^{-5}

4.6 Discussion

4.6.1 Groundwater flow velocities

Groundwater velocities observed in most areas of the surficial aquifer (FP2 to FP4) are comparable to those reported for saturated sandy and silty-sandy soil media (< 1 m/d) (Matthess and Pekdeger, 1985; Fetter et al., 1999; Dingman, 2002; Shwetha et al., 2015). Velocities and Reynolds numbers are consistent with low-head Darcian flow through the well-sorted sands with few fine particle fractions reported for the surface soils in Basin 1 (Chang et al., 2015; Rice, 2018). Observed velocities in FP2-FP4 wells are also within the range of horizontal groundwater velocities observed in other sandy surficial aquifers in non-karst areas in Florida (0.02 to 0.42 m/d) (Corbett et al., 2000). However, the near immediate detection of tracer in FP1 wells indicates that groundwater flows in some parts of the surficial aquifer may fall outside of the range expected by transport through homogeneous sandy media and may be related to the influence of macropores in subsurface strata (Etana et al., 2013) (Figure 17 and Table 10). For example, the maximum groundwater velocities observed in FP1 wells based on the first arrival time of tracer demonstrates

that macropores and subsurface features, as detected by GPR, may allow for advective transport of stormwater in the shallow subsurface. In contrast, the maximum groundwater velocities observed in FP4 wells (wells 4 to 6) could correlate to matrix flow speeds with large contributions of dispersive or diffusive transport (Sudicky et al., 1983).

The maximum groundwater velocities observed in the UFA (233-19,200 m/d) indicate the presence of rapid groundwater flow paths, especially from the UFA under Basin 1 to the Silver River monitoring station (Table 10). The comparison of maximum groundwater velocities observed in Silver Springs when the tracer was injected at a similar location (Basin 1) but at different depths (into the UFA *vs.* the surficial aquifer) indicates that flow through the UFA in the immediate vicinity of Silver Springs was almost twice as fast as flow from the surficial aquifer (Table 10 and Figure 20). While we cannot differentiate groundwater velocity from the transport time of open channel flow, results suggest that groundwater velocity in the UFA from Basin 1 to Silver Springs is fast, potentially within large conduits under high hydraulic gradients as groundwater flows converge to the Silver Springs discharge vents. To reach the spring, tracer injected into the surficial aquifer had to move either through the surficial aquifer to the spring or pass through the intermediate confining layer to reach the UFA. In addition, the maximum groundwater velocities observed in the UFA are comparable to groundwater velocities reported in other karst areas, for example, the McConnell Springs (7,600 m/d, Norris et al., 2016) and Mystery Spring (2,680 m/d, Martin et al., 2019) in Kentucky, and the Blautopf Spring watershed in Germany (1,224 to 13,872 m/d, Lauber et al., 2014). The relatively high groundwater velocity observed in the UFA in this study may be partially associated to the eogenetic karst of the study area, which is characterized by higher matrix porosity relative to the dense telogenetic karst with

lower matrix porosity found in Kentucky (Vacher and Mylroie, 2002; Florea and Vacher, 2006). However, the location of study in Basin 1 in close proximity to the high-magnitude spring vents may also have contributed to the high velocities observed in the spring vicinity. For instance, the lower maximum groundwater velocity observed in the UFA further from the spring vents (233 m/d between Basins 3 and 2) is comparable to maximum velocities previously reported in the UFA near Silver Springs (702 m/d, Knochenmus, 1967).

Despite considerable differences in the maximum groundwater velocities observed in the UFA and surficial aquifer, groundwater velocities estimated based on the times of peak concentrations in the spring (2.3 and 13.5 m/d, respectively) are similar in the two tracer inspections from Basin 1 (Table 11). These are also similar to mean groundwater velocities reported in some earlier tracer studies of the UFA in the vicinity of Silver Springs (10.2 - 91.4 m/d, Phelps, 1994), although greater mean groundwater velocities have also been reported in UFA near Silver Springs (e.g. 350 m/d, Knochenmus, 1967; 213 – 427 m/d, McGurk et al., 2012; and 8.4 - 317 m/d, Yang et al., 2019). Further, mean groundwater velocities reported in this and other studies near Silver Springs are comparable to estimated mean groundwater velocities in other karst areas of Florida (e.g. 42 - 299 m/d near Wekiva Spring, FDEP, 2016; and 31 - 298 m/d in Wakulla Spring, Kincaid et al., 2012).

Tracer concentrations observed in Silver Springs were low, for instance relative to concentrations observed in the monitoring wells in the surficial aquifer, which is expected due to the larger water volumes diluting tracer concentrations in the springs. For the same reason, concentrations of tracer injected into the UFA (Figure 21 A) were also lower in the springs than when injected into the surficial aquifer (Figure 20 E), despite that more mass of RWT had been

applied in the UFA. Although tracer injected into the UFA further from the spring (Eos from Basin 2 or Fl from Basin 3) was not detected in the spring, it cannot be concluded that hydraulic connections do not exist from these areas. It is more likely that concentrations of Eos and Fl in the spring were either too dilute for accurate detection within the period of monitoring or may have arrived at the spring after monitoring ceased. Steady transport of Fl tracer from Basin 3 to Basin 2 was still ongoing at the time monitoring ceased (Figure 21 B).

4.6.2 Contaminant transport from stormwater basins and implication for stormwater management in karst regions

Based on results of geophysical surveys and observed movements of tracer injected into multiple stormwater management basins in the Silver Spring springshed, a conceptual model can be proposed to hypothesize how stormwater contaminants may move between the surficial aquifer, intermediate semi-confining unit and UFA, to eventually reach the spring. Both injections from Basin 1 produced multiple peaks of tracer in Silver Springs, highlighting the diversity of flowpaths that exist (from both the surficial aquifer and the UFA) from the stormwater basin to the springs. The variable groundwater velocities observed indicate that infiltrated stormwater from Basin 1 flows in a complex anisotropic karst groundwater flow condition, potentially through multiple flow paths. Variations in size and hydraulic gradients of underground drainage systems produce diverse groundwater flow velocities, and thus complex transport of contaminants to the Silver Springs discharge points. For instance, following a single pulse delivery of contaminants to Basin 1, one flow pathway may deliver peak contaminant concentrations to the spring within 40 to 70 days, while another flow pathway may produce a contaminant peak around 250 days (Figure 20 and Figure 21).

The similarity in behavior of tracers injected into the UFA and the surficial aquifer reveals hydraulic connections with implications for stormwater management. It is expected that infiltrated stormwater will move within the shallow surficial aquifer according to Darcian flow in porous media, following hydraulic gradients and local hydraulic conductivity of aquifer media (similar to FP 2-4 in Figure 17). Theory predicts that vertical groundwater flow through the semi-confining unit will proceed slowly based on differences in hydraulic gradient between the water level in the unconfined surficial aquifer and the potentiometric water level in the confined UFA. However, the similarity in pulse elapse time of tracer injected to the UFA and surficial aquifer suggests that the role of the intermediate semi-confining layer between the two may be limited, hinting at the influence of heterogeneous subsurface features in connecting different parts of the surficial aquifer (as in FP1 in Figure 17) and the surficial aquifer to the UFA. Expression of karst features at the surface (for example in Basin 2) also highlight this possibility. High conductivity zones associated with subsurface features may allow for greater connectivity between the surficial aquifer and the UFA and springs, which could explain the rapid transit of tracer from the surficial aquifer in Basin 1 to appear in Silver Springs much faster than would have been predicted based on Darcian flow through homogeneous media. Though multiple diverse flowpaths likely exist, we hypothesize that the tracer transported to the springs through at least two different mechanisms: traveling through the soil matrix horizontally in the surficial aquifer, and moving vertically downward to pass through the intermediate confining unit via preferential flowpaths to reach the UFA. From the UFA, the tracer traveled through the highly karstic features of the UFA, i.e., rock matrix and high porosity fractures/conduits.

4.7 Conclusions

The objective of this study was to investigate potential subsurface pathways for urban runoff from stormwater management basins to a high-magnitude freshwater spring in an area of karst hydrogeology. Subsurface heterogeneity of stormwater management basins within the Silver Springs springshed were characterized using ground-based geophysical surveys (ground penetrating radar and frequency domain electromagnetics) and tracer tests were implemented to estimate transport rates of shallow and deep groundwater flows between the basins and Silver Springs. As one of the first studies to investigate transport of stormwater pollutants from concentrated stormwater management areas to and within karst aquifers, study outcomes may be useful to agencies aiming to protect spring and groundwater quality in Silver Springs and other karst regions. For instance, results underscore the influence of karst hydrogeology to contaminant transport from stormwater management areas. Multiple tracer peaks observed in Silver Springs with pulse velocities on the order of 10^{-5}-10^{-4} ms^{-1} suggest that contaminants from stormwater basins may be transported to Silver Springs through multiple heterogeneous flowpaths from surficial and deep aquifers. Rapid detection of tracer in Silver Springs indicated maximum groundwater velocities in the springs vicinity on the order of 10^{-2}-10^{-1} ms^{-1} while slower transport rates (10^{-3} ms^{-1}) were observed further from the springs, suggesting that the immediate vicinity of springs may be particularly vulnerable to stormwater contamination. Maximum flow velocities observed within the surficial aquifer were highly variable (10^{-6} to 10^{-3} ms^{-1}) and transport rates in some areas were much greater than expected. Locations characterized by high transport rates were associated with clusters of subsurface anomalies detected by GPR and low EM signal conductance, potentially indicating the influence of karst features. The observed high transport rates through

both surficial and deep groundwater pathways may limit opportunities for biogeochemical cycling and contaminant reduction, rendering stormwater BMPs in karst areas less effective at reducing loads of some pollutants than in alluvial aquifers. To adequately protect groundwater resources, the design of stormwater BMPs in karst regions should be undertaken in consideration of karst geologic configurations and implications to hydrogeologic transport processes.

4.8 Acknowledgement

This research is supported financially by Florida Department of Transportations. The expressed opinions, findings, and conclusions in this publication are those of the author(s) and not necessarily from the Florida Department of Transportation or the U.S. The authors would like to thank City of Ocala and Florida Department of Transportation for the permission to access the sites and cooperation in this research.

4.9 References

Ahmed, S., Carpenter, P.J., 2003. Geophysical response of filled sinkholes, soil pipes and associated bedrock fractures in thinly mantled karst, east-central Illinois. Environmental Geology, 44(6), 705-716. https://doi.org/10.1007/s00254-003-0812-3

Aley, T., Beeman, S.L., 2015. Procedures and criteria analysis of fluorescent dyes in water and charcoal samplers: fluorescein, eosine, rhodamine wt, and sulforhodamine b dyes. Ozark Underground Laboratory, Inc., Protem, MO. 20 p.

Aley, T., 2019. Groundwater tracing handbook. Ozark Underground Laboratory, Inc., Protem, MO. 44 p.

Bakalowicz, M., 2005. Karst groundwater: a challenge for new resources. Hydrogeology Journal, 13(1), 148-160. https://doi.org/10.1007/s10040-004-0402-9

Behroozi, A., 2019. Reactive solute transport in urban karst-like environments: Implications for the design and layout of stormwater infiltration systems [PhD dissertation]. University of Melbourne, 170 p.

Butler, K., 1984. Microgravimetric and gravity gradient techniques for detection of subsurface cavities. Geophysics 49:1084–1096. https://doi.org/10.1190/1.1441723

Byle, M.J. 2001. Stormwater infiltration practices in karst, in Southeastern Pennsylvania Stormwater Management Symposium, Oct. 2001, Villanova University.

Caminha-Maciel, G., Figueiredo, I., 2013. Error analysis in measured conductivity under low induction number approximation for electromagnetic methods. ISRN Geophysics, https://doi.org/10.1155/2013/720839

Chalikakis, K., Plagnes, V., Guerin, R., Valois, R., Bosch, F.P., 2011. Contribution of geophysical methods to karst-system exploration: an overview. Hydrogeology Journal, 19(6): 1169-1180. https://doi.org/10.1007/s10040-011-0746-x

Chang, N.B., Wanielista, M., Hartshorn, N., 2015. Optimal design of stormwater basins with bio-sorption activated media (BAM) in karst environments phase I: site screening and selection (No. BDV24-977-12). Florida. Dept. of Transportation. 60 p. https://rosap.ntl.bts.gov/view/dot/29673

Corbett, D.R., Dillon, K., Burnett, W., 2000. Tracing groundwater flow on a barrier island in the north-east Gulf of Mexico. Estuarine, Coastal and Shelf Science, 51(2), 227-242. https://doi.org/10.1006/ecss.2000.0606

Czachor, H., 2011. Laminar and Turbulent Flow in Soils. In: Gliński J., Horabik J., Lipiec J. (eds) Encyclopedia of Agrophysics. Encyclopedia of Earth Sciences Series. Springer, Dordrecht. https://doi.org/10.1007/978-90-481-3585-1_80Dingman, S.L., 2002. Physical hydrology. 2nd edition, Prentice-Hall, Inc., Upper Saddle River, NJ, 656 p.

Doolittle, J.A., Collins, M.E., 1998. A comparison of EM induction and GPR methods in areas of karst. Geoderma, 85(1), 83-102. https://doi.org/10.1016/S0016-7061(98)00012-3

Dubrovsky, N.M., Burow, K.R., Clark, G.M., Gronberg, J.A.M., Hamilton, P.A., Hitt, K.J., Mueller, D.K., Munn, M.D., Puckett, L.J., Nolan, B.T., Rupert, M.G., 2010. Nutrients in the nation's streams and groundwater, 1992–2004, (No. 1350). US Geological Survey, Reston, VA, 174 p.

Eller, K.T., Katz, B.G., 2017. Nitrogen source inventory and loading tool: An integrated approach toward restoration of water-quality impaired karst springs. Journal of Environmental Management, 196, 702-709. https://doi.org/10.1016/j.jenvman.2017.03.059

EPA, 2002. The QTRACER2 program for tracer-breakthrough curve analysis for tracer tests in karstic aquifers and other hydrologic systems. U.S. Environmental Protection Agency, Washington, DC, USA.

ERP, 2013. Design requirement for stormwater treatment and management systems, water quality and water quantity. Southwest Florida Water Management District, Applicant Handbook, volume II. 97 p.

Essouayed, E., Annable, M.D., Momtbrun, M., Atteia, O., 2019. An innovative tool for groundwater velocity measurement compared with other tools in laboratory and field tests. Journal of Hydrology X, 2, 100008. https://doi.org/10.1016/j.hydroa.2018.100008

Etana, A., Larsbo, M., Keller, T., Arvidsson, J., Schjønning, P., Forkman, J., Jarvis, N., 2013. Persistent subsoil compaction and its effects on preferential flow patterns in a loamy till soil. Geoderma, 192, 430-436. https://doi.org/10.1016/j.geoderma.2012.08.015

Farmer, N., Blew, B., 2010. Fluorescent dye tracer tests near the Malad Gorge state park (Riddle well test). Idaho Department of Water Resources Open File Report, 36 p.

Faulkner, G.L., 1970. Geohydrology of the Cross-Florida Barge Canal area with special reference to the Ocala vicinity. US Geological Survey Water-Resource Investigation Report 1-73, 117 p.

FDEP., 2006. Fifty-year retrospective study of the ecology of Silver Springs, Florida. Florida Department of Environmental Protection, Tallahassee, Florida, USA.

FDEP., 2012. Nutrient TMDL for Silver Springs, Silver Springs Group, and Upper Silver River (WBIDs 2772A, 2772C, and 2772E). Florida Department of Environmental Protection, Tallahassee, Florida, USA.

FDEP., 2016. Wekiva Basin ground water tracer study for Rock and Wekiwa Springs. Rep. no. WM926. Florida Department of Environmental Protection. Tallahassee, Florida, USA.

Fetter, C.W., Boving, T.B., Kreamer, D.K., 1999. Contaminant hydrogeology. Prentice hall Upper Saddle River, NJ. v. 500.

Ficco, K.K., Sasowsky, I.D., 2018. An interdisciplinary framework for the protection of karst aquifers. Environmental Science & Policy, 89, 41-48. https://doi.org/10.1016/j.envsci.2018.07.005

Field, M.S., Pinsky, P.F., 2000. A two-region nonequilibrium model for solute transport in solution conduits in karstic aquifers. Journal of Contaminant Hydrology, 44(3-4), 329-351. https://doi.org/10.1016/S0169-7722(00)00099-1

Florea, L.J., Vacher, H.L., 2006. Springflow hydrographs: eogenetic vs. telogenetic karst. Groundwater, 44(3), 352-361. https://doi.org/10.1111/j.1745-6584.2005.00158.x

Flury, M., Wai, N.N., 2003. Dyes as tracers for vadose zone hydrology. Reviews of Geophysics, 41(1). https://doi.org/10.1029/2001RG000109

Ford, D., Williams, P.D., 2013. Karst hydrogeology and geomorphology. John Wiley & Sons. Chichester, England.

Gao, Y., Libera, D.A., Wang, D., Kibler, K., Chang, N.B., 2020. Evaluating the performance of BAM-based blanket filter on nitrate reduction in a karst spring. Journal of Hydrology, 591, p.125491. https://doi.org/10.1016/j.jhydrol.2020.125491

German, E.R., 2010. Evaluation and recomputation of daily-discharge for Silver Springs near Ocala, Florida, special publication SJ2010-SP9. St. Johns River Water Management District, Palatka, FL. 121 p.

Geyer, T., Birk, S., Licha, T., Liedl, R., Sauter, M., 2007. Multitracer test approach to characterize reactive transport in karst aquifers. Groundwater, 45(1), 36-45. https://doi.org/10.1111/j.1745-6584.2006.00261.x

Glibert, P.M., 2017. Eutrophication, harmful algae and biodiversity—Challenging paradigms in a world of complex nutrient changes. Marine Pollution Bulletin, 124(2), 591-606. https://doi.org/10.1016/j.marpolbul.2017.04.027

Goldscheider, N., 2008. A new quantitative interpretation of the long-tail and plateau-like breakthrough curves from tracer tests in the artesian karst aquifer of Stuttgart, Germany. Hydrogeology Journal, 16(7), p.1311. https://doi.org/10.1007/s10040-008-0307-0

Goldscheider, N., Chen, Z., Auler, A.S., Bakalowicz, M., Broda, S., Drew, D., Hartmann, J., Jiang, G., Moosdorf, N., Stevanovic, Z., Veni, G., 2020. Global distribution of carbonate rocks and karst water resources. Hydrogeology Journal, 28(5), 1661-1677. https://doi.org/10.1007/s10040-020-02139-5

Günay, G., Ekmekçi, M., 1997. Importance of public awareness in groundwater pollution, *In* G. Günay, and A. I. Johnson (eds.), Karst waters and environmental impacts, Balkema, Rotterdam, p. 3–10.

Harper, H.H., Baker, D.M., 2007. Evaluation of current stormwater design criteria within the state of Florida. Florida Department of Environmental Protection, 327 p.

Hartmann, A., Goldscheider, N., Wagener, T., Lange, J., Weiler, M., 2014. Karst water resources in a changing world: Review of hydrological modeling approaches. Reviews of Geophysics, 52(3), 218-242. https://doi.org/10.1002/2013RG000443

Heffernan, J.B., Albertin, A.R., Fork, M.L., Katz, B.G., Cohen, M.J. and Slomp, C.P., 2012. Denitrification and inference of nitrogen sources in the karstic Floridan Aquifer. Biogeosciences, 9(5), 1671-1690. https://doi.org/10.5194/bg-9-1671-2012

Heffernan, J.B., Liebowitz, D.M., Frazer, T.K., Evans, J.M. and Cohen, M.J., 2010. Algal blooms and the nitrogen-enrichment hypothesis in Florida springs: evidence, alternatives, and adaptive management. Ecological Applications, 20(3), 816-829. https://doi.org/10.1890/08-1362.1

Hicks, R.W., Holland, K., 2012. Nutrient TMDL for Silver Springs, Silver Springs Group, and Upper Silver River (WBIDs 2772A, 2772C, and 2772E). Ground Water Management Section, Florida Department of Environmental Protection, Tallahassee, FL.

Husic, A., Fox, J., Adams, E., Pollock, E., Ford, W., Agouridis, C. and Backus, J., 2020a. Quantification of nitrate fate in a karst conduit using stable isotopes and numerical modeling. Water Research, 170, p.115348. https://doi.org/10.1016/j.watres.2019.115348

Husic, A., Fox, J., Mahoney, T., Gerlitz, M., Pollock, E., Backus, J., 2020b. Optimal transport for assessing nitrate source-pathway connectivity. Water Resources Research, 56, e2020WR027446. https://doi.org/10.1029/2020WR027446

Jardani, A., Revil, A., Santos, F., Fauchard, C., Dupont, J.P., 2007. Detection of preferential infiltration pathways in sinkholes using joint inversion of self-potential and EM-34 conductivity data. Geophysical Prospecting 55(5): 749–760. https://doi.org/10.1111/j.1365-2478.2007.00638.x

Kačaroğlu, F., 1999. Review of groundwater pollution and protection in karst areas. Water, Air, and Soil Pollution, 113(1-4), 337-356. https://doi.org/10.1023/A:1005014532330

Katz, B.G., 2001. A multitracer approach for assessing the susceptibility of ground water contamination in the Woodville Karst Plain, Northern Florida, In: Kuniansky, ed., U.S.

Geological Survey Karst Interest Group Proceedings: Water-Resources Investigations Report 01-4011, 167–176.

Katz, B.G., 2019. Nitrate contamination in karst groundwater. In: Culver, D., White, W., (Eds.), Encyclopedia of Caves. Elsevier Science, Amsterdam, Netherlands, 756-760. https://doi.org/10.1016/B978-0-12-814124-3.00091-1

Kibler, K.M., Chang, N.B., Wang, D., Wanielista, M.P., Shokri, M., Ordonez, D., Gao, Y., Valencia, A., Hagglund, C., Corrado, A. 2020. Innovative and Integrative BMPs for Surface and Groundwater Protection. Florida Department of Transportation, report number BDV24-977-25, 134 p.

Kincaid, T., Davies, G., Werner, C., DeHan, R., 2012. Demonstrating interconnection between a wastewater application facility and a first magnitude spring in a karstic watershed: Tracer study of the Southeast Farm Wastewater Reuse Facility, Tallahassee, Florida. Florida Geological Survey, 192 p.

Knochenmus, D.D., 1967. Tracer studies and background fluorescence of ground water in the Ocala, Florida, area, Open-File Report. https://doi.org/10.3133/ofr67132

Knowles, L., Katz, B.G., Toth, D.J., 2010. Using multiple chemical indicators to characterize and determine the age of groundwater from selected vents of the Silver Springs Group, central Florida, USA. Hydrogeology Journal, 18(8), 1825-1838. https://doi.org/10.1007/s10040-010-0669-y

Knowles J.L., O'Reilly, A.M., Adamski, J.C., 2002. Hydrogeology and simulated effects of the ground-water withdrawals from the Floridan aquifer system in Lake County and in the

Ocala National Forest and vicinity, north-central Florida. Water-Resources Investigations Report, 2-4207. U.S. Geological Survey.

Knowles, L., 1996. Estimation of evapotranspiration in the Rainbow Springs and Silver Springs Basins in north-central Florida. U.S. Geological Survey Water-Resources Investigation Report 96-4024. https://doi.org/10.3133/wri964024

Kovalevsky, V.S., Kruseman, G.P., Rushton, K.R., 2004. Groundwater studies: an international guide for hydrogeological investigations. IHP-VI Series on Groundwater No. 3, Unesco. 430 p.

Lauber, U., Ufrecht, W., Goldscheider, N., 2014. Spatially resolved information on karst conduit flow from in-cave dye tracing. Hydrology and Earth System Sciences, 18(2), 435-445. https://doi.org/10.5194/hess-18-435-2014

Martin, D.P., Brown, C.M., Currens, B.J., 2019. Dye trace study of karst groundwater flow at Mystery Spring and Wildcat Culvert in Lexington, Fayette County, Kentuciy. The North Kentucky University Journal of Student Research, 1: 43-48, http://hdl.handle.net/11216/3171

Massei, N., Wang, H.Q., Field, M.S., Dupont, J.P., Bakalowicz, M., Rodet, J., 2006. Interpreting tracer breakthrough tailing in a conduit-dominated karstic aquifer. Hydrogeology Journal, 14(6), 849-858. https://doi.org/10.1007/s10040-005-0010-3

Matthess, G., Pekdeger, A., 1985. Survival and transport of pathogenic bacteria and viruses in ground water. Ground Water Quality, John Wiley and Sons, New York NY. 472 - 482.

McGurk, B.E., Davis, J.B., Stokes, J.A., Toth, D.J., Colona, W., Butt, P., 2012. Silver Springs nutrient pathway characterization project, final report. St. Johns River Water Management District Special Publication SJ, 805 p.

McNeill JD. 1980. Electromagnetic Terrain Conductivity Measurements at Low Induction Numbers. Technical Note TN-6, Geonics Limited, Mississaugua, Ontario, Canada, 13 p.

Milanovic, P., 1981, Karst Hydrogeology, Water Res. Publ., Littleton, Colorado, U.S.A. 434 p.

Militzer, H., Rösler, R., Lösch, W., 1979. Theoretical and experimental investigations for cavity research with geoelectrical resistivity methods. Geophysical Prospecting 27: 640-652. https://doi.org/10.1111/j.1365-2478.1979.tb00991.x

Moore, H., Beck, B., 2018. Karst terrane and transportation issues. In: Meyers, R.A., (ed.), Encyclopedia of sustainability science and technology, 1-33, https://doi.org/10.1007/978-1-4939-2493-6_206-4

Morales, T., de Valderrama, I.F., Uriarte, J.A., Antigüedad, I., Olazar, M., 2007. Predicting travel times and transport characterization in karst conduits by analyzing tracer-breakthrough curves. Journal of Hydrology, 334(1-2), 183-198. https://doi.org/10.1016/j.jhydrol.2006.10.006

Mull, D.S., Liebermann, T.D., Smoot, J.L., Woosley, L.H., 1988. Application of dye-tracing techniques for determining solute-transport characteristics of ground water in karst terranes (No. PB-92-231356/XAB; EPA-904/6-88/001). Environmental Protection Agency, Atlanta, GA (United States). Region IV. 117 p.

NOAA.gov. 2017. National Centers for Environmental Information (NCEI) formerly known as National Climatic Data Center (NCDC) | NCEI offers access to the most significant

archives of oceanic, atmospheric, geophysical and coastal data. [online] Available at: https://www.ncdc.noaa.gov/. [Accessed 15 October 2017].

Nobes DC. 1999. How important is the orientation of a horizontal loop EM system? Examples from a leachate plume and a fault zone. Journal of Environmental and Engineering Geophysics 4 (2) 81-85.

Norris, L.A., Simpson, C.E., Garrison, T., 2016. Relationships between surface and ground water velocities determined from dy trace experiments in McConnell Springs and Preston's Cave Spring, Lexington, Fayette County, Kentucky. Eastern Kentucky University Encompass, 1-17, https://doi:10.1130/abs/2016se-272937

Phelps, G.G., 1994. Hydrogeology, water quality, and potential for contamination of the Upper Floridan aquifer in the Silver Springs ground-water basin, central Marion County, Florida. US Geological Survey Water Resources Investigations Report 92-4159, 69 p.

Phelps, G.G., 2004. Chemistry of ground water in the Silver Springs Basin, Florida, with an emphasis on nitrate. US Department of Interior, US Geological Survey, 54 p.

Phelps, G.G., Walsh, S.J., Gerwig, R.M., Tate, W.B., 2006. Characterization of the hydrology, water chemistry, and aquatic communities of selected springs in the St. Johns Water Management District, Florida, 2004. US Geological Survey Open-File Rep 2006-1107, 51 p.

Puckett, L.J., Cowdery, T.K., 2002. Transport and fate of nitrate in a glacial outwash aquifer in relation to ground water age, land use practices, and redox processes. Journal of Environmental Quality, 31(3), 782-796. https://doi.org/10.2134/jeq2002.7820

Rice, N., 2018. Evaluating hydrologic fluxes through stormwater treatment systems: implication to freshwater springs in a karst environment. [M.Sc. Thesis], University of Central Florida, 131 p.

Shokri, M., Ashjari, J., Karami, G., 2016. Surface and subsurface karstification of aquifers in arid regions: the case study of Cheshme-Ali Spring, NE Iran. Journal of Cave & Karst Studies, 78(1), 25-35. http://dx.doi.org/10.4311/2014ES0020

Shuster, E.T., White, W.B., 1971. Seasonal fluctuations in the chemistry of lime-stone springs: A possible means for characterizing carbonate aquifers. Journal of Hydrology, 14(2), 93-128. https://doi.org/10.1016/0022-1694(71)90001-1

Shwetha, P., Varija, K., 2015. Soil water retention curve from saturated hydraulic conductivity for sandy loam and loamy sand textured soils. Aquatic Procedia, 4, 1142-1149. https://doi.org/10.1016/j.aqpro.2015.02.145

Smith, D.L., 1986. Application of the pole–dipole resistivity technique to the detection of solution cavities beneath highways. Geophysics 51: 833– 837. http://dx.doi.org/10.1190/1.1442135

Stephenson, J.B., Zhou, W.F., Beck, B.F., Green, T.S., 1999. Highway stormwater runoff in karst areas—preliminary results of baseline monitoring and design of a treatment system for a sinkhole in Knoxville, Tennessee. Engineering Geology, 52(1-2), 51-59. https://doi.org/10.1016/S0013-7952(98)00054-4

Sudicky, E.A., Cherry, J.A., Frind, E.O., 1983. Migration of contaminants in groundwater at a landfill: A case study: 4. A natural-gradient dispersion test. Journal of Hydrology, 63(1-2), 81-108. https://doi.org/10.1016/0022-1694(83)90224-X

Taylor, C.J., Greene, E.A., 2008. Hydrogeologic characterization and methods used in the investigation of karst hydrology. Field techniques for estimating water fluxes between surface water and ground water. In: Rosenberry, D.O., LaBaugh, J.W., (Eds.), Field techniques for estimating water fluxes between surface water and groundwater, US Geological Survey Techniques and Methods, Reston, Virginia, 71-114.

Toride, N., Leu, F.J., van Genuchten, M.T., 1993. A comprehensive set of analytical solutions for nonequilibrium solute transport with first-order decay and zero-order production. Water Resources Research 29(7), 2167-2182. https://doi.org/10.1029/93WR00496

Toride, N., Leu, F.J., van Genuchten, M.T., 1999. The CXTFIT code for estimating transport parameters from laboratory or field tracer experiments. Research report, US Salinity Laboratory, USDA, ARS, Riverside, USA. 137 p. Vacher, H.L., Mylroie, J.E., 2002. Eogenetic karst from the perspective of an equivalent porous medium. Carbonates and Evaporites, 17(2), 182-196. https://doi.org/10.1007/BF03176484

Weiss, P.T., LeFevre, G., Gulliver, J.S., 2008. Contamination of soil and groundwater due to stormwater infiltration practices, a literature review. St. Anthony Falls Laboratory. Retrieved from the University of Minnesota Digital Conservancy, https://hdl.handle.net/11299/115341

Wen, D., Valencia, A., Lustosa, E., Ordonez, D., Shokri, M., Gao, Y., Rice, N., Kibler, K., Chang, N.B. and Wanielista, M.P., 2020. Evaluation of green sorption media blanket filters for nitrogen removal in a stormwater retention basin at varying groundwater conditions in a karst environment. Science of The Total Environment, 719, p.134826. https://doi.org/10.1016/j.scitotenv.2019.134826

White, W.B., 1988. Geomorphology and hydrology of karst terrains. New York. Oxford University Press. 464 p.

Worthington, S.R.H., Ford, D.C., 2009. Self-organized permeability in carbonate aquifers. Groundwater, 47(3), 326-336. https://doi.org/10.1111/j.1745-6584.2009.00551.x

Worthington, S.R.H., Soley, R.W., 2017. Identifying turbulent flow in carbonate aquifers. Journal of Hydrology, 552, 70-80. https://doi.org/10.1016/j.jhydrol.2017.06.045

Yang, M., Yaquian, J.A., Annable, M.D., Jawitz, J.W., 2019. Karst conduit contribution to spring discharge and aquifer cross-sectional area. Journal of Hydrology, 578, p.124037. https://doi.org/10.1016/j.jhydrol.2019.124037

Zhou, W., Beck, B.F., 2008. Management and mitigation of sinkholes on karst lands: an overview of practical applications. Environmental Geology, 55(4), 837-851. https://doi.org/10.1007/s00254-007-1035-9

Zhu J, Currens JC, Dinger JS. 2011. Challenges of using electrical resistivity method to locate karst conduits-a field case in the Inner Bluegrass Region, Kentucky. Journal of Applied Geophysics 75 (3): 523–530. https://doi.org/10.1016/j.jappgeo.2011.08.009

CHAPTER 5 CONCLUSIONS

The main contribution of this research was to improve protection of water resources from non-point sources of roadway runoff contaminants, focusing on nutrient as a pervasive and endangering contaminant in Florida water resources. Application and efficacy of engineered infiltration media within roadside VFS was inspected as a new strategy for the purpose of enhanced nutrient removal from roadway runoff. It was recognized that nutrient removal is interrelated with hydraulic capacity of the media, as infiltration is a main component of hydrological process providing the chance of contaminants to be treated by subgrade media within VFS. The particular reason for such study was to test the enhance nutrient removals through engineered point of view, but also contribute to scientific research in the field with filling a knowledge gap regarding uncertainty of VFS in nutrient removal, especially for roadside VFS, which little to no impact or even generating nutrient was reported based on literatures. VFS within roadside shoulders are bounded by many particular factors within the configuration of roadside criteria and typical space limitation, which restrict the design of filter width size. Experiments were designed within two 1:1 scale physical models of vegetated roadway shoulders: a Treatment model containing engineered BAM (CTS BOLD & GOLD^{TM}), and an identical Control model containing AASHTO A-3 sandy soils, commonly found in central Florida. Experiments were conducted in various frequent and infrequent rainfall-runoff events (i.e. rain depth, duration, and pattern of occurrence) for 1-lane

and 2-lane roadways. The outcome of the study indicated that BAM VFS outperformed the A-3 sandy soil significantly in decreasing concentrations of NO_x and TN at 6 m filter width. However, BAM and A-3 soil performed comparably with respect to decrease in concentrations of NH_3 and TP and occurred quickly within 1.5 m filter width. In addition, results indicated that BAM removal capacity is not impacted by storm depth and road lane type and minimum 6 m filter width can provide the greatest and consistently performance with respect to decrease in concentrations of nitrogen species from roadway runoff. In addition, the 6 m filter width can provide 100% infiltration for most frequent and infrequent storm events, considering sufficient depth to the groundwater table. While BAM VFS can be a promising strategy for self-treating roadway runoff events, future studies are suggested to consider more experiments and comparing BAM performance against more textural soil types, especially soils with various organic contents and microbial communities. Detailed mechanism of nutrient removal may be investigated considering thorough water chemistry parameter analysis such as measuring redox, pH, DO, and carbon content.

In another research, nutrients load and delivery within stormwater runoff events from roadways were assessed within various rainfall-runoff events. The specific reason for such study was to inspect dynamic nutrient delivery within runoff events of various rainfall-runoff characteristics for the purpose of exploring the main source of nutrient load and factors affecting nutrient transport. The research was in the interest of targeting the main portion of runoff volume that deliver the major nutrient mass within the most important runoff events, providing insight to better design of BMP strategies. The result of the research revealed that roadway runoff nutrient delivery regulates by mainly two physical components: available nutrient mass and capacity of storm runoff to

transport nutrient in runoff events. Storms following long dry periods produced greater concentrations of nitrogen in runoff events, reflecting greater nutrient mass load on surface of roadways. Three types of runoff events were discerned following multi-criteria analysis including type I events, which were characterized as relatively high nutrient supply and high transport capacity, type II events that have relatively low nutrient supply but high transport capacity, and type III events which have low transport capacity (either high or low nutrient supply). The presented event type approach and classification of runoff events systematically could resolve the deficiencies reported to the traditional M(V) curve analysis, where event size and initial contaminant supply were dismissed, causing uncertainty about detecting first flush concept. The M(V) curve analysis on the discovered event types indicated a greater nutrient mass first flush with statistically significant difference in type I events than type II and type III. Results suggested that type I events are more reliable to wash off nutrient and transport over early part of runoff events. Thus, BMP strategies may be designed based on such type of events. Future researches are suggested to collect more runoff events from different roadways and road-lane types considering detailed water quality parameters including pH, redox, DO, and sediment loads along with nutrient variation over runoff events. Such a type of research may provide information to better understand mechanisms related to nutrient wash off process. Complementary research may be also conducted to measure actual nutrient concentrations and after occurred storms over randomly locations over impervious road surface to confirm percent nutrient removal by the occurred storms. Moreover, to inspect the complex role of rainfall intensity on nutrient transportation and sediment entrainment and load, detailed temporal variation of rainfall intensities and runoff sediment load and chemical variation may be required. Such comprehensive research may provide systematic results to

compare obtained results from the event type approach here against other method of analyzing m(V) curves.

Analyzing stormwater management areas near Silver Springs indicated that BMP stormwater basins can act as hotspots for contamination in karst areas and require particular attention with respect to configuration of basin. The presence of karstic formations such as sinkholes and subsurface features in the basins with potential high infiltration rate of sandy soils in central Florida could facilitate contaminant transport from surface to groundwater aquifer. Highly heterogeneous near-surface and deep karst conditions were obtained in the area through the conducted geophysical and tracer experiments, where pollutant may transfer from surface to groundwater quickly and transport through karst system rapidly to Silver Springs discharge point. The configuration of the bottom of the basins and high groundwater velocities in the karstic formation aquifer dictate needs of specific strategies about stormwater management basins in vulnerable karst areas of Florida for pretreatment strategies of stormwater runoff and regulating infiltration process. Hydraulic connections between the surficial aquifer and UFA indicated that stormwater may transport from semi-confining unit between the surficial aquifer and UFA through preferential flowpaths and potential deep subsurface karst features, where the semi-confining unit may even locally not present and make the UFA more vulnerable to surface contamination. As stormwater management areas are important BMPs to control flood and collect significant amount of runoff volume from streets, roads, and urbanized areas, care must be taken into account for their design, performance, and pretreatment strategies of collected stormwater runoff. The BMP stormwater management basins must be designed by a team of expert hydrogeologists and water resources engineered considering subsurface geological conditions in basins, groundwater level depth and

its fluctuations, and potential infiltration rate in the basins. Deep basins with very shallow groundwater table can make aquifer more vulnerable to contamination and basin depth should not be increased to capture more runoff while groundwater is too shallow. Any potential form of sinkhole and subsurface features, which increase unnecessary infiltration rate and pollutant transport, must be monitored regularly. Remediation strategies should be implemented within a thin epikart zone considering general shallow groundwater table in the area. Future researches may consider testing the application of remediation strategies to not address soluble contamination but also control mobile sediments and suspended particulate colloids from moving into aquifer.

APPENDIX- SUPPLEMENTARY DATA

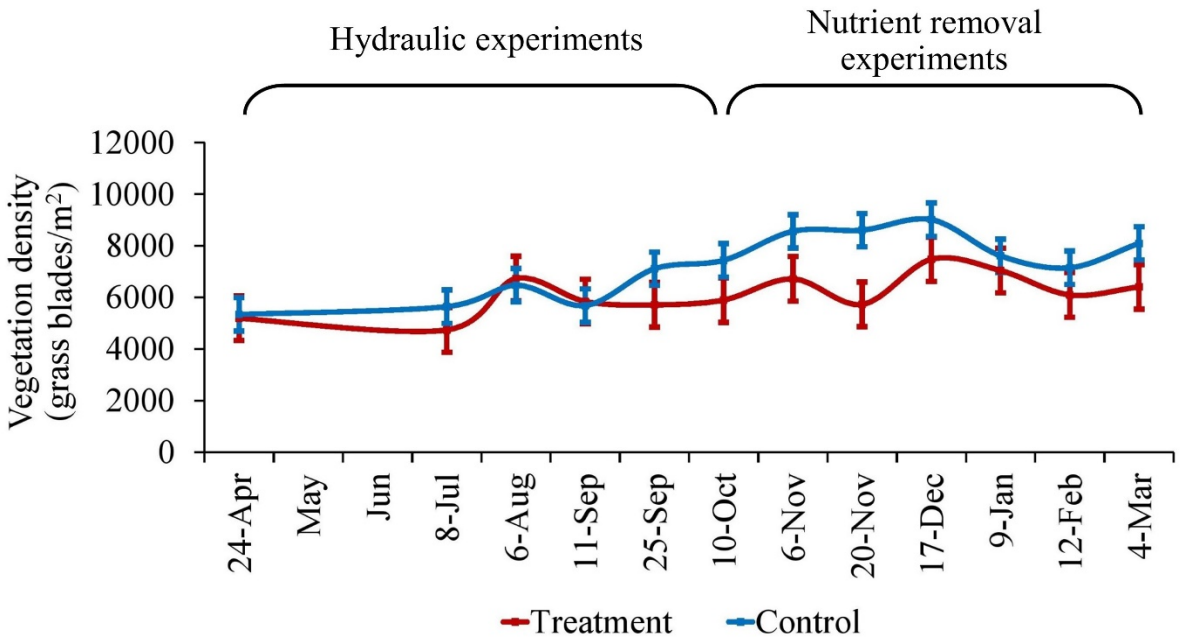

Figure A.1. Mean vegetation density in the Treatment and Control models over the experiments. The values present mean of 7 randomly locations and error bars indicate the range of minimum and maximum measurements. Measurements started in Apr 2018 and ended in May 2019.

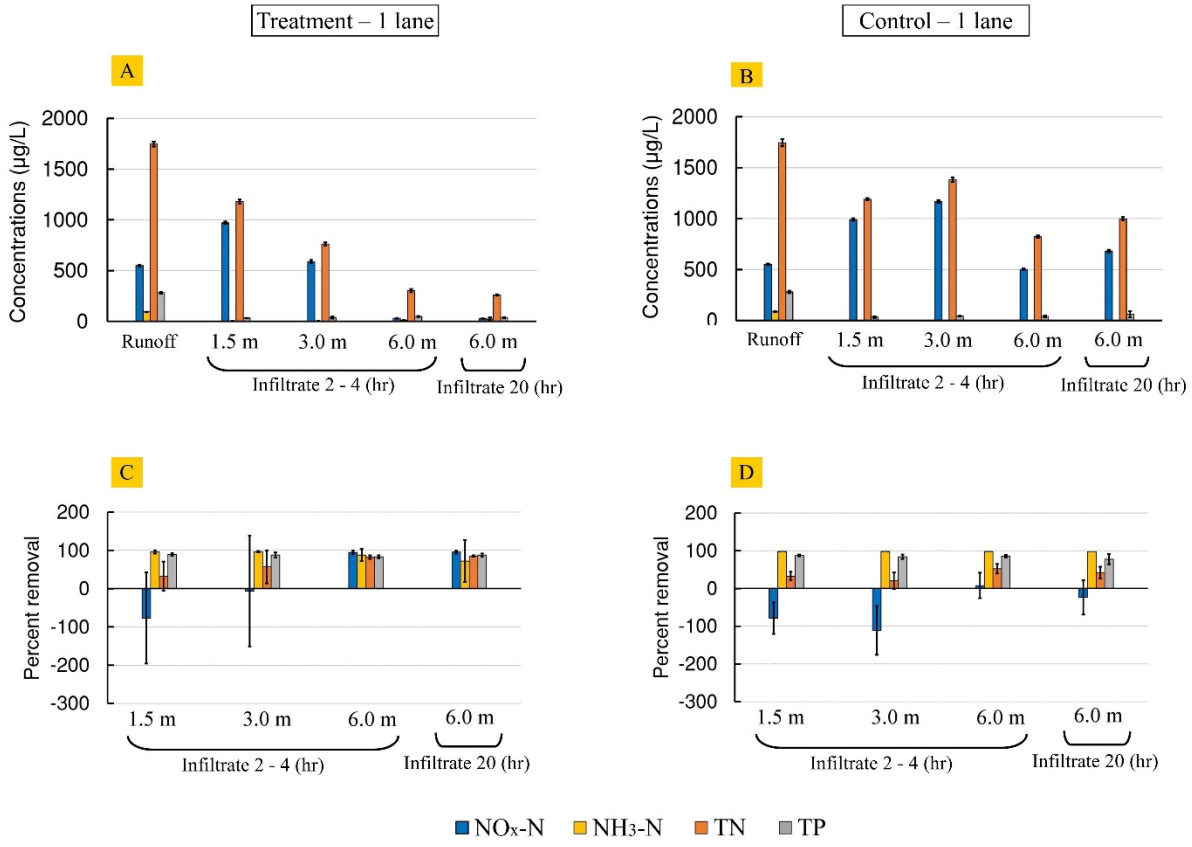

Figure A.2. Arithmatic mean ± SD of nutrient concentrations in runoff and infiltrate water samples at 1.5 m, 3.0 m, and 6.0 m along the filter width in Treatment (A) and Control (B) models for 1-lane roadway. Mean percent removal ± SD of nutrient in infiltrate water with respect to runoff in Treatment (C) and Control (D) models of 1-lane roadway.

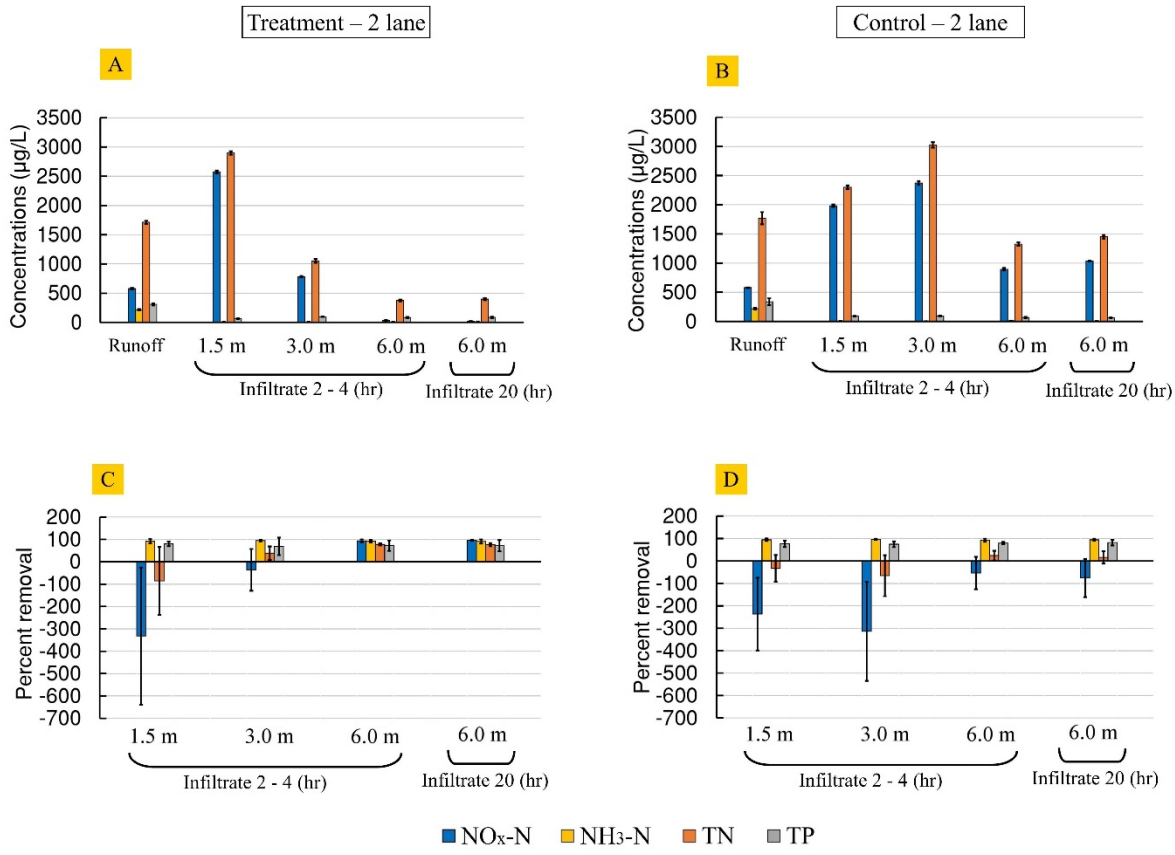

Figure A.3. Arithmatic mean ± SD of nutrient concentrations in runoff and infiltrate water samples at 1.5 m, 3.0 m, and 6.0 m along the filter width in Treatment (A) and Control (B) models for 2-lane roadway. Mean percent removal ± SD of nutrient in infiltrate water with respect to runoff in Treatment (C) and Control (D) models of 2-lane roadway.

Table A.1. Hydraulic performance of Treatment and Control models during high-intensity rainfall-runoff events.

		1-lane roadway								2-lane roadway							
		Treatment model				Control model				Treatment model				Control model			
Storm depth (mm)		25.4	38.1	50.8	76.2	25.4	38.1	50.8	76.2	25.4	38.1	50.8	76.2	25.4	38.1	50.8	76.2
Storm duration (h)		1	1	1	1	1	1	1	1	1	1	1	1	1	1	1	1
Mean intensity (mm/h)		25.4	38.1	50.8	76.2	25.4	38.1	50.8	76.2	25.4	38.1	50.8	76.2	25.4	38.1	50.8	76.2
Q_{in}	Rainfall, (L)	566	849	1133	1699	566	849	1133	1699	566	849	1133	1699	566	849	1133	1699
	Runoff, (L)	226	340	452	678	226	340	452	678	452	679	904	1356	452	679	904	1356
	Total, (L)	792	1189	1585	2377	792	1189	1585	2377	1018	1528	2037	3055	1018	1528	2037	3055
Q_{out}	Infiltrated water, (L)	870	770	1500	1545	731	626	1578	2377	1018	1528	1580	1995	1018	1528	2037	3055
	Surface runoff, (L)	0	0	0	832	0	0	0	0	0	0	458	1060	0	0	0	0
	Total, (L)	870	770	1500	2377	731	626	1578	2377	1018	1528	2038	3055	1018	1528	2037	3055
Infiltration %		100	100	100	65	100	100	100	100	100	100	78	65	100	100	100	100
Runoff %		0	0	0	35	0	0	0	0	0	0	22	35	0	0	0	0
Time to flow generation at 6 m (h)		-	-	-	0.5	-	-	-	-	-	-	0.5	0.3	-	-	-	-
Overland flow length (m)		0.6	1.5 - 2	3	6	0.3	1	1.5 - 2	3.9	2.1	3.9	6	6	0.6 - 1	1.5	5	4.5 - 5

Table A.2. Hydraulic performance of Treatment and Control models during frequently-occurring storm events.

		1-lane roadway								2-lane roadway							
		Treatment model				Control model				Treatment model				Control model			
Storm depth (mm)		12.7	19.1	25.4	38.1	12.7	19.1	25.4	38.1	12.7	19.1	25.4	38.1	12.7	19.1	25.4	38.1
Storm duration (h)		0.5	0.75	0.75	3.75	0.5	0.75	0.75	3.75	0.5	0.75	0.75	3.75	0.5	0.75	0.75	3.75
Mean intensity (mm/h)		25.4	25.4	33	10.16	25.4	25.4	33	10.16	25.4	25.4	33	10.16	25.4	25.4	33	10.16
Q_{in}	Rainfall (L)	283	425	566	849	283	425	566	849	283	425	566	849	283	425	566	849
	Runoff (L)	113	170	226	340	113	170	226	340	226	340	452	680	226	340	452	680
	Total (L)	396	595	792	1189	396	595	792	1189	509	765	1018	1529	509	765	1018	1529
Q_{out}	Infiltrated (L)	396	595	792	1189	396	595	792	1189	509	765	1018	1529	509	765	1018	1529
	Surface runoff (L)	0	0	0	0	0	0	0	0	0	0	0	0	0	0	0	0
	Total (L)	396	595	792	1189	396	595	792	1189	509	765	1018	1529	509	765	1018	1529
Infiltration %		100	100	100	100	100	100	100	100	100	100	100	100	100	100	100	100
Runoff %		0	0	0	0	0	0	0	0	0	0	0	0	0	0	0	0
Time to flow generation at 6 m (h)		-	-	-	-	-	-	-	-	-	-	-	-	-	-	-	-
Overland flow length (m)		0.15	0.9 - 1.2	1.5	0.3 - 0.6	0.15 - 0.3	0.3	0.3 - 0.6	0.15	0.3 - 0.6	2	3	1.5	0.6	1.2	1.5	0.3 - 0.6

Table A.3. Mean concentration with standard deviation of three measurements of the nutrient species from BAM VFS and calculated percent change for a 2-lane roadway.

Storm depth	Location	Mean concentration ± SD				Change			
		NO_x-N (µg/l)	NH_3-N (µg/l)	TN (µg/l)	TP (µg/l)	NO_x-N (%)	NH_3-N (%)	TN (%)	TP (%)
12.7 (mm)	Runoff	531±42	-	1889±10	294±10	-	-	-	-
	1.5 m (4h)	1289±8	-	1848±10	46±1	142	-	-2	-84
	3 m (4h)	1130±6	-	1630±4	39±1	113	-	-14	-87
	6 m (4h)	9±4	-	544±4	45±2	-98	-	-71	-84
	6 m (20h)	10±4	-	649±16	54±2	-98	-	-66	-82
19.1 (mm)	Runoff	546±6	847±35	1863±36	288±1	-	-	-	-
	1.5 m (4h)	962±5	5±0	1464±35	21±1	76	-99	-21	-93
	3 m (4h)	202±6	5±0	533±26	22±1	-63	-99	-71	-92
	6 m (4h)	6±4	5±0	471±19	46±7	-99	-99	-75	-84
	6 m (20h)	2±0	5±0	507±17	41±1	-100	-99	-73	-86
25.4 (mm) (1st)	Runoff	590±4	105±6	1791±30	310±11	-	-	-	-
	1.5 m (4h)	4120±64	27±4	4635±109	122±12	598	-74	159	-60
	3 m (4h)	706±7	11±5	1164±166	390±21	20	-90	-35	26
	6 m (4h)	25±11	10±9	427±64	257±34	-96	-90	-76	-17
	6 m (20h)	23±9	11±9	481±53	276±15	-96	-89	-73	-11
25.4 (mm) (2nd)	Runoff	641±25	128±16	1240±39	365±25	-	-	-	-
	1.5 m (4h)	6739±45	17±2	6556±10	99±11	951	-86	429	-73
	3 m (4h)	789±56	13±1	904±4	93±1	23	-90	-27	-75
	6 m (4h)	37±7	14±2	282±2	42±5	-94	-89	-77	-88
	6 m (20h)	22±1	36±3	341±8	64±18	-96	-71	-72	-82
25.4 (mm) (3rd)	Runoff	576±4	62±2	1692±19	305±19	-	-	-	-
	1.5 m (4h)	1025±2	2±0	1500±8	52±5	78	-96	-11	-83
	3 m (4h)	601±3	3±0	765±6	38±1	4	-95	-55	-87
	6 m (4h)	43±7	3±0	316±4	50±1	-92	-95	-81	-84
	6 m (20h)	2±0	3±0	282±7	48±5	-100	-95	-83	-84
38.1 (mm)	Runoff	572±4	61±0	1767±43	312±45	-	-	-	-
	1.5 m (4h)	1345±12	2±0	1569±14	73±2	135	-97	-11	-77
	3 m (4h)	1831±6	2±0	2008±13	71±2	220	-97	14	-77
	6 m (4h)	2±0	2±0	277±3	94±1	-100	-97	-84	-70
	6 m (20h)	31±1	2±0	274±9	80±5	-95	-97	-84	-74
76.2 (mm)	Runoff	571±1	87±1	1733±16	282±2	-	-	-	-
	1.5 m (4h)	2541±37	0±0	2711±23	26±0	345	-100	56	-91
	3 m (4h)	196±2	0±0	368±6	30±1	-66	-100	-79	-89
	6 m (4h)	117±1	14±1	319±6	54±2	-79	-83	-82	-81
	6 m (20h)	47±10	4±0	251±13	39±28	-92	-95	-85	-86

Note: Ammonia was not measured for samples during storm depth 12.7 mm.

Table A.4. Mean concentration with standard deviation of three measurements of the nutrient species from BAM VFS and calculated percent change for a 1-lane roadway.

Storm depth	Location	Mean concentration ± SD				Change			
		NO_x-N (µg/l)	NH_3-N (µg/l)	TN (µg/l)	TP (µg/l)	NO_x-N (%)	NH_3-N (%)	TN (%)	TP (%)
12.7 (mm)	Runoff	550±3	72±1	1730±56	275±7	-	-	-	-
	1.5 m (4h)	-	-	-	-	-	-	-	-
	3 m (4h)	-	-	-	-	-	-	-	-
	6 m (4h)	9±2	2±0	484±81	48±1	-98	-97	-72	-82
	6 m (20h)	12±1	116±118	322±16	48±7	-98	60	-81	-83
19.1 (mm)	Runoff	566±5	80±1	1828±42	260±4	-	-	-	-
	1.5 m (4h)	91±2	2±0	251±13	35±1	-84	-98	-86	-87
	3 m (4h)	70±2	2±0	223±0	26±0	-88	-98	-88	-90
	6 m (4h)	16±0	2±0	220±4	44±1	-97	-98	-88	-83
	6 m (20h)	26±1	2±0	220±11	37±0	-95	-98	-88	-86
25.4 (mm) (1st)	Runoff	544±4	89±4	1713±21	321±26	-	-	-	-
	1.5 m (4h)	327±0	2±0	493±15	51±6	-40	-98	-71	-84
	3 m (4h)	103±4	2±0	257±10	86±51	-81	-98	-85	-73
	6 m (4h)	2±0	3±1	239±14	76±18	-100	-96	-86	-76
	6 m (20h)	2±0	2±0	215±2	53±25	-100	-98	-87	-83
25.4 (mm) (2nd)	Runoff	522±2	132±5	1762±9	292±3	-	-	-	-
	1.5 m (4h)	738±1	2±0	1016±12	16±0	41	-98	-42	-94
	3 m (4h)	326±15	2±0	592±6	16±2	-38	-98	-66	-94
	6 m (4h)	2±0	12±1	315±1	46±3	-100	-90	-82	-84
	6 m (20h)	2±0	2±0	280±12	11±0	-100	-98	-84	-96
25.4 (mm) (3rd)	Runoff	559±3	64±1	1553±21	290±5	-	-	-	-
	1.5 m (4h)	1077±7	2±0	1239±9	32±2	93	-97	-20	-89
	3 m (4h)	326±1	2±0	480±6	31±0	-42	-97	-69	-89
	6 m (4h)	34±2	2±0	256±8	43±2	-94	-97	-84	-85
	6 m (20h)	34±1	2±0	239±0	37±1	-94	-97	-85	-87
38.1 (mm)	Runoff	558±21	80±1	1818±13	275±8	-	-	-	-
	1.5 m (4h)	1744±44	11±1	1862±24	29±2	212	-86	2	-89
	3 m (4h)	2384±41	6±2	2518±60	33±4	327	-93	38	-88
	6 m (4h)	72±13	40±0	297±2	48±2	-87	-50	-84	-82
	6 m (20h)	29±3	15±0	255±1	38±0	-95	-81	-86	-86
76.2 (mm)	Runoff	547±12	120±4	1824±11	255±3	-	-	-	-
	1.5 m (4h)	1850±17	0±0	2219±52	20±1	238	-100	22	-92
	3 m (4h)	327±29	3±6	504±7	22±1	-40	-97	-72	-91
	6 m (4h)	65±2	18±0	302±3	25±0	-88	-85	-83	-90
	6 m (20h)	70±2	6±5	288±4	19±0	-87	-95	-84	-92

Note: Drainage ports at 1.5 m and 3 m filter during storm depth 12.7 mm were dry.

Table A.5. Mean concentration with standard deviation of three measurements of the nutrient species from Control model and calculated percent change for a 2-lane roadway.

Storm depth	Location	Mean concentration ± SD				Change			
		NO_x-N (µg/l)	NH_3-N (µg/l)	TN (µg/l)	TP (µg/l)	NO_x-N (%)	NH_3-N (%)	TN (%)	TP (%)
12.7 (mm)	Runoff	552±4	-	1931±30	302±7	-	-	-	-
	1.5 m (4h)	1298±16	-	1793±19	38±3	135	-	-7	-87
	3 m (4h)	2190±81	-	3405±68	48±2	297	-	76	-84
	6 m (4h)	381±19	-	1118±16	81±4	-31	-	-42	-73
	6 m (20h)	397±13	-	1161±17	72±1	-28	-	-40	-76
19.1 (mm)	Runoff	547±3	887±50	2023±245	313±37	-	-	-	-
	1.5 m (4h)	1020±4	5±0	1715±19	38±1	87	-99	-15	-88
	3 m (4h)	4815±25	5±0	7283±97	62±2	780	-99	260	-80
	6 m (4h)	402±45	20±2	1143±14	70±2	-26	-98	-43	-78
	6 m (20h)	389±1	11±2	1168±6	65±1	-29	-99	-42	-79
25.4 (mm) (1st)	Runoff	595±2	115±21	1850±47	528±263	-	-	-	-
	1.5 m (4h)	2136±18	5±0	2522±57	263±13	259	-96	36	-50
	3 m (4h)	3003±26	5±0	3463±54	289±14	404	-96	87	-45
	6 m (4h)	1044±32	13±6	1474±64	62±17	75	-89	-20	-88
	6 m (20h)	1382±3	7±3	1805±43	43±4	132	-94	-2	-92
25.4 (mm) (2nd)	Runoff	633±1	114±4	1602±304	353±2	-	-	-	-
	1.5 m (4h)	4379±51	19±6	4321±62	141±16	591	-83	170	-60
	3 m (4h)	2275±53	7±0	2338±42	89±7	259	-94	46	-75
	6 m (4h)	1046±32	23±1	1369±11	74±18	65	-80	-15	-79
	6 m (20h)	1769±8	17±0	1932±30	153±18	179	-85	21	-57
25.4 (mm) (3rd)	Runoff	567±16	48±9	1489±31	320±58	-	-	-	-
	1.5 m (4h)	1852±22	3±0	1969±7	47±2	227	-94	32	-85
	3 m (4h)	2162±20	3±0	2264±19	55±1	281	-94	52	-83
	6 m (4h)	1164±3	3±0	1437±39	71±13	105	-94	-4	-78
	6 m (20h)	1357±5	3±0	1600±24	53±2	139	-94	7	-83
38.1 (mm)	Runoff	582±6	51±5	1739±24	261±25	-	-	-	-
	1.5 m (4h)	1068±10	2±0	1515±45	56±3	84	-96	-13	-79
	3 m (4h)	1412±18	2±0	1486±19	75±14	143	-96	-15	-71
	6 m (4h)	1651±10	2±0	1917±21	65±12	184	-96	10	-75
	6 m (20h)	1404±11	2±0	1741±76	4±1	141	-96	0	-98
76.2 (mm)	Runoff	567±8	93±1	1754±46	284±11	-	-	-	-
	1.5 m (4h)	2129±18	0±0	2257±9	33±0	276	-100	29	-88
	3 m (4h)	740±3	0±0	927±18	48±1	31	-100	-47	-83
	6 m (4h)	579±2	0±0	822±35	44±1	2	-100	-53	-85
	6 m (20h)	547±1	0±0	760±12	42±1	-4	-100	-57	-85

Note: Ammonia was not measured for samples during storm depth 12.7 mm.

Table A.6. Mean concentration with standard deviation of three measurements of the nutrient species from Control model and calculated percent change for a 1-lane roadway.

Storm depth	Location	Mean concentration ± SD				Change			
		NO_x-N (µg/l)	NH_3-N (µg/l)	TN (µg/l)	TP (µg/l)	NO_x-N (%)	NH_3-N (%)	TN (%)	TP (%)
12.7 (mm)	Runoff	545±13	76±8	1691±62	287±9	-	-	-	-
	1.5 m (4h)	-	-	-	-	-	-	-	-
	3 m (4h)	-	-	-	-	-	-	-	-
	6 m (4h)	315±2	2±0	582±4	47±1	-42	-97	-66	-84
	6 m (20h)	368±4	2±0	725±16	63±0	-32	-97	-57	-78
19.1 (mm)	Runoff	590±12	84±4	1891±33	268±2	-	-	-	-
	1.5 m (4h)	1475±8	2±0	1670±4	32±0	150	-98	-12	-88
	3 m (4h)	1026±3	2±0	1244±26	32±0	74	-98	-34	-88
	6 m (4h)	453±6	2±0	736±12	43±1	-23	-98	-61	-84
	6 m (20h)	696±2	2±0	982±21	37±0	18	-98	-48	-86
25.4 (mm) (1st)	Runoff	539±6	98±9	1708±38	301±45	-	-	-	-
	1.5 m (4h)	885±8	2±0	1057±2	41±37	64	-98	-38	-86
	3 m (4h)	1052±20	2±0	1221±29	82±5	95	-98	-28	-73
	6 m (4h)	848±15	2±0	1187±37	36±50	57	-98	-31	-88
	6 m (20h)	1133±23	2±0	1433±16	67±30	110	-98	-16	-78
25.4 (mm) (2nd)	Runoff	514±2	91±3	1757±44	304±13	-	-	-	-
	1.5 m (4h)	870±5	2±0	1102±11	22±1	69	-98	-37	-93
	3 m (4h)	1434±9	2±0	1772±26	22±2	179	-98	1	-93
	6 m (4h)	548±1	2±0	976±10	22±5	7	-98	-44	-93
	6 m (20h)	735±3	2±0	1127±19	35±3	43	-98	-36	-88
25.4 (mm) (3rd)	Runoff	555±6	64±1	1509±16	279±7	-	-	-	-
	1.5 m (4h)	605±1	2±0	773±20	37±1	9	-97	-49	-86
	3 m (4h)	1307±8	2±0	1507±11	43±1	135	-97	0	-84
	6 m (4h)	610±2	2±0	905±3	45±1	10	-97	-40	-84
	6 m (20h)	665±3	2±0	978±5	46±1	20	-97	-35	-84
38.1 (mm)	Runoff	585±4	77±1	1802±20	277±6	-	-	-	-
	1.5 m (4h)	1120±46	2±0	1303±14	40±1	91	-97	-28	-86
	3 m (4h)	1672±24	2±0	1779±34	44±1	186	-97	-1	-84
	6 m (4h)	300±22	2±0	662±6	48±2	-49	-97	-63	-82
	6 m (20h)	818±40	2±0	1128±16	42±0	40	-97	-37	-85
76.2 (mm)	Runoff	532±12	108±4	1857±21	248±8	-	-	-	-
	1.5 m (4h)	992±4	0±0	1239±8	30±1	87	-100	-33	-88
	3 m (4h)	520±10	0±0	771±5	40±1	-2	-100	-58	-84
	6 m (4h)	450±3	0±0	709±4	39±1	-15	-100	-62	-84
	6 m (20h)	356±7	2±1	621±11	135±174	-33	-98	-67	-46

Note: Drainage ports at 1.5 m and 3 m filter during storm depth 12.7 mm were dry.